

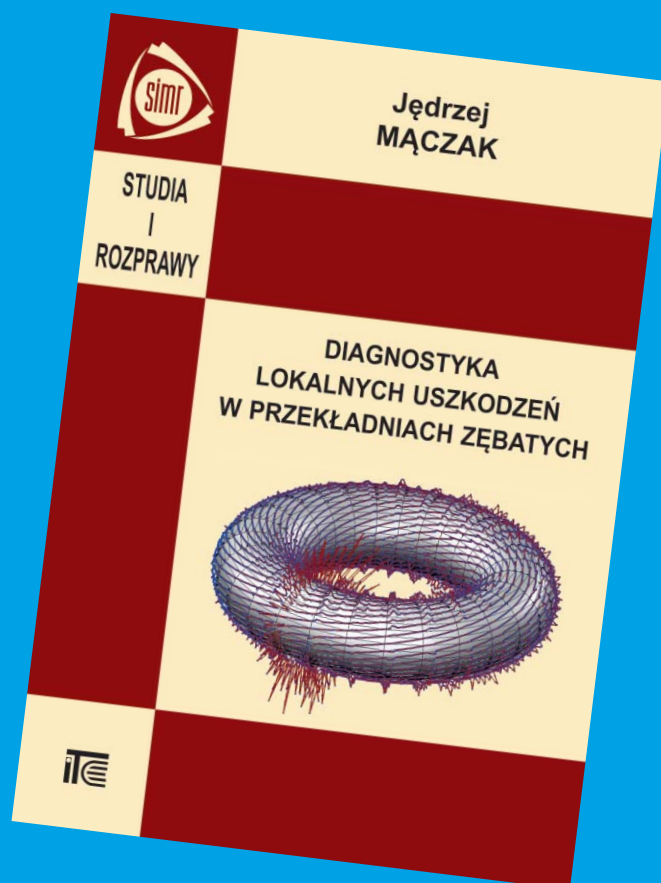
DIAGNOZA - GENEZA - PROGNOZA => PODSTAWA KAŻDEJ DECYZJI



Diagnostyka

Applied Structural Health,
Usage and Condition Monitoring

ISSN 1641-6414



Vol. 14, No. 3

PTDT, Warszawa, 2013

RADA PROGRAMOWA / PROGRAM COUNCIL

PRZEWODNICZĄCY / CHAIRMAN:

prof. dr hab. dr h.c. mult. **Czesław CEMPEL** *Politechnika Poznańska*

REDAKTOR NACZELNY / CHIEF EDITOR:

prof. dr hab. inż. **Wiesław STASZEWSKI** *AGH w Krakowie*

CZŁONKOWIE / MEMBERS:

prof. dr hab. inż. **Jan ADAMCZYK**
AGH w Krakowie

prof. **Francesco AYMERICH**
University of Cagliari – Italy

prof. **Jérôme ANTONI**
University of Technology of Compiègne – France

prof. dr. **Ioannis ANTONIADIS**
National Technical University Of Athens – Greece

dr inż. **Roman BARCZEWSKI**
Politechnika Poznańska

prof. dr hab. inż. **Walter BARTELMUS**
Politechnika Wroclawska

prof. dr hab. inż. **Wojciech BATKO**
AGH w Krakowie

prof. dr hab. inż. **Adam CHARCHALIS**
Akademia Morska w Gdyni

prof. **Li CHENG**
The Hong Kong Polytechnic University – China

prof. dr hab. inż. **Wojciech CHOLEWA**
Politechnika Śląska

prof. dr hab. inż. **Zbigniew DĄBROWSKI**
Politechnika Warszawska

prof. **Charles FARRAR**
Los Alamos National Laboratory – USA

prof. **Wiktor FRID**
Royal Institute of Technology in Stockholm – Sweden

dr inż. **Tomasz GAŁKA**
Instytut Energetyki w Warszawie

prof. **Len GELMAN**
Cranfield University – England

prof. **Mohamed HADDAR**
National School of Engineers of Sfax – Tunisia

prof. dr hab. inż. **Jan KICIŃSKI**
IMP w Gdańsku

prof. dr hab. inż. **Daniel KUJAWSKI**
Western Michigan University – USA

prof. **Graeme MANSON**
University of Sheffield – UK

prof. dr hab. **Wojciech MOCZULSKI**
Politechnika Śląska

prof. dr hab. inż. **Stanisław RADKOWSKI**
Politechnika Warszawska

prof. **Bob RANDALL**
University of South Wales – Australia

prof. dr **Raj B. K. N. RAO**
President COMADEM International – England

prof. **Riccardo RUBINI**
University of Modena and Reggio Emilia – Italy

prof. **Massimo RUZZENE**
Georgia Institute of Technology – USA

prof. **Vasily S. SHEVCHENKO**
BSSR Academy of Sciences Mińsk – Belarus

prof. **Menad SIDAHMED**
University of Technology Compiègne – France

Prof. **Tadeusz STEPINSKI**
Uppsala University - Sweden

prof. **Wiesław TRĄMPCZYŃSKI**
Politechnika Świętokrzyska

prof. dr hab. inż. **Tadeusz UHL**
AGH w Krakowie

prof. **Vitalijus VOLKOVAS**
Kaunas University of Technology – Lithuania

prof. **Keith WORDEN**
University of Sheffield – UK

prof. dr hab. inż. **Andrzej WILK**
Politechnika Śląska

dr **Gajraj Singh YADAVA**
Indian Institute of Technology – India

prof. dr hab. inż. **Radosław ZIMOROZ**
Politechnika Wroclawska

prof. dr hab. inż. **Bogdan ŻÓLTOWSKI**
UTP w Bydgoszczy

WYDAWCA:

Polskie Towarzystwo Diagnostyki Technicznej
ul. Narbutta 84
02-524 Warszawa

REDAKTOR NACZELNY:

prof. dr hab. inż. **Wiesław STASZEWSKI**

SEKRETARZ REDAKCJI:

dr inż. **Sławomir WIERZBICKI**

CZŁONKOWIE KOMITETU REDAKCYJNEGO:

dr inż. **Krzysztof LIGIER**
dr inż. **Paweł MIKOŁAJCZAK**

ADRES REDAKCJI:

Redakcja Diagnostyki
Katedra Budowy, Eksploatacji Pojazdów i Maszyn
UWM w Olsztynie
ul. Oczapowskiego 11, 10-736 Olsztyn, Poland
tel.: 89-523-48-11, fax: 89-523-34-63
www.diagnostyka.net.pl
e-mail: redakcja@diagnostyka.net.pl

KONTO PTDT:

Bank PEKAO SA O/Warszawa
nr konta: 33 1240 5963 1111 0000 4796 8376

NAKLAD: 500 egzemplarzy

Spis treści / Contents

Maria Cristina VALIGI – University of Perugia, Italy, Susanna PAPINI – University of Florence, Italy	3
Analysis of chattering phenomenon in industrial S6-high rolling mill	
Marco SPAGNOL, Luigi BREGANT – Università degli Studi di Trieste, Italy	9
Instantaneous angular speed: encoder-counter estimation compared with vibration data	
Marcin ŁUKASIEWICZ, Tomasz KAŁACZYŃSKI, Michał LISS, Tomasz KASPROWICZ – University of Technology and Life Sciences, Bydgoszcz,	15
Diagnostics investigations of DMG-1A transmission with operational modal analysis methods application <i>Badania diagnostyczne przekładni DMG-1A z zastosowaniem metod eksploatacyjnej analizy modalnej</i>	
Jerzy KWAŚNIEWSKI – AGH University of Science and Technology in Kraków, Józef GRZYBOWSKI, Damian KORDOS – Rzeszów University of Technology	23
System of geometric parameters monitoring during cutting of steel plates process <i>System monitorowania parametrów geometrycznych podczas cięcia blach stalowych</i>	
Tomasz CIECHULSKI – Wojskowa Akademia Techniczna w Warszawie	29
GSM localization and monitoring in electronic transport security systems <i>Lokalizacja GSM i monitoring wizyjny w transportowych elektronicznych systemach bezpieczeństwa</i>	
Tomasz WÓJCICKI – Institute For Sustainable Technologies – National Research Institute in Radom	35
Model of a computer support for the design of AOI systems aimed at the detection of surface defects <i>Model komputerowego wspomaganie projektowania systemów AOI detekcji wad powierzchniowych</i>	
Ivan Prudyus, Volodymyr Shkliarskyi, Yuriy Matiieshyn, Anatoliy Pedan, Yuriy Balanyuk, Volodymyr Vasylyuk – National University in Lviv, Ukraine	41
Scanning television optical microscope for diagnostics of microobjects in medicine <i>Skanujący telewizyjny optyczny mikroskop dla diagnostyki mikroobektów w medycynie</i>	
Adrian D. NEMBHARD, Jyoti K. SINHA, K. ELBHBAH – The University of Manchester, A. J. PINKERTON – Lancaster University	45
Fault diagnosis of rotating machines using vibration and bearing temperature measurements	
Tomasz BARSZCZ, Marcin STRĄCZKIEWICZ – AGH University of Science and Technology in Kraków	53
Novel intuitive hierarchical structure for condition monitoring system of wind turbines <i>Nowatorska intuicyjna struktura hierarchiczna systemu monitorowania stanu turbin wiatrowych</i>	
Phong Ba DAO – AGH University of Science and Technology in Kraków	61
Cointegration method for temperature effect removal in damage detection based on lamb waves <i>Wykrywanie uszkodzeń przy pomocy fal lambda - kompensacja wpływu temperatury oparta o metodę kointegracji</i>	
Wojciech SAWCZUK, Franciszek TOMASZEWSKI - Poznan University of Technology	69
Evaluation of the wear of friction pads railway disc brake using selected frequency characteristic of vibrations signal generated by the disc brake <i>Ocena zużycia okładzin ciernych kolejowego hamulca tarczowego na przykładzie wybranych charakterystyk widmowych sygnału drganiowego generowanego przez hamulec</i>	
Warto przeczytać / Worth to read	75

ANALYSIS OF CHATTERING PHENOMENON IN INDUSTRIAL S6-HIGH ROLLING MILL

Maria Cristina VALIGI¹, Susanna PAPINI²

¹ Department of Industrial Engineering, University of Perugia, Italy
E-mail: mariacristina.valigi@unipg.it

² Department of Industrial Engineering, University of Florence, Italy
E-mail: susanna.papini@unifi.it

Abstract

Chatter in rolling mills is the undesirable vibration observed in most of the rolling mills operating at high speed and rolling thin strip. In this work the authors discuss some problems relative to the vibrations occurring in a S6-high cold rolling mill. It can result in not good surface finish for some applications and, rare cases, in gauge variations in the rolled strip and it is considered to be the result of interaction between rolling mill structure and rolling-process. Three basic types of chatter can be classified in rolling mills: torsional, third-octave mode, and fifth-octave-mode chatter.

S6-high rolling mill is an innovative mode to work the steel: it allows the use of very small work rolls laterally guided by individually adjustable side support rolls, which are supported by two rows of roller bearings mounted in cassettes. It has six rolls able to roll steel strip coming directly from hot rolling mill train.

A proposed solution based on empirical observations, vibration analysis and considerations of a model is described with the aim to improve the quality of the product and increasing production.

Keywords: Chatter, vibration analysis, S6-high rolling mill.

1. INTRODUCTION

Due to their excellent features, the S6-high rolling mills are increasingly used for steel strip rolling. The integrated tandem S6-high rolling mill studied in this paper is positioned at the entry section of the annealing and pickling line. Using the integrated treatment line at S6-High, the strip is transported to the processing line, laminated, annealed and pickled in one step thus obtaining a semi-finished product but already laminated, workable again (also on the same line) or marketable. The market share of products perfectly stackable is relevant and the use of this technology offers new scenarios for the steel industry of the future. The attention is focused on the vibrations generated in the rolling mill with the aim to investigate the problem of chatter marks generation. Such marks are regular, parallel marking across the width of strip metal that not only significantly affects the mill performance, but also reduces surface quality of the strip steel. The defects of the strip are the consequence of insurgence of vibrations, generically denominated 'chatter'. Its manifestation is the classical regular, parallel marking across the width of strip metal called "chatter marks" or skid marks [1–5]. There are several types of rolling mill vibration that can have a significant impact on the quality and productivity of the cold rolling process. Under extreme conditions of chatter, strip rupture or damage to the rolling mill can also occur.

Chatter in rolling is considered to be the result of interactions between the mill structure and the rolling

process. The dynamic forces which are generated in the rolling process deflect the structure of the mill, leading to variations in the roll gap, rolls speed, tension, etc. These, in turn, result in further variations in the rolling forces. Self-excited systems begin to vibrate of their own accord spontaneously, the amplitude increasing until some non-linear effect limits any further increase. Chatter is a particular case of self-excited vibrations: the alternating force that sustains the motion is created by the motion itself and stops when the motion stops. Three basic types of rolling chatter have been observed in rolling mills which causes significant chatter bands across the strip and small thickness fluctuations. Torsional chatter, occurs in the 5–25Hz range. Third-octave-mode chatter, which produces large thickness variations and strip rupture, lies in the 125–240Hz range. Fifth-octave-mode chatter occurs in the 500–800Hz range. The third-octave-mode chatter is considered the most critical because it generates large gauge variations in the rolled materials. It therefore has the most detrimental effects in terms of loss productivity due to the lower rolling speeds required to avoid the phenomenon [6-11]. To understand the conditions which lead to the dynamic instability of the rolling process suggests the solutions able to limit the phenomena. Thus, the interaction between the structural dynamics of the mill and the dynamics of the rolling process must be investigated [12-13]. This investigation is often carried out by modelling the rolling mill and the rolling process and their interaction. Figure 1 describes the closed loop diagram

representing schematically the interaction between the structure and the process [14-16].

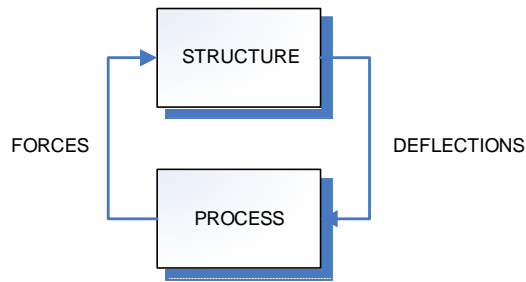


Fig. 1. Diagram scheme

A number of model have been proposed and developed to better understand the rolling process [17].

Unimodal e multimodal structural models have been developed together with models of the rolling process [18-21]. Lumped parameter models have been widely used to represent the mill dynamic [22-26].

1 S6-HIGH ROLLING MILL: CHATTER MARKS AND VIBRATION ANALYSIS

The S6-high cold rolling has six rolls with different diameters arranged horizontally one above each other and symmetrically to the neutral rolling plane. The six rolls are: the work rolls (WRs) the intermediate rolls (IRs), and the backup rolls (BURs). The IRs are the only ones motorized ad transmit the rotation to the stand through gear-boxes linked by means of spindles. In addition there are four cassettes fixed with an additional cylinder called Side Support Roll (SSR). The aim of the SSR is to support the

horizontal load created on the work roll during the process (Figure 2).

The vertical rolling force is transmitted through an hydraulic system that acts on back-up rolls which then transmit the force up to the work rolls. The cassettes have the function to get a rolls packing condition helpful to provide a sufficient compression inside the rolling stand. The two rows of roll bearings have the axis parallel to the side support roll and they have the function to reduce the strokes originated by work rolls during the process. During the rolling process the WR is pushed on SSR because of the horizontal force and transmitted to the roll bearings with the aim to restrain the force. Little fluctuations on the process parameters take to little fluctuations on the forces values so that WR is pushed towards SSR with a vibration mode. When the WR pushes SSR towards its roll bearings with little force, SSR must react to follow the WR contact in order to damp the stroke effects of the following load increasing. This is the important role played by the springs located on the extremities of the SSRs necks into the cassette. The SSRs rolls have a limited grinded life of about some hundreds of rolled strip because they have to resist to the horizontal loads and because they are made with a softer material than the WRs [25-26].

The analyzed plant presents the problem of chatter marks on the strip.

The aim of this paper is to investigate the reason of chatter-marks using a vibration analysis and understand which of parameters is involved in the self-exciting behaviour and how a rolling mill can be adjusted to ensure highest quality and maximum productivity.

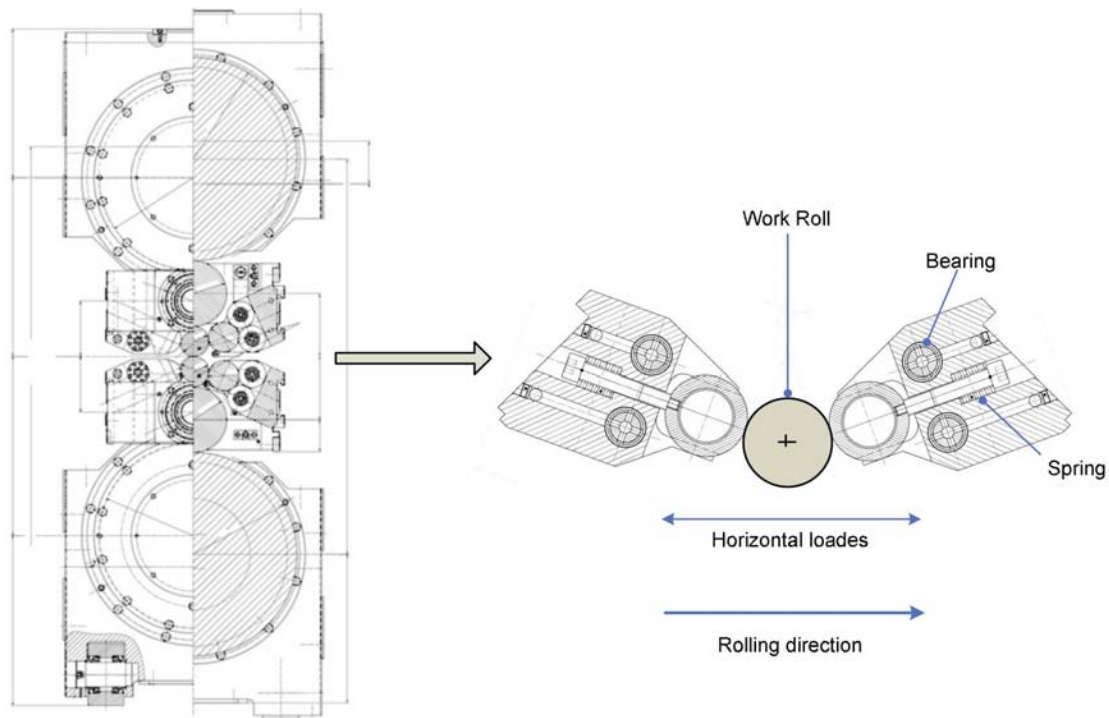


Fig. 2. S6-high rolling mill and side support cassettes

Since the start-up of the plant a series of chatter marks, perpendicular to the rolling direction, compromising the aesthetically quality of the product was noted.

The frequency of the skid marks was about two marks per centimeter so that for a rolling speed of 40 m/min gives a characteristic frequency of about 130 Hz. Because an inaccurate grinding of involved rolls in the process can be a cause of defects a promptly analysis of the grinding process parameters, measurements and inspection reports checks was carried out but results excluded this hypothesis. Experimental evidences showed that the gravity occurrence of chatter marks followed a periodic trend of rolling mill campaigns with to the replacement of SSR cassettes. Particularly chatter marks were noted on SSRs' surfaces the so called facets so that after just 150 km of rolled strip the cassettes had to be replaced. Disappearing the problem with the replacement of the cassettes, the immediate relationship between the age of the SSR rolls and the chatter marks on the strip was deduced. Vibration measurements made directly on the motor gear-box systems and the rolling mill stands for the rolling speeds 40 m/min in order to investigate the origin of chatter.

Since the vibration behavior of the gear-box systems presents a prevalent and admissible component attributable to tooth mesh frequency the gear-box system was left out the possible origin of self-excited vibration.

The vibration measurements made directly on the rolling stand before (in red) and after (in blue) the change of the cassettes, showed a critical value of 124.5 Hz at 40 m/min rolling speed (Figure 3) and 249 Hz at 80 m/min (Figure 4). This results show the origin of the chatter inside the stand and specifically in the cassettes.

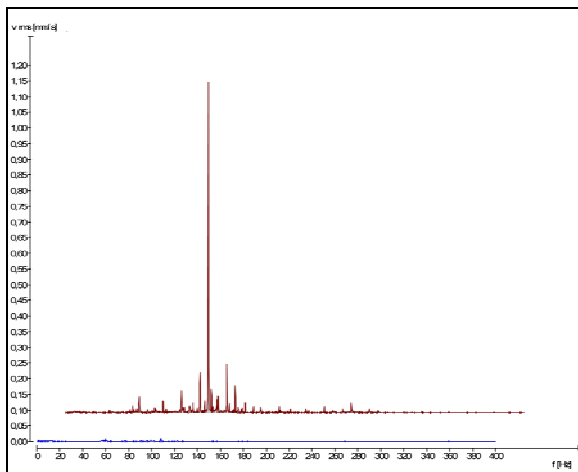


Fig. 3. Measures at 40 m/min

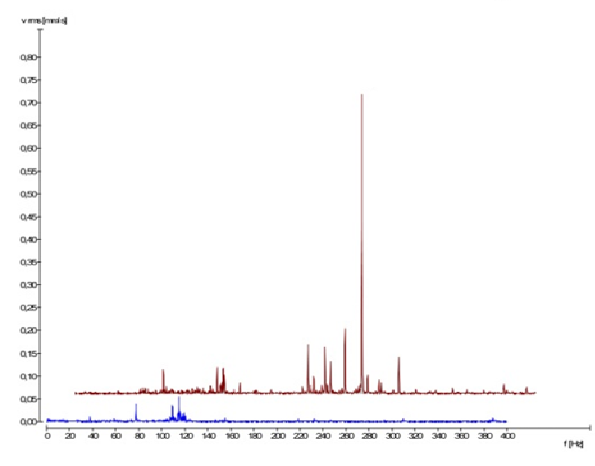


Fig. 4. Measures at 80 m/min

3. PROPOSED MODEL

In order to investigate the influence of individual parameters on the dynamic instability, a lumped parameter model of the rolling mill have been proposed, as the conventional, linear-mass-damping-spring system [21] [24-26]. Firstly a model having ten degree of freedoms (Figure 5-a) where the masses are reduced to the ten rolls involved in the process can be considered but, to simplify the problem, the stand was assumed symmetrical in relation to the rolled strip and symmetrical to the vertical axis of the stand so that the ten degrees of freedoms model was reduced into the simplest system with two degree of freedoms (Figure 5-b).

Equations for the two degree of freedoms model are:

$$\begin{bmatrix} m_1 & 0 \\ 0 & m_2 \end{bmatrix} \begin{Bmatrix} \ddot{y}_1 \\ \ddot{y}_2 \end{Bmatrix} + \begin{bmatrix} c_1 & 0 \\ 0 & 0 \end{bmatrix} \begin{Bmatrix} \dot{y}_1 \\ \dot{y}_2 \end{Bmatrix} + \begin{bmatrix} k_1+k_2 & -k_2 \\ -k_2 & k_2+k_3 \end{bmatrix} \begin{Bmatrix} y_1 \\ y_2 \end{Bmatrix} = \begin{Bmatrix} F \\ 0 \end{Bmatrix} \quad (1)$$

This model takes into account the equivalent mass m_1 of the working rolls, the intermediate rolls and the back-up rolls and the equivalent mass m_2 of the side support rolls.

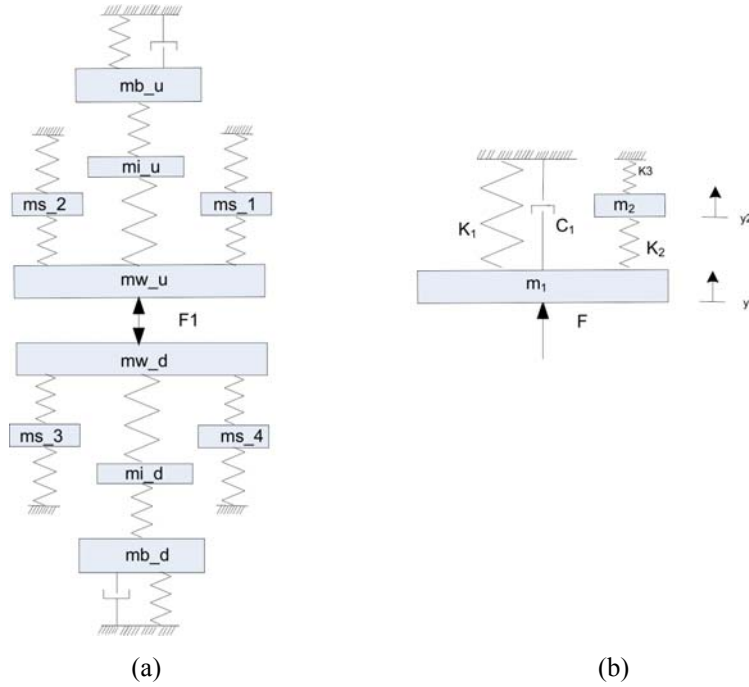


Fig. 5. Lumped parameter model with 10 DOF (a) reduced to a model with 2 DOF (b)

Then k_1 e c_1 represent the stiffness and the damping of the mass frame connection, k_2 the contact stiffness between working rolls and side support rolls, and k_3 is the stiffness of spring in the cassettes. The vertical component F of the rolling force acting between strip and working rolls can be evaluated by a wide used model: the slab theory (Figure 6).

$$dp = 2 \frac{k}{y} dy \pm \frac{\mu P}{y} + 2dk \quad (2)$$

It supposes infinitesimal segments in deformation delimited by two surfaces that remain flat during the process where p is the rolling pressure, μ is the coefficient of friction and k is the mean yield stress in plane strain [1][22]. The model determines the rolling force that, assuming that the roll radius is constant, may be implicitly written as a function of several variables :

$$F = F(y_e, y_d, \sigma_{xe}, \sigma_{xd}, \mu, \lambda) \quad (3)$$

where y_e , y_d , are the half thickness of rolled strip at the entry and at the exit of the stand, σ_{xe} , σ_{xd} , are the horizontal tensile stress at entry and at exit of the stand and λ is the resistance to deformation dependent on strain hardening characteristics [23-25].

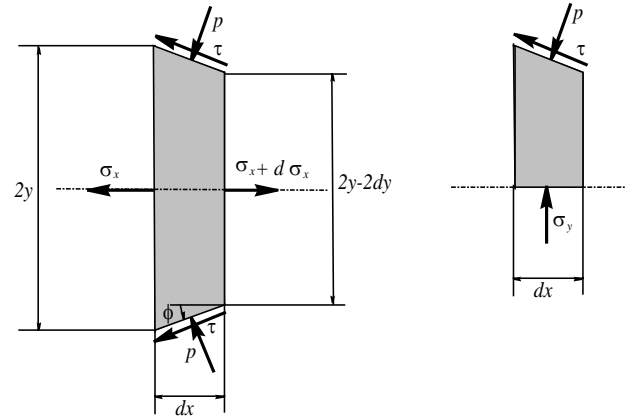


Fig. 6. Slab analysis

4. PROPOSED SOLUTION

The disturbances and the variations of the strip thickness due to roll vibration generate the dynamic component of the rolling force. This dynamic component deflects the structure of the mill leading to variations in the roll gap, y_1 , which in turn result in further variations in the rolling force. Under certain conditions, however, this interaction between the structure and process leads to dynamic instability. By applying the Laplace transform to the above equations (1), the following relationships are obtained:

$$\left\{ \begin{array}{l} \frac{L[y_1]}{L[F]} = G1(s) = \frac{(m_2 s^2 + k_{sw} + k_s)}{(m_1 s^2 + c_0 s + k_0 + k_{sw})(m_2 s^2 + k_{sw} + k_s) - k_{sw}} \\ \frac{L[y_2]}{L[F]} = G2(s) = \frac{k_{sw}}{(m_2 s^2 + k_{sw} + k_s)} \frac{(m_2 s^2 + k_{sw} + k_s)}{(m_1 s^2 + c_0 s + k_0 + k_{sw})(m_2 s^2 + k_{sw} + k_s) - k_{sw}} \end{array} \right. \quad (4)$$

On the basis of the model a proposed solution for improve the productivity of the plant is the change of spring stiffness in the cassettes in order to have an anti-resonance at 124 Hz. Figure 7 shows the diagrams of $G1(s)$ with two different values of k_s : the red line regards the system with the current value of 260 N/mm and the blue one with the proposed value of 485 N/mm. Immediately after replacing the springs the presence of skid marks appeared after 350 km of rolled strip so that the proposed solution has resulted in doubling of the side support rolls life [25-26].

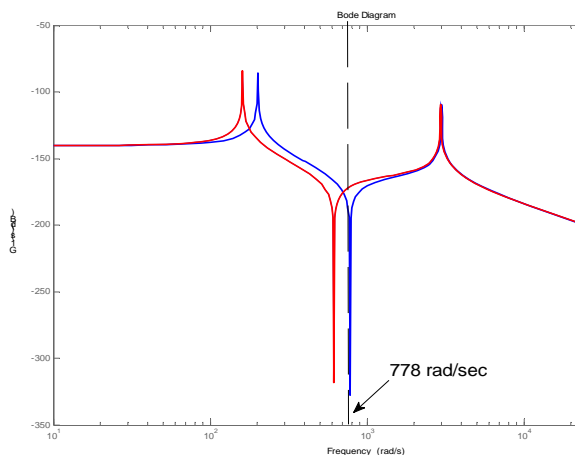


Fig. 7. Frequency response $G1(s)$: the blue line with the proposed value of k_s the red line with the current value of k_s

5. CONCLUSION

In this work the source of the chatter in a rolling mill was identified in side support rolls so that a proposed solution based on a linearized two degrees of freedoms model has improved the mill performances. This just the beginning of the study of chatter problem in the analyzed plant; the authors are going to investigate the phenomenon with a more complex models using non-linear models in closed loop and considering more refined model of the process (e.g. the Orowan's model) with the aim to analyze the problem and further increase the productivity of the mill.

Acknowledgements

This work is a result of collaboration between the Acciai Speciali Terni Spa and University of Perugia. The authors desire to thank the competent consultant team of A.S.T. in particular the engineers S. Cervo and A. Petrucci. Furthermore a special thanks to Prof. Paolo Toni for the careful supervision at the activity.

References

- [1] L. Chefneux, J.-P. Fischbach, J. Gouzou, *Study and control of chatter in cold rolling*. (1980) Iron and Steel Engineer 17–26.
- [2] R.-M. Guo, A. C. Urso. *Analysis of chatter vibration phenomena of rolling mills using finite element method*. (1993) Iron and Steel Engineer Jan. 29–39.
- [3] D. L. Paton, S. Critchley. *Tandem mill vibration: its cause and control*. (1985) Iron and Steel Making 37–43.
- [4] I. S. Yun, W. R. D. Wilson, K. F. Ehmann. *Review of chatter studies in cold rolling*. International (1998) Journal of Machine Tools & Manufacture 38 1499–1530.
- [5] W. L. Roberts. *Four-h mill-stand chatter of the fifth octave mode*. (1978) Iron Steel Engineering, 55, 41-47.
- [6] Evans, P. R., Hill, D. E., and Vaughan, N. D. *Dynamic Characteristics of a Rolling Mill*. (1996), Proc. Instn. Mech. Engrs., V210 259-271.
- [7] J. Tlustý, G. Chandra, S. Critchley, D. Paton, *Chatter in cold rolling*. (1982) Annals of the CIRP, 31, 195.
- [8] M. Malvezzi, M. Rinchi. *Control systems of strip tension in hot steel rolling mills trains*. Proceedings of Nineteenth IASTED International Conference -MIC 2000 - Modelling, Identification and Control, Innsbruck, Austria, February 14-17, 2000.
- [9] M. Rinchi; A. Rindi. *Fenomeni vibratori autoeccitati nei laminatoi finitori*. In: XIV Congresso Nazionale AIMETA, Como, 6-9 ottobre 1999.
- [10] Pei-Hua Hu Huyue Zhao K F Ehmann. *Third-octave-mode chatter in rolling. Part 1: Chatter model*. (2006), Proceedings of the Institution of Mechanical Engineers, Part B: Journal of Engineering Manufacture August 1, 220: 1267-1277.
- [11] Y Chen, S Liu, T Shi, S. Yang, G. Liao. *Stability analysis of the rolling process and regenerative chatter on 2030 tandem mills*. (2002) Imech Part C: J Mechanical Engineering Science, 216 1225-1235.
- [12] D. R. Bland, H. Ford. *The calculation of roll force and torque in cold strip rolling with tensions*. (1948) Proceedings of the Institute of Mechanical Engineers 159 144–163.
- [13] I. S. Yun, W. R. D. Wilson, K. F. Ehmann. *Review of chatter studies in cold rolling*. (1998) International Journal of Machine Tools & Manufacture 38 1499–1530.
- [14] J. M. Alexander. *On the theory of rolling*. Proceedings of the Royal Society of London A326 (1972) 535–563.
- [15] T. Tamiya, K. Furui, H. Hida. *Analysis of chattering phenomenon in cold rolling*. (1980) Proceedings of International Conference on Steel Rolling, 2, 1191-1207.

- [16] G. L. Nessler, J. F. Cory, "Identification of chatter sources in cold rolling mills", (1993), *Iron and steel Engineer*, 40-45.
- [17] P.-H. Hu, K. F. Ehm. *A dynamic model of the rolling process. Part I: homogeneous model.* (2000) *International Journal of Machine Tools & Manufacture* ,40, 1–19.
- [18] I. Yarita, K. Furukawa, Y. Seino. *An analysis of chattering in cold rolling of ultrathin gauge steel strip.* (1978) *Transactions ISIJ* 19 (1) 1–10.
- [19] K. Misonoh. *Analysis of chattering in cold rolling of steel strip.* (1980) *Journal of the JSTP* 21 (238) 1006–1010.
- [20] R. Venter, A. Abd-Rabbo, "Modelling of the rolling process—part I", (1980), *International Journal of Mechanical Science* 22 , 83–92.
- [21] A. Swiatonoswki, A. Bar. *Parametrical Excitement vibration in tandem mills-mathematical model and its analysis.* (2003) *Journal of material processing Technology* 134 214-224.
- [22] Malvezzi M, Valigi M. C., (2008) "Cold rolling mill process: A numerical procedure for industrial applications. *Meccanica* 43 (1) 1-9
- [23] Johnson, R. E., and Qi, Q. *Chatter Dynamics in Sheet Rolling,*" (1994) *Int. J. Mech. Sci.*, 36(7). pp. 617–30.
- [24] Gryllias, K. C. , Antoniadis, I. A. *Modeling and experimental analysis of a 6-High industrial rolling mill vibration response.* in Proc. The Seventh International Conference on Condition Monitoring and Machinery Failure Prevention Technologies, Ettington Chase, Stratford-upon-Avon, England June ,22-24,(2010).
- [25] Valigi, M. C., Cervo, S., Petrucci, A. *Chatter Marks and Vibration Analysis in a S6-high cold rolling mill.* in Proc. III Inter. Conference on Condition Monitoring of Machinery in Non-Stationary Operations (CMMN02013), Ferrara ,Italy, May,8-10,(2013).
- [26] Valigi,M. C., Papini S. *Chatter in a S6-high rolling mill.* XXI Congresso AIMETA,Torino, Italy,17-20 Settember (2013).

INSTANTANEOUS ANGULAR SPEED: ENCODER-COUNTER ESTIMATION COMPARED WITH VIBRATION DATA

Marco SPAGNOL¹, Luigi BREGANT²

¹ Università degli Studi di Trieste, via A. Valerio 10, 34127 Trieste TS Italy

mspagnol@units.it

² Università degli Studi di Trieste, via A. Valerio 10, 34127 Trieste TS Italy

bregant@units.it

Abstract

In rotating machinery, actions of the moving parts take place at specific angular positions rather than at specific times. For this reason, having a geometrical reference, such as the one provided by an encoder, and studying the Instantaneous Angular Speed (IAS) variations can provide a large amount of information about the health status of the machine. In fact, from the variation of the IAS during the machine loads' cycle it is possible to identify defects and faults. The current work focuses on the estimation of the IAS through the Elapsed Time (ET) method, using a counter in order to measure the time elapsed between the pulses of an encoder. Both IAS and vibration measurement are conducted on an asynchronous four poles electrical motor driven by 50Hz line current, without load. The study compares the order analysis of both signals. The bearing's Fundamental Train Frequency is detected using IAS estimation.

Keywords: instantaneous angular speed, encoder, elapsed time method, AC DC electrical machine, slip effect.

1. ENCODER-COUNTER SYSTEM

Among the different processing strategies to obtain IAS [Li et al - 2005], in this study, the Elapsed Time (ET) method is used. In this case, the counter measures the time elapsed between two successive pulses of the encoder. With this approach there are as many measurement values as there are pulses/revolution of the encoder. The frequency of the counter and the number of pulses determine the resolution of the IAS estimates. The method is strictly correlated to the real rotational angle of the shaft, except from the encoder tolerances. [André, et al - 2012], [Youssef, et al - 2011], [Renaudin, et al - 2010]. A National Instruments 80MHz counter is used for the measurements described in the following paragraphs. The selected board allows a choice between three counting methods: the Elapsed Time (ET) method, using one counter, and the High-Frequency (HF) and Large-Range (LR) methods, using two counters. A comparison between these methods is reported in [Spagnol, et al - 2013]. In this paper ET method is used: the rising edge of the input signal of the encoder triggers the counting of the timebase ticks (Fig. 1). Since the timebase is of a known frequency, the frequency of the input signal can be obtained as (3).

$$f_{count} = 80MHz \quad (1)$$

$$\Delta t_{count} = f_{count}^{-1} = 1,25 \times 10^{-8} s \quad (2)$$

$$f_{input} = \frac{1}{n_{count} \Delta t_{count}} \quad (3)$$

IAS measurement errors come from different sources. Generally speaking, the absolute error value, increases linearly with the speed and the resolution of the encoder, considering that the upper measured speed limit is the ratio between the encoder's resolution and the clock frequency of the counter.

The ideal encoder assumes exactly equal geometric segments and any variation causes the ET to be sampled on a non-uniform angular basis. Since the spacing pattern repeats itself after each revolution, the error manifests itself as high-level content at integer multiples of the shaft running speed. It is possible to use the synchronous averaged encoder passage times to correct for the uneven encoder spacing [Resor, et al - 2005]. These errors are unavoidable, but the production standards are very high and great precision can be obtained.

The ET measurement depends on the achievable time resolution, governed by the clock rate and the zero crossing detection circuit. These lead to two main problems: the counting method and the clock stability. Different authors [Youssef, et al - 2011], [André, et al - 2012] have analysed the problems and have suggested appropriate remedies.

Further errors can be experienced if the sensor undergoes lateral movement, if it is installed with eccentricity or misalignment, or if any light-path transmission variations are present, as shown from the test setup (Fig. 2).

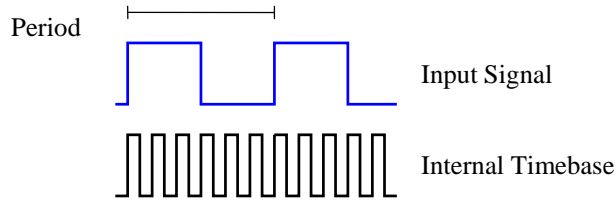


Fig. 1. Digital signal frequency measured with ET method

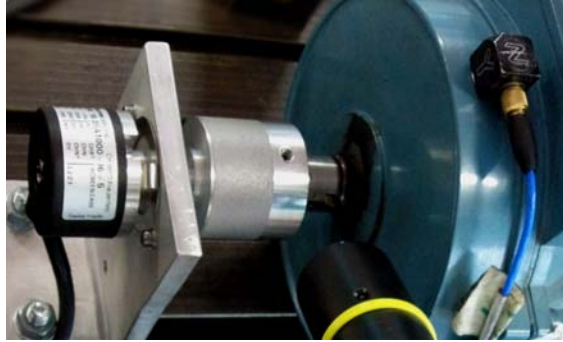


Fig. 2. Test setup: encoder 1000ppr, accelerometer PCB, 1kW 4 poles induction motor

2. EXPERIMENTAL RESULTS

In this paper, the IAS is compared to the vibration measurement obtained from accelerometer data . The motor used for the test is a 1kW 4 poles electric induction motor. It is driven by 50Hz line current 380V. The test was conducted without load in order to emphasize speed variations. The encoder has 1000 pulse per revolution (ppr) and its shaft is rigidly connected to the motor’s one. The encoder’s body is fixed at the baseplate through a spring. The accelerometer is a PCB 356A16 with the X axis in tangential, the Y in the axial and the Z in the radial direction. The acquisition system is based on National Instruments hardware. Analog signals are collected at 51.2kHz, while the encoder’s signal uses a 80MHz counter.

A MATLAB software does the necessary signal processing. Due to the motor type, the slip effect is present. It is possible to view this phenomenon in Fig. 3, where signals from an AC and a DC motor are compared. The main component of the signal is the electro-magnetic force seen by the rotor and its frequency is given by (4), where p is the number of poles, f_m is the mechanical rotational frequency and f_e is the electrical rotational frequency. In time/angular-domain, it appears as a shifting waveform due to the fact that there is a difference between the rotating speed to the magnetic field and the rotor. This effect doesn’t appear with synchronous or DC machines because mechanical and electrical speeds are synchronized.

$$f_e = \frac{f_m \cdot p}{1 - s} \Rightarrow o_e = \frac{1}{1 - s} \cdot \frac{p}{2} \quad (4)$$

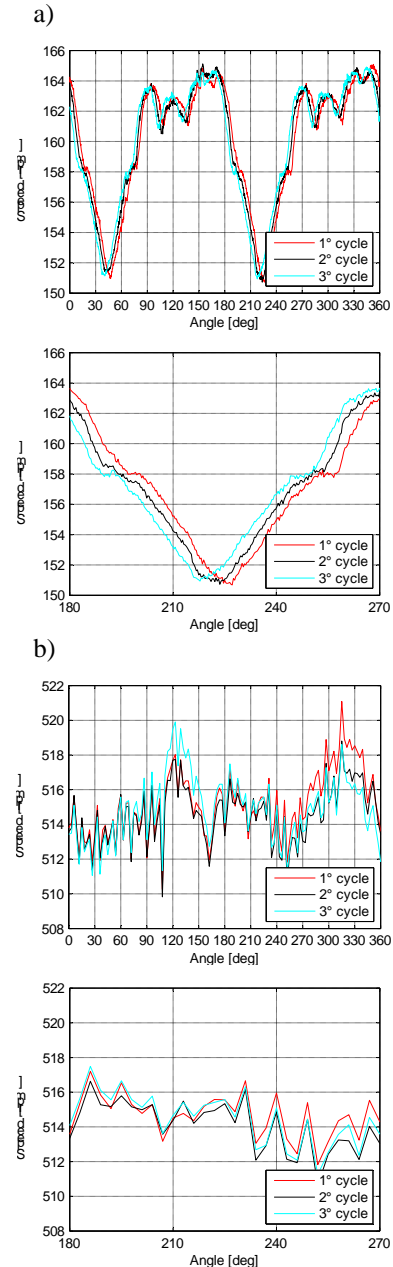


Fig. 3. Three cycles at 0-360° and zoom at 180-270°: a) AC motor, 150rpm, encoder 1000ppr, with slip effect; b) DC motor, 515rpm, encoder 120ppr, without slip effect

Table 1. Characteristic orders, bearing 6204-2RS1

Defect	Order
Bass Pass Frequency - BPFI	4.948
Inner	
Bass Pass Frequency - BPFO	3.052
Outer	
Fundamental Train FTF	0.382
Frequency (Cage)	
Ball Spin Frequency BSF	1.992
(Rolling element)	

The motor under test has a working history. The measurements present electric phase imbalance since the fourth order is dominant. The characteristic frequencies of the installed bearing (type 6204-2RS1) are listed in Table 1.

In order to compare the measurements from the encoder and the accelerometer, an order analysis is performed. To visualize the results the order domain is chosen. The encoder signal is already in the proper domain, while the accelerometer output needs an angular resampling. The comparison presents the IAS orders obtained with the ET of the 1000ppr encoder signal and the accelerometer signals resampled at 1000ppr. The encoder signal shows that at low order, the signal is good, while at higher order there is some quantization error, [André, et al - 2012]. The higher the speed, the bigger the quantization effect.

The order analysis from IAS and accelerometer data presents similar sidebands in the low order region. f_m is the mechanical frequency, f_e is the electrical supply frequency, f_s is the synchronous frequency and depends on the number of poles. The motor actual speed is 1497 rpm while the theoretical is 1500rpm. The slip (6) between the two is 0.002, that appears in the orders plot.

$$f_s = \frac{2f_e}{p} = \frac{2}{4} 50Hz = 25Hz \quad (5)$$

$$s = \frac{f_s - f_m}{f_s} = \frac{25 - 24.95}{25} = 0.002 \quad (6)$$

It is present an order 0.008 due to the slip and pole pass. In this case there are four poles, so pps is obtained in (7).

$$pps = p \cdot s = 4 \cdot 0.002 = 0.008 \quad (7)$$

Due to (4), the phase imbalance is present at $2o_e$, obtaining order 4.008, (9).

$$o_e = \frac{1}{1-s} \frac{p}{2} = \frac{1}{1-0.002} \frac{4}{2} = 2.004 \quad (8)$$

$$2o_e = 2 \cdot 2.004 = 4.008 \quad (9)$$

$$4o_e = 4 \cdot 2.004 = 8.016 \quad (10)$$

$$6o_e = 6 \cdot 2.004 = 12.024 \quad (11)$$

Figure 4 presents four plots around orders 2, 4, 8 and 12. Orders at slip frequency harmonics are shown. The 4.008 order has the highest amplitude. There are sidebands at 0.008 around each peak.

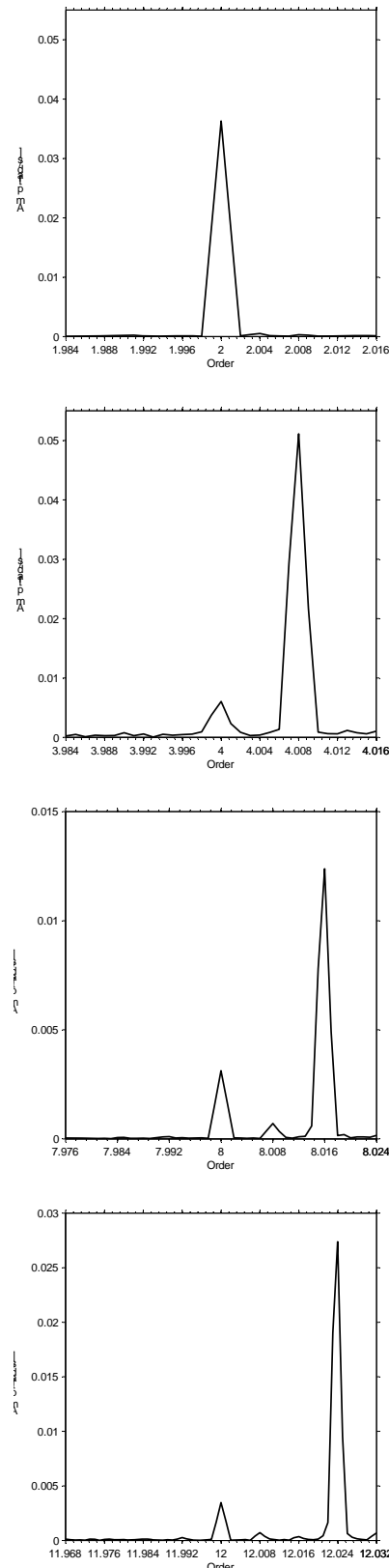


Fig. 4. IAS: slip order 2.004 and its harmonics 4.008, 8.016 and 12.024

Figures 5-7 show IAS plots from encoder's data in the first subplot, while in the following three, acceleration's data in the three directions are reported. Figure 5a presents the measurement from 0 to the maximum order (500), while Fig. 5b zooms from 0 to the 10 order. Encoder's main orders are 1, 2, 4.008, while acceleration's main orders are 1, 4.008 and 8.016. Figure 6 zooms around the fourth order where the 4.008 order appears in all signals. All the peaks are surrounded by sidebands at 0.008. These are more evident at higher orders, especially in accelerometer data. IAS also shows sidebands at FTF order 0.382. The same sidebands are present in accelerometer data, but at higher orders and the peaks are smeared. Other sidebands are present at order 0.064. These are related to the number of rotor bars, 32. Figure 7 zooms around the 8 order. The 8.016 order is shown and sidebands at 0.008 are present. The sidebands at 0.064 are not symmetrical.

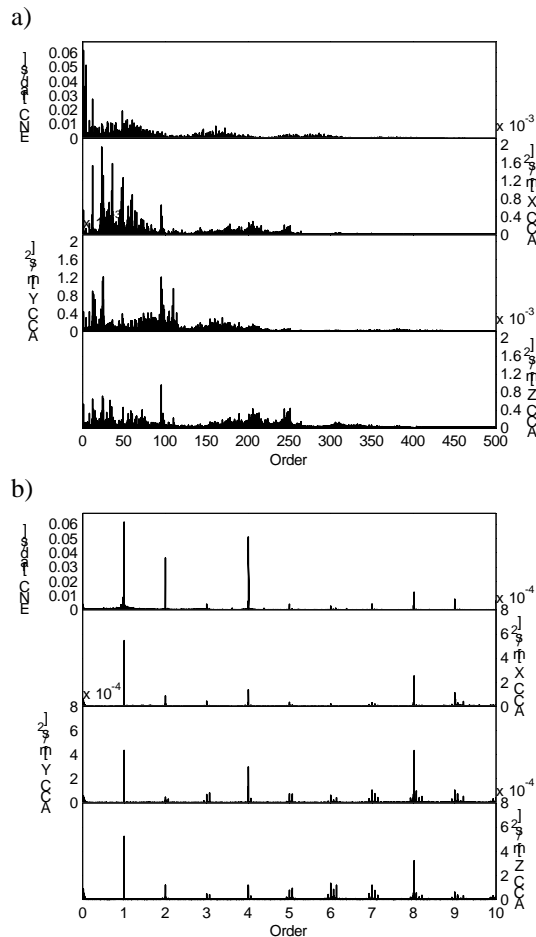


Fig. 5. IAS and accelerometer order analysis. The first subplot represents the encoder's data, while the three under are the accelerometer's data in X, Y, and Z directions. a) full scale plot, 0-500 order; b) zoom plot 0-10 order

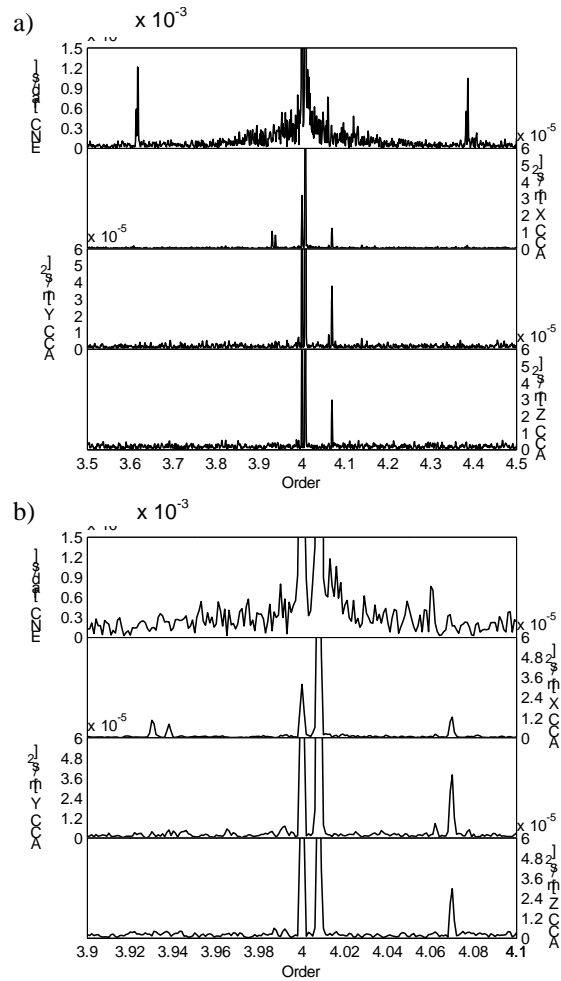


Fig. 6. IAS and accelerometer order analysis. The first subplot represents the encoder's data, while the three under are the accelerometer's data in X, Y, and Z directions. a) zoom plot, 3.5-4.5 order; b) zoom plot 3.9-4.1 order

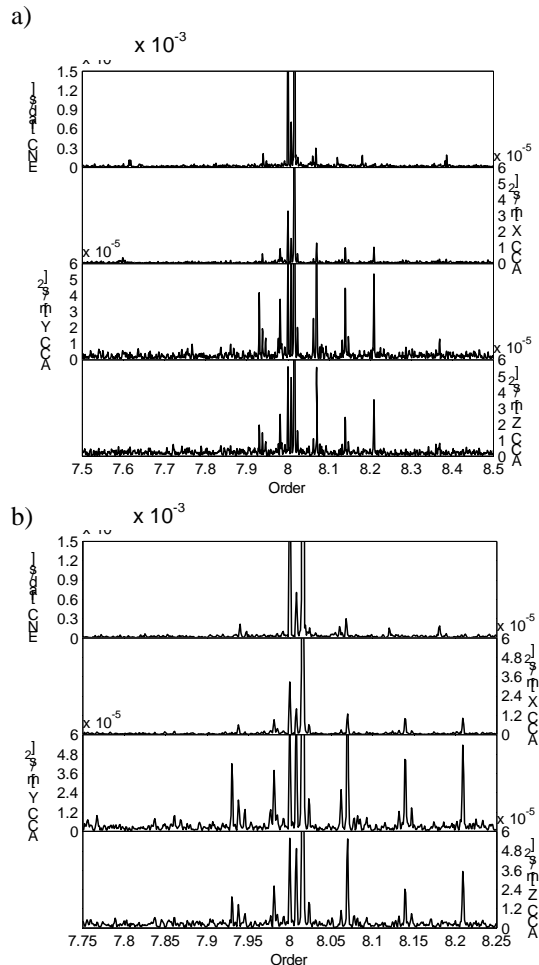


Fig. 7. IAS and accelerometer order analysis. The first subplot represents the encoder's data, while the three under are the accelerometer's data in X, Y, and Z directions. a) zoom plot, 7.5-8.5 order; b) zoom plot 7.75-8.25 order

3. CONCLUSIONS

This research shows the capability of IAS to identify FTF bearing defect. The electrical behaviour is the principal element of IAS order analysis, so the method can be used for diagnosis for electrical and mechanical defects. Further analysis has to be done to improve the signal processing technique but the comparison between IAS and acceleration measurements showed interesting differences.

Acknowledgements

This research is supported by Università degli Studi di Trieste, Nidec ASI S.p.A. and "Programma Operativo del Fondo Sociale Europeo 2007/2013 della Regione Autonoma Friuli Venezia Giulia".

References

- [1] André, H. Bourdon, A. Antoni, J. Remond, D. (2012). *Precision of the IAS monitoring system based on the elapsed time method in the spectral domain*. Proceedings of the International Conference on Noise and Vibration Engineering ISMA 2012, Belgium, pp. 1126-1142.
- [2] Li, Y. Gu, F. Harris, G. Ball, A.D. Bennett, N. Travis, K. (2005). *The measurement of instantaneous angular speed*. Mechanical Systems and Signal Processing, Vol. 19, no. 4, pp. 786-805.
- [3] National Instruments (2013). *Frequency Measurements: How-To Guide*. Tutorial 7111
- [4] Renaudin, L. Bonnardot, F. Musy, O. Doray, JB. Remond, D. (2010) *Natural roller bearing fault detection by angular measurement of true instantaneous angular speed*, Mechanical Systems and Signal Processing, Vol. 24, no. 7, pp. 1998-2011.
- [5] Resor, BR. Trethewey, MMW. Maynard, KPK. (2005). *Compensation for encoder geometry and shaft speed variation in time interval torsional vibration measurement*. Journal of Sound and Vibration, Vol. 286, no. 4-5, pp. 897-920.
- [6] Spagnol, M. Bregant, L. Boscarol, A. (2013) *Instantaneous Angular Speed: comparisons between Torsional Laser Vibrometer and Encoder-Counter estimations*. Proceedings of COMADEM2013.
- [7] Youssef, W. Guillet, F. Elbadaoui, M. (2011) *Characterization of counter technique for instantaneous angular speed measurement: Application on gear box signal*. Proc. of the ICS6, Université Technologique de Compiègne, France.

DIAGNOSTICS INVESTIGATIONS OF DMG-1A TRANSMISSION WITH OPERATIONAL MODAL ANALYSIS METHODS APPLICATION

Marcin ŁUKASIEWICZ, Tomasz KAŁACZYŃSKI, Michał LISS, Tomasz KASPROWICZ

University of Technology and Life Sciences, Faculty of Mechanical Engineering
Kaliskiego 7, 85-789 Bydgoszcz, Poland, e-mail: mlukas@utp.edu.pl
kalaczynskit@utp.edu.pl; mliiss@wp.pl; kasprowicz.tomasz@gmail.com

Summary

The modern engineering applications using virtual environment to simulating calculations conducting finds wider use in the process of projecting and structure dynamic analysis of machine engines and devices. Utilization of the modal analysis, aiming on the aid of transmission technical state description process brought to obtainment of three modal model parameters that describing the studied object. The analysis of results allowed to the qualification of characteristic modal parameters set for chosen technical state and introducing the natural frequency shapes for given modal model parameters of the studied mechanical construction. The LMS Test.Lab software with Modal Analysis Lite module was used for modal analysis. The results of investigations were a modal model parameters and mode shapes of investigated transmission.

Keywords: operational modal analysis, diagnostic inference

BADANIA DIAGNOSTYCZNE PRZEKŁADNI DMG-1A Z ZASTOSOWANIEM METOD EKSPLOATACYJNEJ ANALIZY MODALNEJ

Streszczenie

Metoda eksploatacyjnej analizy modalnej jest jedną z wielu technik wirtualnych wykorzystywanych w aspekcie diagnozowania maszyny i urządzeń. Istotną zaletą, szczególnie dla przemysłu jest fakt, że eksploatacyjna analiza modalna umożliwia identyfikację parametrów modelu modalnego jedynie w oparciu o pomiar odpowiedzi tego układu w trakcie eksploatacji. Podstawowym założeniem w tej metodzie jest to, że wymuszenie w trakcie pracy układu mechanicznego ma charakter losowy, a mierzony sygnał odpowiedzi układu na to wymuszenie jest niestacjonarny w czasie. W artykule przedstawiono metodę eksploatacyjnej analizy modalnej jako skuteczną formę diagnozowania maszyn. Przeanalizowano ponadto zachowanie się tej metody w przypadku wprowadzanych zmian do układu mechanicznego. Eksploatacyjną analizę modalną zastosowano do identyfikacji parametrów modalnych rzeczywistego układu mechanicznego jakim była przekładnia zębata DMG-1A.

Słowa kluczowe: eksploatacyjna analiza modalna, wnioskowanie diagnostyczne

1. Introduction

The development and progress of the human civilization is guided by the desire of difficult questions solving often connected with the varied fields of the science. However very often takes place the situation that introduced solutions are more difficult than on the beginning. In modern technical constructions this problems are also similar. From that reasons new devices and new diagnostics methods are developing which will be able to provide a valuable information about technical state of that products.

Vibroacoustics is one from these fields of the science which rise on the needs of diagnosing the current machine engines and devices technical condition. Using emitted vibrations, received during machine engine exploitation process as a valuable

information about dynamic properties drawing ahead machine and other aspects or possible relationships among them. The most valuable information about current machine engine technical state we could obtain during machine natural loads without disturbing this process. This kind of information obtainment is the basic domain of the technical diagnostics. Up to now an existing diagnostic procedures based on state symptoms slowly changes into diagnostics process based on machine engines models that describing their properties analysis.

Used in the diagnosing process models are identified basis on the real object investigative results. During diagnostics process we could create two kinds of diagnostic models: functional or structural. In diagnostics aspects of investigations, the structural models are more valuable, because they enable to show relations between current

elements of construction and model specific properties. The diagnostics procedure for structural model requires the identification guidance of the model parameters and monitoring of these parameters changes on the basis of measurements guided during exploitation. Therefore this relationship between individual parameters and pointed construction elements are the basis for estimation of current dynamic state of investigated machine. Periodical monitoring of this relationship may manage to detection, locating and evaluation of the waste stage or damages of given mechanical unit.

Nowadays one of the most known way to structural model creation of machine engines is modal analysis models utilization: experimental or operational modal analysis methods. The method choice depends on this what kind the input function character of the investigative object during the experiment has to have. Operational modal is the name for the technique to do modal analysis on operational data - cases where we do not excite the structure artificially but just allow the natural operating loads to excite the structure. Thanks to this during investigations we receive investigative data for real object working process in chosen measure points in relation to reference points.

Preparation process for diagnostics investigations in these methods contain measure and reference points disposal and also frequency range define. The advantage of this method in use to identification of objects dynamic profiles is shore conditions and loads retain that are characteristic for these objects exploitation. Basis on measured signals on the output of object received in chosen measure and reference points for unknown natural loads of the arrangement, the estimation of modal parameters is proceed. Modal poles and natural frequencies are identified ant then the mode shapes are estimated.

This way of parameters estimation could procure some doubt – we have to take it into consideration during final analysis. The biggest problem of this method is that we do not know the value of exciting force on the arrangement. The exciting forces with random character doesn't have one point of reaction on investigated mechanical structure so received exploitation forces structural schedule is unable to identification.

The more important is also fact that lots of machine engines used in industry cooperates with other technical objects, not necessarily with the same characters of dynamics loads. Best way to solve this problem will be separation from others machines the investigated machine engine. Unfortunately it refer with the machine engines working process stop so this action is unacceptable in this method usage. Disturbances triggered from next machine engines could causes the formation of additional poles on the created stabilization diagram.

2. Modal parameters estimation

In modal analysis we had two ways of modal model parameters estimation: in time and frequency domain. Time domain estimation basis on information from vibrations in time domain and arrangement response. Estimation of modal model parameters in frequency domain basis on the input and output signal spectrum

Nowadays during investigative process we often use the modal model estimation in frequency domain because there is possibility of limitation frequency range to this value in which we could recognize change of vibroacoustics signal during machine exploitation. The most valuable advantages of this method are:

- easiest possibilities of investigative data averaging which is used for noise reduction from signal,
- high precision of received results in case when exist an influence of vibration that lay behind of investigative range of vibrations,
- high precision of received results in case when is the high value of damping.

The frequency domain disadvantages are:

- the possibility of local minimum existence for signals with high noise level,
- the possibilities of troublesome mistakes connected with spectrum leak, existence of incorrect frequencies component in the signal and others.

Introduced below disadvantages and advantage of time domain modal model parameters estimation has similar sights to frequency domain, but this method is better in case, when we have to estimate:

- data with high level of noise,
- wide range of frequency during estimation.

It is also possible to use both of these methods in case, when we have measured vibrations in time domain booth from input and output source.

The LMS Test.Lab software with Modal Analysis Lite module was used for modal model poles estimation and analysis of mode shapes for multidegree arrangements with PolyMAX method.

PolyMAX method in frequency domain basis on the proper matrix formulation in frequency domain in shape:

$$[H(j\omega_f)] = [B][A]^{-1}, \quad [1]$$

where:

$[H(j\omega_f)]$ – FRF matrix with spectrum functions between all inputs m and all outputs l ,

$[B(j\omega_f)] = \sum_{k=0}^q [\beta_k] s_f^k$ – polynomial matrix numerator,

$[A(j\omega_f)] = \sum_{k=0}^q [\alpha_k] s_f^k$ – polynomial matrix denominator.

Marking of mode shapes of mechanical construction is connected with utilization of Least

Squares Frequency Domain (LSFD) method in frequency domain.

3. DMG-1A transmission investigations

The investigations of transmission DMG-1A were conducted in the investigative laboratory in UTP Bydgoszcz. During investigations mass and springily properties of transmission were analysed. The main parts of transmission were:

- commutated engine,
- spur gear transmission,
- toothed pump.



Figure 1. DMG-1A transmission [own picture]

DMG-1A transmission enable to provide measurement for chosen technical states. During investigations there were simulated four transmission cases:

- transmission in fit condition,
- transmission with broken tooth,
- transmission with skew axis,
- broken tooth and skew axis of transmission.

Figure no 2 presents the simulated technical state of transmission, when transmission is exploited with broken tooth.

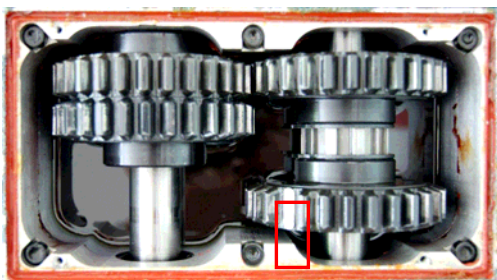


Figure 2. Transmission with the broken tooth [own picture]

Investigations were realized for three different rotation speed: (400, 600, 800 [min⁻¹]). Measure points were put on the bearing chassis of transmission. In each of measure points were realized measurements in three mutually perpendicular directions. Figure no 3 presents transmission DMG-1A geometrical model used for analysis with signal acquisition points.

The dynamic signal LMS SCADAS III recorder was used for signal acquisition. During investigations conducted 8 measuring sessions in which were recorded 13 signals of vibration acceleration, one of them was from reference point. The highest measure frequency range were definite

till 400 [Hz]. In case of proper qualification of measure frequency range for DMG-1A transmission investigations the preliminary measurements were conducted with use of the impulse input function for chosen construction areas.

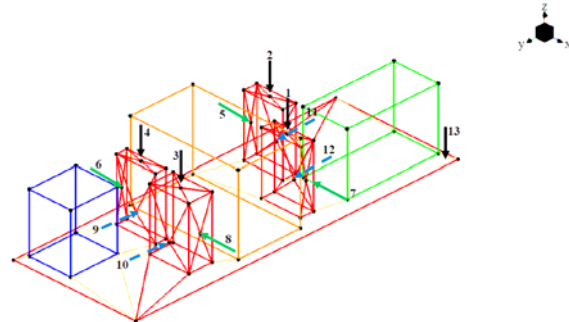


Figure 3. Transmission DMG-1A geometric model with mark of signal acquisition points [own source]

There were recorded per 300 seconds time response function with 512 [Hz] testing frequency. The essential aspect of the conducted investigative process was the proper modal model for the given construction technical condition obtainment. Observations of modal model individual parameters changes could enable to establish what influence of introduced changes call out in the construction through investigations in reference to transmission in fit condition. On figure no 4 were introduced respective stages of conducted investigations.

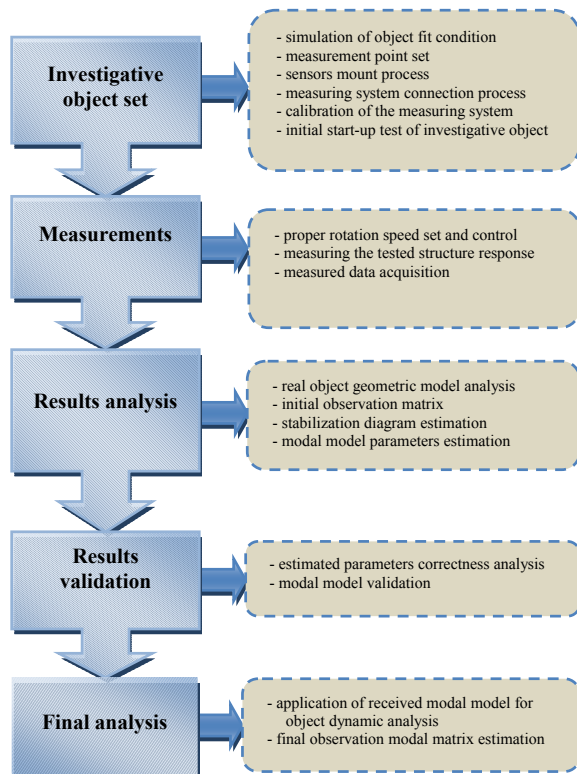


Figure 4. Respective stages of conducted investigations [own source]

It was decided during the experiment realization that measurement of time response courses will be

realized both for the input function and for the arrangement answer on this input function – this possibility will enable the estimated poles proving process in both (time and frequency) domain. For the proper data usage in Modal Analysis Lite module the recorded time response signals have to be transformed to the spectral figure (Crosspower) using Op. Data Collection module. Figure no 5 presents sample of Op. Data Collection module window during investigations.

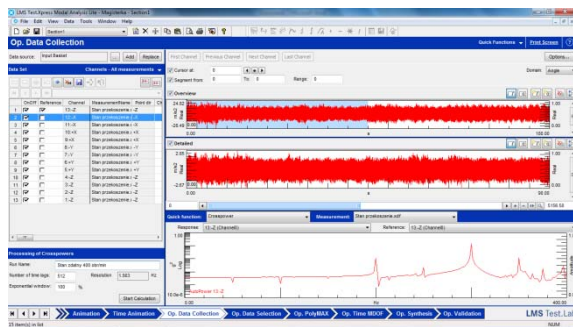


Figure5. Sample of Op. Data Collection module window during investigations [own source]

This data transformation enable to modal model estimation basis on stabilisation diagram analysis, where we mark order of modal model and damping factor for estimated natural frequency of object. Figure no 6 presents sample of stabilisation diagram with usage of PolyMax method during investigations for modal parameters estimation.

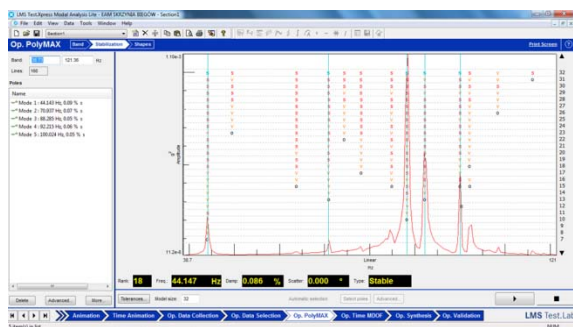


Figure6. Sample of stabilisation diagram with usage of PolyMax method used for results obtainment [own source]

Analysing individual simulated cases on the investigative transmission during investigation received set of stabilization diagrams, on which stable poles were mark. The stable pole marks parameters: frequency, modal damping and the mode shapes vector. The stabilization process ran with tolerance of individual modal parameters: 1% for frequency, 5% for modal damping and 2% for mode shapes vector. In such case as this, where the operational modal analysis is applied, there is only this mode shapes identification possibility which became sufficiently well extorted during the experiment identification.

Table no 1, 2 and 3 presents only the chosen part

of results received during modal identification of transmission for transmission with broken tooth for five sensors (the first one was reference sensor) after stabilization diagrams analysis.

Table 1. Observation matrix for transmission with broken tooth for 400 min⁻¹ rotation speed

Transmission with broken tooth			
Point	Rotation speed [min ⁻¹]		
	400		
	Natural Frequency [Hz]	Damping factor [%]	Modal model Order
C1-reference point	49,916	0,57	9
	100,295	0,65	11
	199,925	0,05	9
	250,888	0,75	12
	299,966	0,01	12
	371,516	1,23	24
	384,296	2,15	8
C2	49,916	0,57	9
	100,295	0,65	11
	199,925	0,05	9
	250,888	0,75	12
	299,966	0,01	12
	371,018	1,02	20
	383,860	2,15	11
C3	49,916	0,57	9
	100,295	0,65	11
	199,925	0,05	9
	250,888	0,75	12
	299,966	0,01	12
	372,020	1,17	26
	382,921	1,72	19
C4	49,916	0,57	9
	100,295	0,65	11
	199,925	0,05	9
	250,888	0,75	12
	299,966	0,01	12
	372,029	1,21	23
	382,921	1,72	19
C5	49,916	0,57	9
	100,295	0,65	11
	199,925	0,05	9
	250,888	0,75	12
	299,966	0,01	12
	372,029	1,21	23
	384,296	2,15	8

Table 2. Observation matrix for transmission with broken tooth for 600 min⁻¹ rotation speed

Transmission with broken tooth			
Point	Rotation speed [min ⁻¹]		
	600		
	Natural Frequency [Hz]	Damping factor [%]	Modal model Order
C1-reference point	20,628	0,93	21
	50,070	0,75	19
	99,889	0,15	14
	199,898	0,01	14
	299,875	0,01	19
	370,101	2,96	10
C2	20,628	0,93	21
	50,070	0,75	19
	99,889	0,15	14
	199,898	0,01	14
	299,875	0,01	19
	370,628	2,90	7
C3	20,628	0,93	21
	50,070	0,75	19
	99,889	0,15	14
	199,898	0,01	14
	299,875	0,01	19
	370,628	2,96	10
C4	20,628	0,93	21
	50,070	0,75	19
	99,889	0,15	14
	199,898	0,01	14
	299,875	0,01	19
	370,628	2,96	10
C5	20,628	0,93	21
	50,070	0,75	19
	99,889	0,15	14
	199,898	0,01	14
	299,875	0,01	19
	370,628	2,96	10

On the basis of results introduced in tables we could conclude, that with growth of transmission rotation speed the number of estimated stable poles and recognised natural frequency decrease. The proper recognition of stable poles has influence directly on the respective mode shapes of construction. Under introduced figures presents most interesting mode shapes of transmission recognized during investigations, that shows more important construction properties. Comparing got results and individual mode shapes were noticed the change of all modal parameters. In case of modal model parameters manifested itself by natural frequency and damping factor value change. The transmission with broken tooth case is the best example for analysis of damping factor and suitable natural frequency value increase changes. The mode shapes change analysis is also valuable tool for construction analysis between all simulated transmission conditions that will marks the differences for all

estimated natural frequencies. For example the figure no 7 present a sample of mode shapes visualization for transmission in fit condition, in which all estimated shapes has very similar character of movement. In this case of mode shapes, we could recognize only the movement of bearings casing.

Table 3. Observation matrix for transmission with broken tooth for 800 min⁻¹ rotation speed

Transmission with broken tooth			
Point	Rotation speed [min ⁻¹]		
	800		
	Natural Frequency [Hz]	Damping factor [%]	Modal model Order
C1-reference point	100,013	0,37	21
	199,948	0,01	8
	299,931	0,08	22
	372,545	2,23	11
C2	100,013	0,37	21
	199,948	0,01	8
	299,931	0,24	22
C3	100,013	0,37	21
	199,948	0,01	8
	299,931	0,01	22
C4	100,013	0,37	21
	199,948	0,01	8
	299,931	0,28	22
C5	100,013	0,37	21
	199,948	0,01	8
	299,931	0,89	22

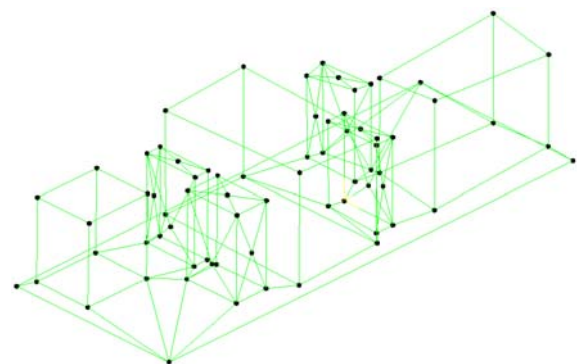


Figure 7. Mode shapes visualization for 49,917 [Hz] frequency for 400rpm [own source]

In case of transmission with broken tooth, the most important marked natural frequency was 384,296 [Hz] and their visualization. The extreme movement of mode shapes for this frequency present figure no 8.

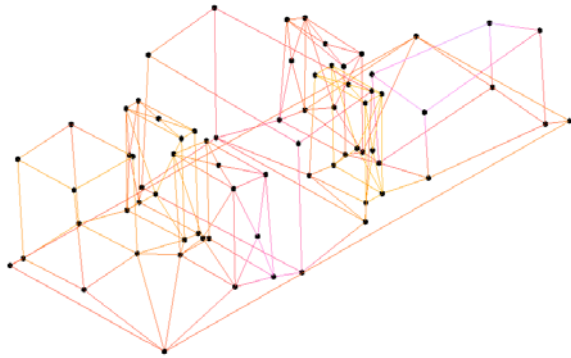


Figure 8. Mode shapes visualization for 384,296 [Hz] frequency for 400rpm [own source]

Only one broken tooth in DMG-1A transmission caused significant change for all mechanical arrangement. The most visible was the specific deformation of bearing casing in direction of axis x , on which was situated shaft with broken toothed gear. The estimated mode shapes for frequency 384,296 [Hz] has bend phenomena.

In case of transmission with skew axis simulations the most important marked natural frequency was 49,716 [Hz] that has most complex phenomena. This frequency has shapes with swirl and bend phenomena on this transmission construction. Figure no 9 present estimated mode shapes visualization for transmission with skew axis simulations.

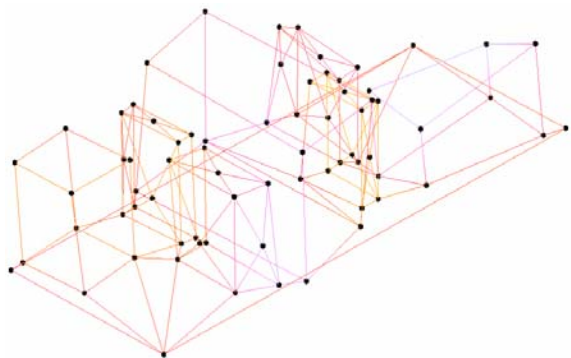


Figure 9. Mode shapes visualization for 49,716 [Hz] frequency for transmission with skew axis for 400rpm [own source]

In case of simulation of broken tooth and skew axis of transmission, two most important natural frequencies were recognized – each for one simulated damage of transmission. The first natural frequency 374,400 [Hz] in case of gear with broken tooth and the second frequency 379,022 [Hz] in case of skew axis of transmission.

The most important aspects of these diagnostics investigations is facts, that all marked natural frequencies are directly connected with simulated technical state and they are not marked for transmission in fit condition. This testifies about this, that in case of appearing damage in the transmission the completely new natural frequency

appears in stabilization diagram, that is directly connected with specific kind of simulated damage. Also interesting phenomena is fact, that the mode shapes descend from transmission toothed gear damage is strictly connected with damping factor value increasing. In this case of mode shapes, the average value of damping factor has value in range from 2,07 [%] till 2,23 [%]. The average value of damping factor for other estimated mode shapes has value in range from 0,01 [%] till 0,93 [%].

4. Conclusions

The results of investigations were a modal model parameters and mode shapes estimations of complex mechanical object and structures basis on transmission DMG-1A investigations example. The most important natural frequencies and mode shapes were recognized. The sample results were introduced in tables and figures. As a final results we obtain the dynamic state description of real technical object with estimation of predominant properties of natural frequency and mode shapes.

The advantage of this method is fact that investigated object could be recognized during normal process of exploitation and modern engineering applications using virtual environment to simulating calculations lowering costs of investigations with higher precision of estimated results basis on real data measured during exploitation.

This paper is a part of investigative project WND-POIG.01.03.01-00-212/09.

REFERENCES

- [1] Heylen W., Lammens S., Sas P.: *Modal Analysis Theory and Testing*, Katholieke Universiteit Leuven, Heverlee 2007.
- [2] Kurowski P.: *Badanie modeli modalnych fundamentów dużych maszyn energetycznych*, Diagnostyka, 2006, Vol. 4, No. 40, pp. 119-126.
- [3] Łukasiewicz M., 2010: *Vibration measure as information on machine technical condition*, Studies & Proceedings of Polish Association for Knowledge Management 35, ISSN 1732-324X, Bydgoszcz.
- [4] Łukasiewicz M, Kałaczyński T, Liss M.: *Zastosowanie metody MDOF oraz PolyMAX w badaniach stanu skrzynek przekładniowych*, Inżynieria i Aparatura Chemiczna 3/2012 (s.70-73), Bydgoszcz 2012r.
- [5] Łukasiewicz M., 2010: *Vibration measure as information on machine technical condition*, Studies & Proceedings of Polish Association for Knowledge Management 35, ISSN 1732-324X, Bydgoszcz.
- [6] Uhl T.: *Komputerowo wspomagana identyfikacja modeli konstrukcji*

mechanicznych, Wydawnictwo Naukowo – Techniczne, Warszawa 1997.

- [7] Żółtowski B., Łukasiewicz M.: *Diagnostyka drganiowa maszyn*, ITE Radom, Bydgoszcz – Radom 2012, ISBN 978-83-7789-138-4.



Marcin ŁUKASIEWICZ PhD is an assistant in Department of Vehicle and Diagnostics at Bydgoszcz University of Technology and Life Science.

In the scientific work deal with the problems of the dynamics of machine engines, vibroacoustics problems, modal analysis theory and modal investigations, the technical diagnostics and the questions of building and the exploitation of mechanical vehicles.



Tomasz KAŁACZYŃSKI PhD is an assistant in Department of Vehicle and Diagnostics at Bydgoszcz University of Technology and Life Science.

In the scientific work deal with the problems of the dynamics of machine engines, vibroacoustics problems, cars construction and exploitation, the technical diagnostics and the questions of building and the exploitation of mechanical vehicles.



Michał LISS MSc is a technician in Department of Vehicle and Diagnostics at Bydgoszcz University of Technology and Life Science.

In the scientific work deal with the problems of the dynamics of machine engines, vibroacoustics problems and the exploitation of mechanical devices.



Tomasz KASPROWICZ BSc is a technician staff in Department of Vehicle and Diagnostics at Bydgoszcz University of Technology and Life Science.

SYSTEM OF GEOMETRIC PARAMETERS MONITORING DURING CUTTING OF STEEL PLATES PROCESS

Jerzy KWAŚNIEWSKI¹, Józef GRZYBOWSKI², Damian KORDOS²

¹ AGH University of Science and Technology in Kraków
Faculty of Mechanical Engineering and Robotics, Department of Rope Transport

² Rzeszów University of Technology
Faculty of Mechanical Engineering and Aeronautics, Department of Avionics and Control Systems
e-mail: jozef.grzybowski@pilc.pl

Summary

The steel plate cutting is performed on a special production lines to enable longitudinal and lateral cut. Input material is usually a metal ring of weight about 32 tons. The cutting process is preceded by an operation of straightening the cutting section. So far, during this operation parameters such as wave cut off sheets, the thickness of the material were not monitored. This paper presents a system of continuous monitoring of sheets parameters constructed by the authors. It was mounted on the process line-cutting and slitting of one of the companies cutting sheet metal. Such approach allows to improve quality control.

Keywords: diagnostics, steel plate cutting.

SYSTEM MONITOROWANIA PARAMETRÓW GEOMETRYCZNYCH PODCZAS CIĘCIA BLACH STALOWYCH

Streszczenie

Proces rozkroju blach stalowych wykonywany jest na specjalnych liniach technologicznych umożliwiających cięcie poprzeczne oraz wzdłużne. Materiałem wejściowym jest zwykle krąg blachy o wadze ok. 32 ton. Operacja cięcia poprzedzona jest procesem prostowania przy rozkroju poprzecznym. Dotychczas przy wykonaniu tej operacji nie monitorowano parametrów rozkroju takich jak falistość uciętych arkuszy, grubość materiału. W pracy przedstawiono wykonany przez autorów system ciągłej kontroli parametrów blachy. Został on zamontowany na linii technologicznej cięcia poprzecznego oraz cięcia wzdłużnego w jednym z przedsiębiorstw rozkroju blach. Zastosowanie powyższego rozwiązania umożliwiło poprawę kontroli jakości produkcji.

Słowa kluczowe: diagnostyka, cięcie blach stalowych.

1. INTRODUCTION

The process of cutting steel sheets takes place on the special process lines in order to enable longitudinal and transverse shearing. Usually, the process starts with introducing a coil of 32 tons. The cutting process is preceded by straightening, especially in case of transverse shearing. At this point, parameters of cuttings, sheets corrugation, metal thickness and its level of crescent shape were not examined. Presented in this paper, the system of constant monitoring of sheets parameters was installed on transverse and longitudinal cutting lines. Measurements of thickness, corrugation and the level of crescent shape of a sheet, performed by laser transducers is linked to the system of production process monitoring.

2. ANALYSIS OF METAL ROLLING DEFECTS

Minor defects of surface which result directly from rolling, but do not influence parameters of the final product are accepted. It refers to the top side of sheets or the outside of coils. Physical and technological properties should suit requirements given in the PN-EN 10025:2002.

Sheet surface defects include:

- surface defects – the surface of the rolled metal should contain no cracks, blisters nor tears, remains of the shrinkage cavity, delamination and cracks which are visible to the naked eye are not acceptable,

- surface defects such as cracks, minor scales and overlapping, non-metallic inclusions, corrosion pits, bulging, dents, mill scales and roughness are acceptable on condition that:

- they do not exceed deviation limits,

- they do not exceed 0,5 mm for 25 mm thick coils, 0,7 mm for thicker coils.

Moreover, it is important to determine the longitudinal and transverse corrugation of the initial material and cut sheets.

Rolling defects always result from differences of sheet thickness and its width. This difference defines zones of tension which seem flat and zones of bumps which resemble a kind of 'pocket' folds. Through constructing rollers it is possible to form working rolls in order to press their longitudinally fibre-pulled parts so that they are pushed to the free zones.

Depending on the place in which 'pockets' are, rollers are precisely set in

a specific way. It must be always checked whether the end line does not have a double tail. Entering material into the straightening machine may damage straightening rolls. Figure 1 shows the screen of the system which controls the rollers power and allows removing sheet waves. Figures 2-5 illustrates forms of transverse waviness.

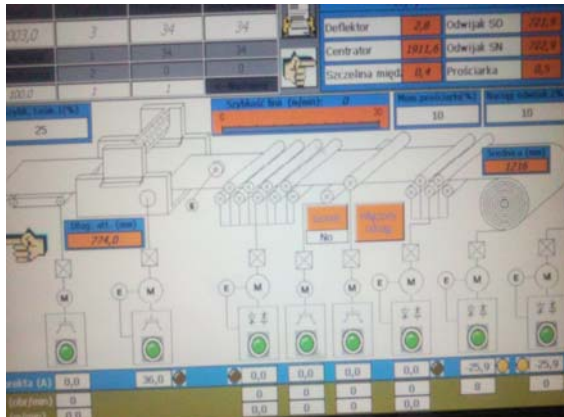


Fig.1. Screen of the system which controls the rollers power enabling the removal of sheet waviness

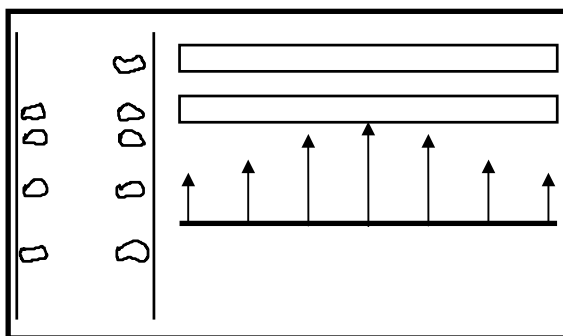


Fig.2. Outline of side wave formation process

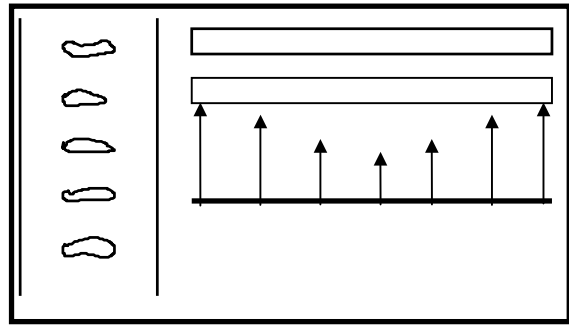


Fig.3. Outline of central wave formation process

The above-mentioned wavy parts of sheets are removed through pressing them by rollers set in so-called negative parabola.

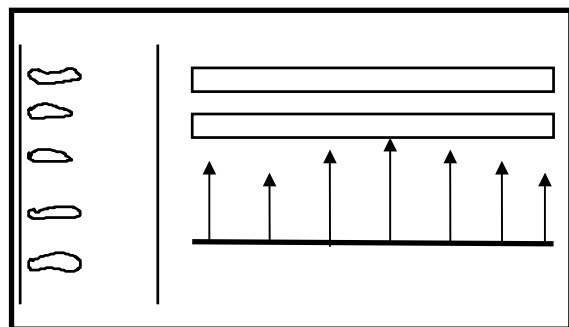


Fig. 4. Outline of one-sided wave formation process

Straightening of this wave is possible by lowering down rollers in the deformed areas

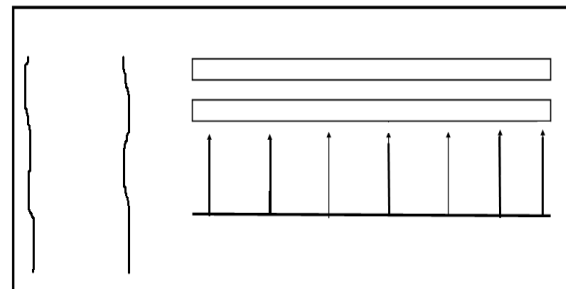


Fig. 5. Outline of the longitudinal waviness

3. MEASUREMENTS OF SHEET PARAMETERS ON THE TRANSVERSE CUTTING LINE

Within this process of monitoring sheet parameters system, measurements of sheet thickness and waviness of its surface had to be separated. Measuring devices were installed in two different places.

Waviness measurement of the sheet 1 which was from 250 to 2050mm wide is performed on the transporting table 2 (fig. 6). Measurement is recorded by two detectors 5 located around 50 mm from the edge of the sheet. Detectors are

automatically spaced according to the set sheet thickness with the aid of the drive 6. Detectors 5 are located on trucks 4 moving on the lead 3. The sheet waviness is examined with reference to the laid down criterion of a given sheet thickness. The sheet which does not fulfill the criterion is classified as the one of lower quality.

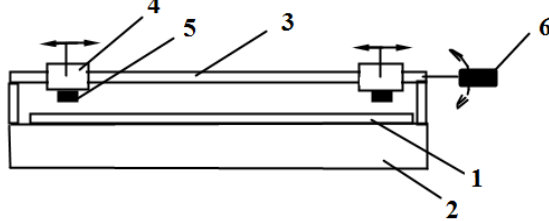


Fig. 6. Outline of the sheet waviness measuring machine

Waviness measuring is constantly recorded and accompanied by its simultaneous graphic and sign presentation. Thickness measuring is recorded by detectors located in the differential gear in the place the most convenient because of the risk of unexpected transverse vibrations of the sheet (especially at the end of the unrolling sheet). Figure 7 illustrates the measuring system installed on the transverse cutting line.



Fig. 7. Waviness measuring system on the transverse cutting line, on the right carriage from the wired side

A special rail protecting detectors against bumps of the end of cut sheet was installed on the line. The monitoring system of sheet transverse cutting is based on the independent measuring system with the parameters presentation seen on a separate screen. The screen shown on the figure 8 presents digital information of the thickness parameter and under it the waviness parameter of the left side, then the one of the right side. Measurement of waviness is performed at the individual programmed distance for sheets, usually it is 50 mm. Differences between measurement points of waviness and thickness cause a delay of thickness parameters comparing to the waviness ones resulting from the distance between detectors. On the right side of the screen (fig. 8) operators' identifiers and parameters of the working material. When the programmed tolerance threshold are exceeded, numbers become red and a red column signaling device is activated (optionally with the sound information).

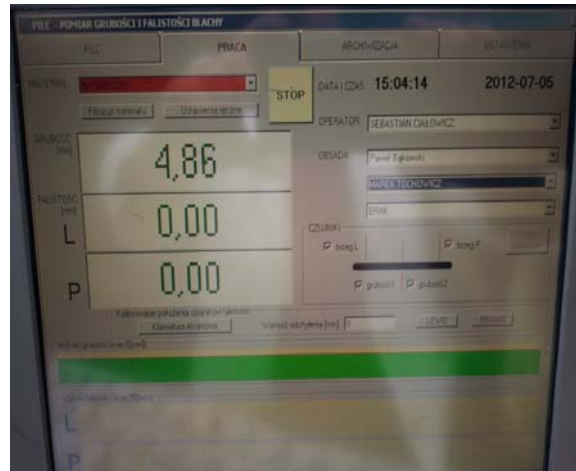


Fig. 8. Screen of the thickness and waviness measuring system

Figure 9 shows the location of transducers for the differential measurement of sheet thickness.

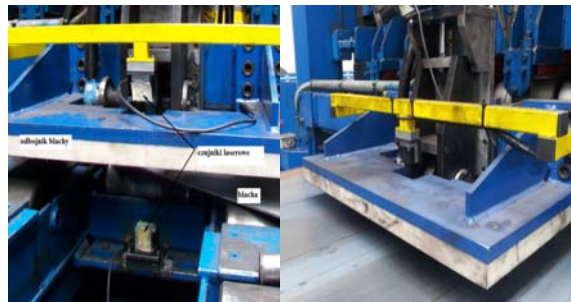


Fig. 9. Measuring system of sheet thickness

Laser transducers of LD type OMRON company, starting signals of which are initially processed by a single-integrated circuit microcomputer. Within waviness measuring system, the same computer is responsible for the control of trucks locating laser transducers. Computer data are transferred through the interface RS485 to the controlling computer storing data and monitoring sheet cutting process. On the touchscreen (fig. 10), important changes of initial parameters may be done as well as they can be observed while being measured.



Fig. 10. Location of the measuring system screen (in the middle)

4. MEASURING SHEET PARAMETERS ON THE LONGITUDINAL CUTTING LINE

Straightness measurement (the sheet is longitudinally wavy which needs to be specified before longitudinal cutting) is performed after straightening unrolling line. A technical system in accordance with the patent 185472 entitled „Device measuring straightness of moving and/or fixed” was implemented on this line; it uses a projection device and a slider with a measuring detector moving along the object 1 (of a cut sheet) where straightness of the latter is measured.

Within the implementation of the above-mentioned technical system described in the patent, the projection device which constitutes a straightness model (fig.11) consists of a fixed axis 2 with a ball screw; on the axis there are sliders 3 with measuring detectors 5 moving along the cut sheet 1. A step motor was used as a drive. The location of sliders depends on the width of the sheet, and detectors measure the straightness of the sheet thanks to the implementation of an appropriate measuring system. As detectors, measuring strips 5 can be used, they consist of magnetic circuit, a keeper of which is fixed and connected with the slider 3 and active elements (magnetic field detectors) are located above the projection device 2 in the air slit 6 situated between permanent magnets and connected to the keeper. The measuring strips connected with the slider through elastic elements protecting against possible vibrations which occur during sheet cutting process.

During the measurement, measuring magnetic circuit which consists of permanent magnets, keepers and the air split goes along the examined edge of the sheet and simultaneously moves along the projection device. The magnetic field detector functions as a measuring element; it measures transverse movement of the magnetic circuit depending on the sheet waviness.

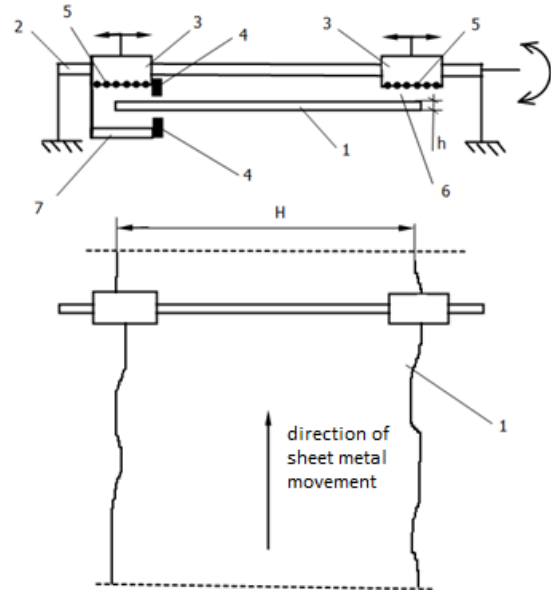


Fig.11. Outline of the adopted technical system

The use of this device will enable to eliminate segments of sheet strips of undesired thickness and the ones which do not satisfy longitudinal waviness edge requirements.

5. PROGRAM SOLUTIONS APPLIED IN PARAMETER MEASUREMENTS IN THE ASSEMBLY LINE

Software enabling permanent measurement of both the thickness and waviness is used in the parameter measurements in the assembly line. Data shown on the screen of the controlling computer are presented in the alphanumeric form as well as diagrams of the thickness and two waviness detectors (fig. 12).

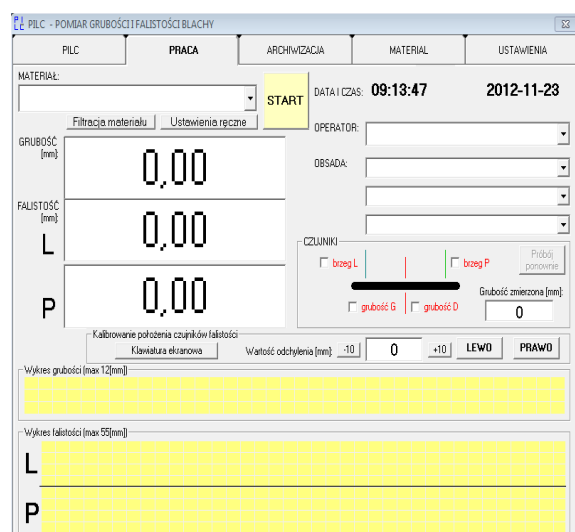


Fig. 12. Main window of the measuring program on the transverse cutting line

In order to quickly space measuring devices, the program uses the data base about sheet metal. The data may be changed and extended by workers responsible for the process. In order to enter data more quickly, the automatic generation of tolerance values calculated on the basis of entered sheet parameters can be applied (fig. 13).

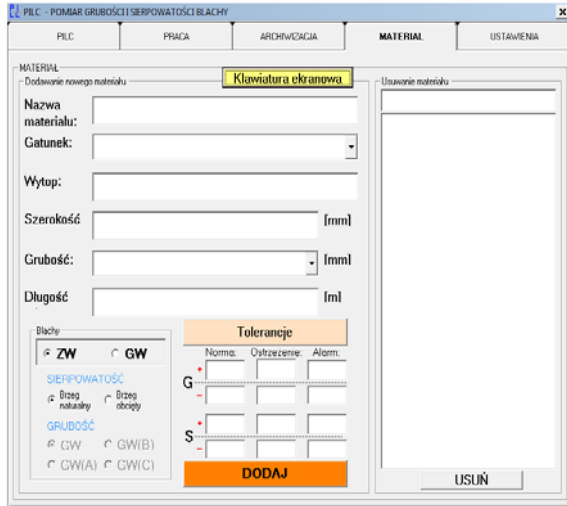


Fig. 13. Tab enabling the material base management

Moreover, workers team responsible for the process is also recorded. All information registered by detectors, including data of the working material and workers responsible for the process is stored on the controlling computer. The archive is saved in *.xls files which allows to see quickly data, and with the use of MS Office scripts it is possible to generate immediately diagrams of both the waviness (fig. 14) and the thickness of a given sheet.

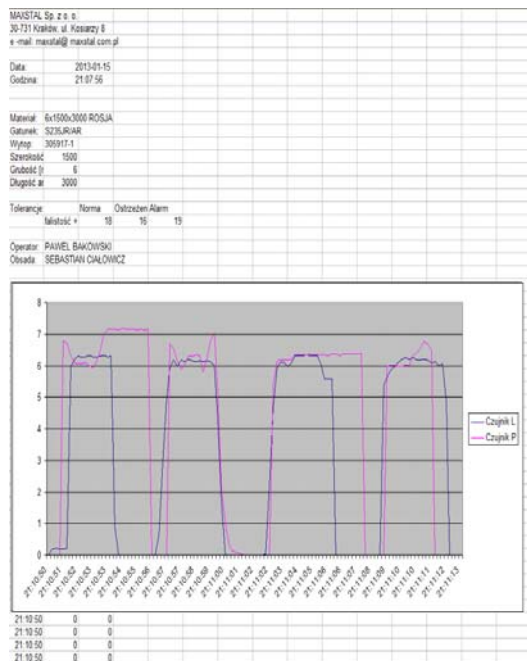


Fig. 14. Example excerpt from the waviness diagram

The access to saved data can be direct on the computer responsible for the process, through the user's interface (fig.15) or indirect through the LAN network.

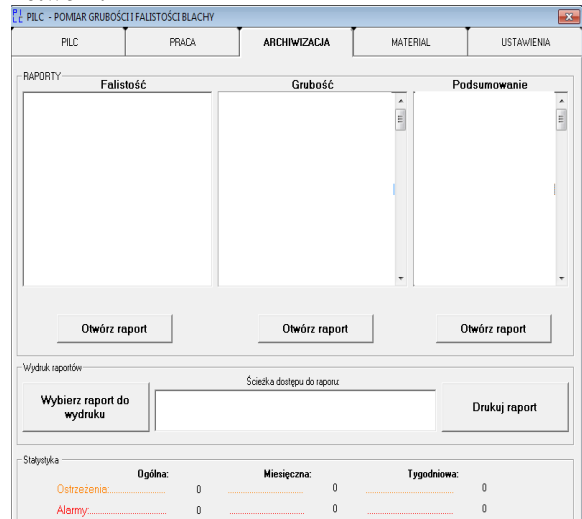


Fig. 15. User's interface enabling archive checking

The quick access from any computer connected with the network is possible thanks to the program attached which additionally renders the management of the working sheet base possible (fig. 16).

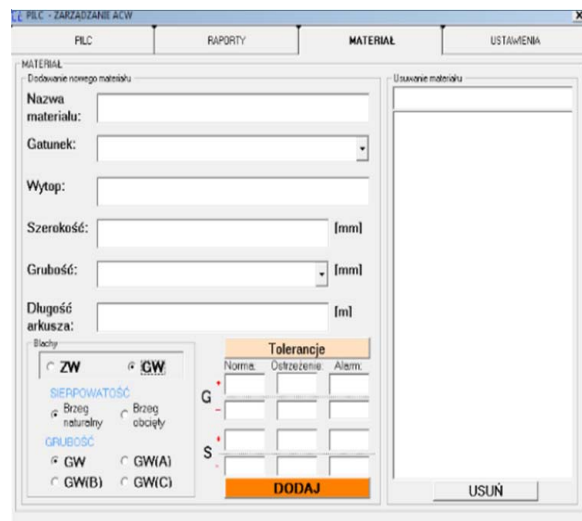


Fig. 16. Tab to manage the material base from computers connected to the LAN network

6. CONCLUSION

The measuring system of sheet parameters on the transverse and longitudinal cutting that has been designed and constructed functions as an independent product quality control system. The implementation of the automatic control and reporting is the basis for the introduction of the quality management. At the stage of improving metrological characteristics of the system, it was indispensable to use the system of program filters adjusted specially to the

confounders. Recursive filters with selectable factors which include: material type, vibration level and sampling frequency were used as basic filters. The acquisition of greater knowledge thanks to the examined process will enable further improvement of the program tools.

#



**Prof. Jerzy
KWAŚNIEWSKI, PhD
Eng.**

Professor at Rope Transport
Department at AGH
University of Science and
Technology in Kraków.



**Józef GRZYBOWSKI, PhD
Eng.**

Assistant professor at
Department of Avionics and
Control Systems at Rzeszow
University of Technology.



Damian KORDOS, M. Eng.
Assistant at Department of
Avionics and Control
Systems at Rzeszow
University of Technology.

GSM LOCALIZATION AND MONITORING IN ELECTRONIC TRANSPORT SECURITY SYSTEMS

Tomasz CIECHULSKI

Instytut Systemów Elektronicznych, Wydział Elektroniki
Wojskowa Akademia Techniczna, ul. Kaliskiego 2, 00-908 Warszawa
tciechulski@wat.edu.pl

Summary

The article contains survey and analysis of electronic security systems used in the public transport. The systems are based on comprehensive approach to many security issues such as monitoring (e.g. railway station), access control (e.g. access to service rooms of railway station), GPS tracking (e.g. private or service car), fire protection systems (e.g. passenger train), wireless alarm signals transmission through GSM modules (e.g. car anti-theft systems).

Keywords: security systems, video monitoring, transport, CCTV, GSM.

LOKALIZACJA GSM I MONITORING WIZYJNY W TRANSPORTOWYCH ELEKTRONICZNYCH SYSTEMACH BEZPIECZEŃSTWA

Streszczenie

Artykuł zawiera przegląd i analizę systemów zabezpieczeń opartych na lokalizacji GSM i monitoringu wizyjnym, wykorzystywanych w środkach transportu. Systemy te charakteryzują się kompleksowym podejściem do problematyki bezpieczeństwa. Obejmują one monitoring (na przykładzie zastosowania na dworcu kolejowym), kontrolę dostępu (w przypadku dostępu do służbowych pomieszczeń dworca kolejowego), namierzanie GPS (w przypadku samochodu prywatnego lub służbowego), a także transmisję sygnałów alarmowych drogą bezprzewodową poprzez moduły GSM (w przypadku systemów zabezpieczających przed kradzieżą samochodu).

Słowa kluczowe: systemy bezpieczeństwa, monitoring, transport, telewizja przemysłowa, GSM.

1. INTRODUCTION

Current state of the telecommunication solutions and satellite navigation allows to use the integrated network services based on determining the position of vehicles and trains in real time. It also allows to control and automatic supervision of the state of the cargo. Traffic telecommunication is very important factor of effective control systems of vehicles and trains.

Positioning system allows to observe the vehicles routes, searching vehicles, and changing the strategy or their destinations. Continuous monitoring gives important information in case of theft, change of logistic decisions or in the event of unexpected difficulties in traffic. The main receiver of such services are: transport industry and national railways where the information received from monitoring systems are connected directly with the company operating income.

Localization system is also very helpful in managing the transport of dangerous or very valuable cargo, limiting the risk of traffic disaster, thefts, and helping to localize the vehicle in case of theft. Effective response in real time to events such

as disruptions in planned routes is important not only because the optimal use of trains but more likely because the security of transport.

Availability of satellite monitoring and localization of the vehicles in every place and time has significant value wherever there is poor infrastructure and many roads are in bad condition, for example in Poland and other countries of Eastern Europe.

It is very important that systems to be created in the future will be available to localize the vehicles and to transmit data, basing on the Global System for Mobile Communications (GSM). In the same time they could be reliable source of information about location of companies' objects [3].

2. GSM TERMINAL LOCALIZATION USED IN ALARM SYSTEMS

TDoA¹ is one of methods which manages to determine the subscriber localization with big accuracy. It relies on terminal localization which is

¹ Time Difference of Arrival.

determined as a source of electromagnetic waves. The time of propagation of the signal measured in different positions is compared to each other. It is required that the subscriber terminal should be at range of at least three BTS's² equipped with a time measure device.

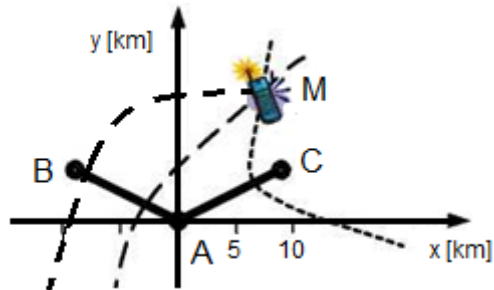


Fig. 1. Determination of electromagnetic wave source position. (M – emission source, A, B, C – BTS).

Station A is the master, and stations B, C are slaves. In this case, the differences between times of signal propagation to the stations can be determined as follows:

$$\Delta t_{Aj} = \frac{1}{c} (R_{jM} - R_{AM}) \quad (1)$$

where:

$j = B$ or C ;

R_{jM} – distance between emission source to B or C;

R_{AM} – distance between emission source to A;

$c \approx 3 \cdot 10^8$ m/s (velocity of electromagnetic wave).

Distance differences can be stated as follows:

$$\Delta R_{Aj} = R_{jM} - R_{AM} \quad (2)$$

The TDoA method also known as reverted hyperbolic system, is characterized by good accuracy, despite of using antennas with non-directional characteristics. Theoretical model of this thread assumes that signals transmitted by the source reach the i th transceiver after time t_i . Measured time t_i is not very useful at that time. The parameters used in the TDoA method is the difference between times of signal propagation between pairs of stations. And that differences give information which is used to forward signal processing.[1]

According to fig. 1 the following devices need to be added to Base Transceiver Stations: block of the time standard, receiver and the sampling module for received signal. Output product of added block is precisely marked sequence of signal samples transmitted by terminal and received by the BTS. This information can be transmitted forward to the TDoA processor localized inside or outside any BTS. Compared sequences of time samples in

the processor could determine time differences of their arrival and on this basis the precise location of terminal is possible. This data can be transmitted to the monitoring centre where they can be implemented on digital maps.

3. VISION MONITORING IN RAILWAYS

The development of technology allowed to connect the cameras with computer networks in direct way. According to this there are wide possibilities of watching images from camera located in very different localizations from whichever camera by using any computer connected to the network in any place in the world (we can use PC or laptop). The network camera has network interface and has assigned its own IP address.

IP monitoring is the kind of technology designed especially for new-built installations. While in small, local monitoring systems there will be built systems based traditionally on digital record on hard disks, insomuch that in large systems, in diffuse objects, in new-built houses with modern structure of teletechnical communication installations there is need to imply monitoring based on CCTV³ IP technology. The usage of monitoring inside the network based on TCP/IP protocol gives widespread possibilities of organizing large and extensive installations.[9]

One of many international companies constructing monitoring systems, integrates under its services more than 290 monitored buildings spread in 60 countries. In this installation there is more than 2700 cameras working condensed in one system.

In such form general monitoring of i.e. petrol station or water intake sources in one region territory is not considered as very difficult task. However, because of the simplicity of structure and big possibilities of replacement of the staff through the software support these systems are worth of building for only few cameras. There are predictions that in next five years the monitoring IP will be the standard of security installations. The structure and architecture of monitoring IP is very similar as the proper computer network. The devices used for image signal processing have their own IP addresses. It is possible to use the analog parts of monitoring systems such as cameras, wall of analog cameras applying analog to digital signal converters considered as webservers. In the opposite way the communication is supported by decoders.

The recording of the signal can be carried on locally in traditional DVRs⁴ as well as in stream signal recorder using remote control.

² Base Transceiver Station.

³ Closed-Circuit Television.

⁴ Digital Video Recorder.

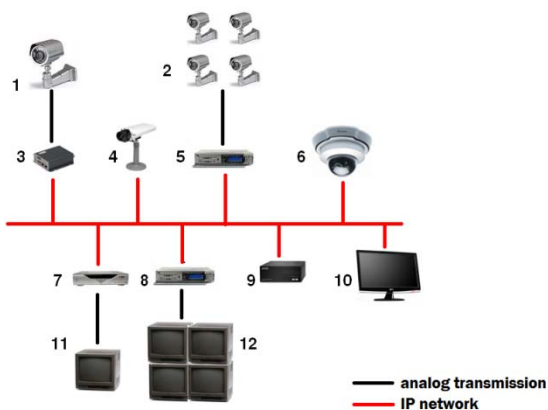


Fig. 2. Simplified scheme showing the genesis of the CCTV installation in IP network, where:

- 1 – analog camera, 2 – wall of analog cameras,
- 3 – one-channel webserver, 4 – IP camera,
- 5 – four-channel webserver, 6 – rotary IP camera,
- 7 – digital to analog decoder,
- 8 – multichannel digital to analog decoder,
- 9 – Network Video Recorder (NVR),
- 10 – digital monitor, 11 – analog monitor,
- 12 – wall of analog monitors

In fig. 2 there is presented simplified scheme of CCTV installation in IP network, where there are included analog as well as digital parts of installation (black colour – analog part, red colour – digital IP part).

This type of system as well as in more advanced configurations can be easily applied in new-built transport objects.

Fig. 2 shows that structure of CCTV network is quite simple and its modernization with adding new cameras is easy. The cameras can be plugged in whichever place and sharing the image can be easily configured. For example part of the recorded images in CCTV can be shared with technical supervision and serve inspection of the building. Other images from the network can be shared with security guards and other forces. The most important images can be send to the police in real time. The basic and the new one element of such installations is IP camera which in special conditions is considered as computer. IP camera can be plugged directly into LAN or wireless network through FME connector with bandwidth 10/100 Mb/s (RJ45 jack). IP cameras are independent network devices which can be used to monitoring offices, warehouses, shops, etc. They are equipped with ports RJ45 (Fast Ethernet), WLAN 54 Mb/s and client station 802.11b/g⁵ (WiFi). Built-in WWW server allows to do remote configuration of the cameras and sending images to Internet browsers. The cameras can be configured also from the managing software level which

⁵ One of the WLAN standards with bandwidth up to 54 Mb/s.

allows to watch images from many cameras at one time and to save them on the hard drives continuously or automatically. The new items in the system are also independent and freestanding devices designed for saving the images from IP cameras – NVR recorders. Some IP cameras own the alarming port which allows to connect outside sensors and RS-485 port allowing to connect the camera turntable. The cameras can also be adapted for outdoor installations through applying hermetic case. Few models using built-in infrared illuminators have possibility for working at night and can record the sound.[4]

IP camera digitizes the analog video signal. The computational efficiency of built-in processor is very important factor because it is strictly connected with the quality of image sent through the network and thereby installation functionality – so significant for extensive transport objects and systems. The camera with frame rate 25 fps and with QCIF⁶ can be applied only in systems with small responsibility in opposite to camera with 25 fps and Full D1⁷.

Very important features of IP cameras are:

- connection to the Internet allows every user to watch in real time the images from office, hotel, city or transport object (i.e. railway station, airport, etc.);
- they allow to watch images from other location;
- in case of using the analog cameras there is possibility for usage network video server to allow watching images from any place or quickly and cheaply expand the supervision system;
- the usage of network camera does not require additional costs, instead of buying separate monitor for camera, the already working PC monitor can be used;
- there is no need to organize new wiring, already existing computer wiring is used;
- network cameras technology eliminates the necessity of replacement the tapes in video recorder – the images are saved on PC hard disk or in NVR recorder.[2]

4. VISION MONITORING SYSTEM INCLUDING THE TCP/IP PROTOCOL

The client-server architecture and TCP/IP protocol can be used for wide communication in different types of data networks. The system allows to transmit to monitoring centre the view, the sound or any other digitized signal. The basic architecture of such system is showed in fig. 3.

⁶ Quarter Common Intermediate Format – recording format with resolution 176 x 144 pixel.

⁷ Resolution of 720 x 576 for PAL and 720 x 480 for NTSC.

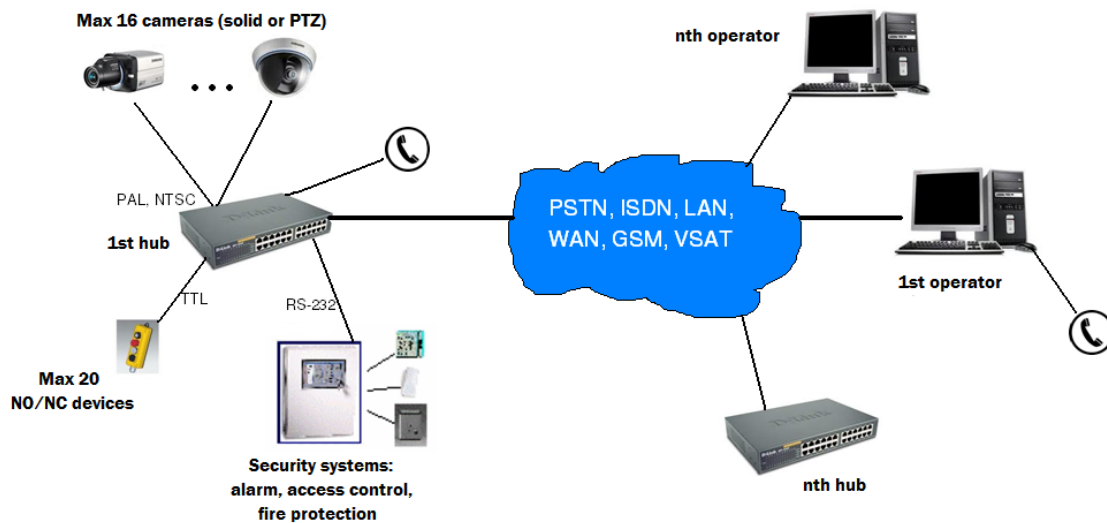


Fig. 3. Architecture of electronic security system including vision monitoring and other alarm systems of M³S type

The main element of the M³S⁸ system is the multimedia hub M²C which collects every data incoming from local systems (cameras, microphones, sensors, etc.). The hub converts them to the digital signals, compress them and saves. Every data can be transmitted through the network to the managing station in monitoring centre. Every hub has 4÷16 video inputs and 5÷20 programmable bistable inputs (NO/NC⁹). Image coding is implemented by programmed coder working in JPEG or Wavelet standard. Hubs provide the communication with Pan-Tilt-Zoom¹⁰ cameras allowing their remote control. Alarm systems, fire protection or access control systems can also be added to hubs. In one system there could be many M²C working at one time and their number is limited only by network bandwidth.

The managing station for M³S system is concerned as a personal computer with adequate software, including graphic user interface for administration and monitoring the signals incoming from the hubs. This station has role of the digital map that shows working of every connected systems, receives and decodes the video stream and allows to control the cameras. There is possibility of observing the view from 16 cameras at one time on one monitor and view from one camera can be displayed in full screen mode on one monitor. Operating of managing station is supported by so-called quick automatic response scenarios. [8]

The existence of defined event in alarm system or movement detection in view of camera causes

automatic reaction of M³S system (notification of the operator, start of recording, change of recording mode, start of video stream transmission from defined camera, notification of the security service, etc.). The architecture of the security system presented on fig. 3 including vision monitoring and other alarming systems is characterized by:

- remote monitoring and supervision of distant and distracted on large area objects throughout available transmission links (networks PSTN¹¹, ISDN¹², GSM, GPRS¹³, Ethernet, Token ring, Frame Relay, ATM, VSAT);
- digital recording of events with possibility of simultaneous replaying of the recording and on-line preview;
- high and stable quality of recorded image and long time of recording (limited only by hard disk drive capacity);
- parameters such as recording, transmission, control are defined independently for each camera;
- digital transmission of encoded video streams and signals incoming from other electronic security systems plugged into M³S system;
- coding of video streams in JPEG and Wavelet standards;
- remote control of Pan-Tilt-Zoom cameras;
- video multicast allowing to view the image from one camera by many operators;
- sound communication between operator and monitored object is provided by duplex transmission;

⁸ Multi Media Monitoring and Surveillance.

⁹ Normally Open/Normally Closed.

¹⁰ Pan-Tilt-Zoom – provides remote control (rotary movement, zoom, etc.)

¹¹ Public Switched Telephone Network.

¹² Integrated Services Digital Network.

¹³ General Packet Radio Service.

- observation of the state of alarm inputs and possibility of change of the state of control outputs;
- NO/NC sensors handling;
- monitoring of working of other electronic security systems, i.e. access control, fire protection system with cautionary sound system;
- event recording in the data base with description including date, time of occurrence and description of the event;
- automatic connection setup with managing station after alarm occurrence;
- support of video stream in PAL¹⁴ and NTSC¹⁵ standards;
- archiving of video record on DAT tapes and DVD–RAM disks;
- recorded images archive management;
- cooperation with Uninterruptible Power Supply (UPS) devices;
- easiness of adding new cameras and operating stations;
- simple management of the system, easy configuration, open architecture.

5. SUMMARY

Constant radio connection with at least three Base Transceiver Stations is necessary for precise definition of terminal localization. This case is fulfilled in urban agglomerations, city areas or their nearest neighbourhoods where there is one network operator. In weakly urbanized areas the condition of subscriber connection with three BTS's will be very difficult to fulfill or impossible. The cooperation between network operators in rescue–alarm surface will be solution to this situation. System cooperating with European emergency telephone number (112) improves the security of the subscribers and allows to provide them prompt assistance in emergency of life and health treats.

Vision monitoring based on TCP/IP protocol largely facilitates administrative activities in the system. It allows to operator to control the whole system in real time. It gives the user elastic possibility of checking the state of the system from every place connected to the Internet. The specifications of the system allow digital recording and archiving of the image and diagnostic parameters on optical data carriers and hard disk drives. The system is protected against sudden decline of power by using the UPS's and immediate notification of the operator about emergency situation that has occurred. It is provided by Internet communication or GSM cellular network.

LITERATURE

1. Czopik G., Roszak M., Witczak A., *Lokalizacja terminala GSM dla potrzeb ratownictwa*, Warszawa 2001.
2. Kołakowski J., Cichocki J., *UMTS system telefonii komórkowej trzeciej generacji*, Warszawa 2003.
3. Krawczak R., *Metody określania położenia terminali w systemie GSM*, Warszawa 2001.
4. Liderman K., *Podręcznik administratora bezpieczeństwa teleinformatycznego*, Warszawa 2003.
5. Liderman K., *Bezpieczeństwo teleinformatyczne*, Warszawa 2001.
6. Liderman K., *Analiza ryzyka i ochrona informacji w systemach komputerowych*, Warszawa 2008.
7. Mielnik P., Witczak A., Poniecki A., *Synchronizacja czasu z wykorzystaniem GPS – wnioski i doświadczenia*, Warszawa 2000.
8. Praca zbiorowa, *Vademecum teleinformatyka*, Warszawa 2004.
9. Wesołowski K., *Systemy radiokomunikacji ruchomej*, Warszawa 2003.



Tomasz CIECHULSKI, M.Sc, is a teaching and research employee in the Faculty of Electronics of Military University of Technology. He holds Master of Science degree in electronics and telecommunication since 2012. He is 1st year D.Sc. candidate in the Institute of Electronic Systems. His research area of interest includes electronic security systems, GSM and GPS localization, neural networks and analysis of load distribution in power systems.

¹⁴ Phase Alternating Line.

¹⁵ National Television System Committee.

MODEL OF A COMPUTER SUPPORT FOR THE DESIGN OF AOI SYSTEMS AIMED AT THE DETECTION OF SURFACE DEFECTS

Tomasz WÓJCICKI

Institute For Sustainable Technologies – National Research Institute in Radom
Pułaskiego 6/10, 26-600 Radom, Poland, (48) 3644241 int. 261, tomasz.wojcicki@itee.radom.pl

Summary

The article presents an original model supporting the design of AOI systems aimed at the detection of surface defects. The analysis of the state of the art shows that the problem of the design of automated systems employing noninvasive measurement methods, including AOI methods, dedicated to specialist tasks connected with surface quality control, is actually a prospective future research direction, as it is directly connected with the need to speed up and rationalise the design processes. The research problem presented in the article was defined through the determination of the scope of automated tasks aimed at the support of the design of AOI systems and methods for their execution. The research method consisted in the analysis of the available numerical methods and computer simulations enabling the selection of the solution facilitating the effectiveness of the decision-making process.

Keywords: expert system, automatic optical inspection, quality control, designing

MODEL KOMPUTEROWEGO WSPOMAGANIA PROJEKTOWANIA SYSTEMÓW AOI DETEKCJI WAD POWIERZCHNIOWYCH

Streszczenie

Artykuł przedstawia autorski model wspomaganie projektowania systemów AOI przeznaczonych do detekcji wad powierzchniowych. Analiza stanu wiedzy wskazuje, że problematyka projektowania zautomatyzowanych systemów wykorzystujących nieinwazyjne metody pomiarowe, w tym metody AOI, dedykowanych do specjalizowanych zadań związanych z kontrolą jakości powierzchni jest perspektywicznym kierunkiem w rozwoju badań naukowych, co spowodowane jest koniecznością przyspieszenia i jakościowego usprawnienia procesów projektowania. Problem badawczy podejmowany w artykule określony został poprzez ustalenie zakresu zautomatyzowanych działań, których celem jest wspomaganie prac projektowych nad systemami AOI oraz metod przeznaczonych do ich realizacji. Metoda badawcza polegała na przeprowadzeniu analizy dostępnych metod numerycznych, oraz symulacji komputerowych w celu wyłonienia rozwiązania, umożliwiającego skuteczne wspomaganie procesów decyzyjnych.

Słowa kluczowe: system ekspertowy, automatyczna optyczna inspekcja, kontrola jakości, projektowanie

1. INTRODUCTION

The automation of manufacturing processes [1] is a contemporary element of progress. The demand for such systems is constantly growing, which is mainly caused by the decrease in the costs of production and the concurrent increase in the quality of the manufactured goods. Another reason behind the growing interest in the topic of the automation of manufacturing processes is the technological progress connected with the growing complexity of final products and processes for their inspection and control. The organoleptic quality inspection has numerous disadvantages that stem from the limitations of the human senses and manual dexterity [2]. The repeatability also plays a crucial role here. Any human feels the effects of long work, which has a negative influence on the outcomes of the undertaken tasks. The automation of the

production process ensures higher quality and greater repeatability, and therefore results in increased efficiency and effectiveness of a process. With reference to the technical equipment, the automation has an impact on the reliability and the availability of machines participating in the manufacturing processes. It also reduces the costs of servicing and maintenance.

The design of quality inspection systems is a complex issue [3]. The designers of such solutions have to have broad knowledge on mechanics, automation, electronics, information technologies, optics, etc. The design of an effective system that can be incorporated into a technological line requires a lot of experience and makes the entire process costly and time-consuming. What is required in the case of AOI systems [4] is the ability to solve interdisciplinary R&D tasks in the area of acquisition methods, digital image processing and

analysis, metrology, applied informatics, or knowledge and software engineering.

The analysis of the state-of-the-art suggests that the issue of the design of automated systems in which non-invasive measurement methods are used, including AOI methods, and which are dedicated for specialised tasks in the area of the inspection of quality of surfaces, constitutes a potential long-term research direction [5,6,7,8,9], which is particularly due to the following:

- The potentially vast possibilities for the design processes to be speeded up and their quality to be improved by means of the application of knowledge and competencies of the design teams, specialised databases and a holistic direction of the entire design process;

- The possibility for design works to be supported with the procedures for the selection of measurement methods determining the efficiency of the system, and the simulation of system operation for different application options, which enables the quick adjustment to the specific technical and functional requirements defined by the final user;

- The possibility to decide on the configuration of the system, particularly the multifunctional system that can be used in changeable manufacturing conditions, and select AOI methods that are most effective when it comes to the detection of surface defects and the image analysis.

The above listed reasons generate the necessity to develop the models and applications intended for the solution of such tasks. One of the ideas has the form of the developed original model aimed at supporting the design of the automatic quality inspection systems based on optical inspection and enabling the detection of surface defects.

2. MODEL FOR THE SUPPORT OF THE DESIGN OF AOI SYSTEMS

The proposed solution consists in the replacement of the classic and time-consuming design stage [10,11] composed of numerous analyses, the determination of optimisation criteria and the design and synthesizing of a model constituting the solution to the posed research questions, with an expert system linked to the knowledgebase (Fig. 1).

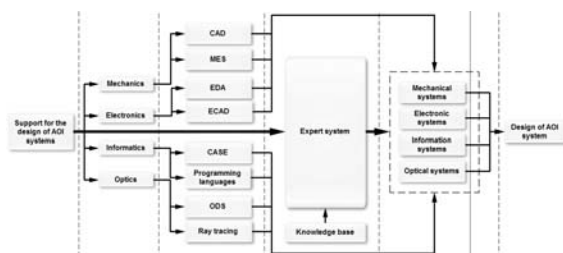


Figure 1. An expert system-based and knowledgebase-coupled model and a traditional model for the design of AOI systems for surface defect detection

The systemised knowledge of the experts [22] accumulated in the knowledgebase facilitates a more efficient creation of systems adjusted to new products or surface defects. The fact that some of the tasks previously executed personally by the designer are now performed by the IT expert system proposed in the model created, enables the costs of the design process to be cut, and the time needed for the development of a solution, satisfactory in terms of its design, reduced. IT models enabling parts of a classic design process to be replaced can differ. They can use simulation systems [13] and complex algorithms based on AI [14], including artificial neural networks, genetic algorithms, cellular automata, fuzzy logic, etc, which aim at the recreation of the phenomenon and the preservation of the real object with the use of numerical models.

In the proposed model, the classic design process was replaced with automatic inference with the configuration of the AOI system (hardware unit of the AOI system), and the structure of a detection algorithm (software unit of the AOI system) (Fig. 2).

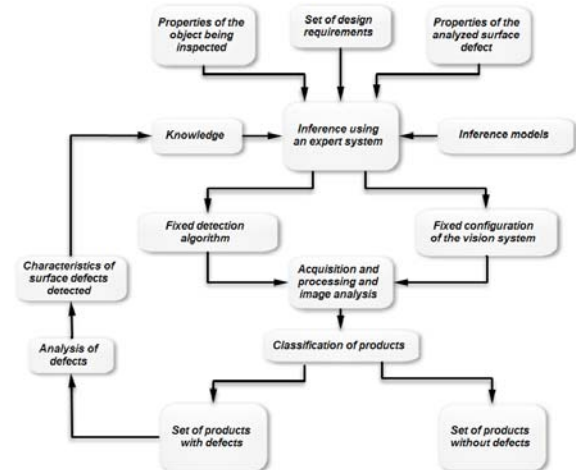


Figure 2. Functional model for the support of the design of AOI systems based on expert system-based inference

A characteristic feature of the developed expert model is, apart from the possibility of its adaptation to different types of surface defects and test objects, the feedback between the set of faulty products and the knowledgebase, which helps to supplement the existing knowledge on the types of surface defects, and therefore increases the effectiveness of the model. The structural model of the developed solution is presented in Fig. 3.

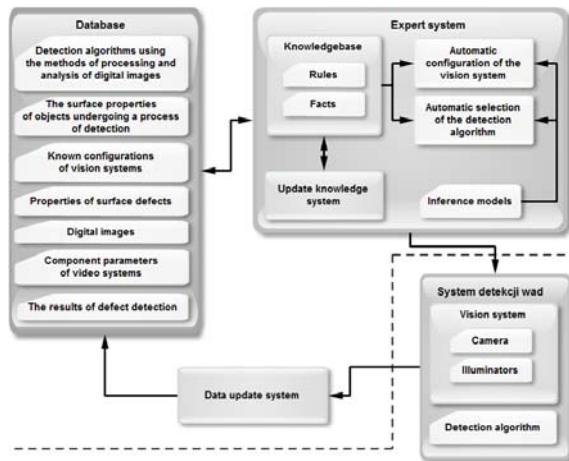


Figure 3. Structural model of the system for the support of the design of AOI systems intended for the detection of surface defects

The main element of the structural model is the expert system composed of two inference modules including the module of the automatic configuration of the vision system, and the automatic model for the selection of the detection algorithm. Other elements of the expert system are a knowledgebase built of facts and rules, a system of knowledge update, and inference models. The other two elements of the model include a database supplying the expert system, and a data update system. The model cooperates with the system for the detection of defects, whose such elements as the vision system or the detection algorithm are selected with the use of the expert system.

3. METHODOLOGY FOR THE CONFIGURATION OF VISION SYSTEM

The model of a vision system intended for the detection of surface defects in machine parts is composed of a camera with an optical system, whose role is to observe the surface of the inspected object onto which a beam of light is projected. The model of the vision system in three different configurations is presented in Fig. 4.

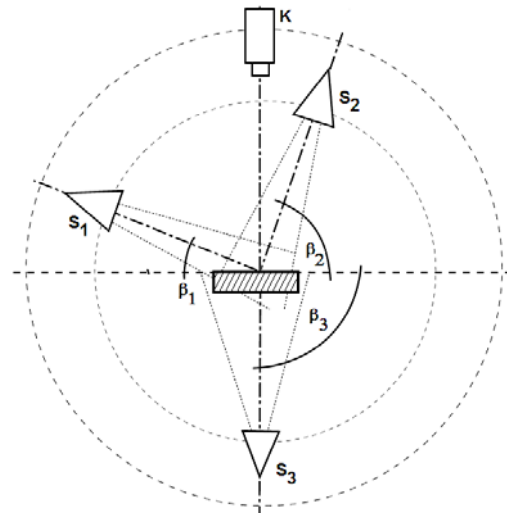


Figure 4. Model of the vision system intended for the detection of surface defects in three configurations of the light source S_1, S_2, S_3 , where K – camera with an optical system; $\beta_1, \beta_2, \beta_3$ – angles at which light is projected

The two essential configurations of the vision system consist in the adjustment of the angle at which light is projected onto the surface of the inspected object, and the adjustment of the light range in a way enabling the defect to stand out with reference to the remaining area of the surface of the object.

The configuration of the vision system is a multistage process that requires knowledge on numerous issues. The proposed methodology for the configuration of the vision system assumes the following stages: the determination of the lighting range, the setting of the angle at which the light is projected, the setting of camera parameters, the selection of the camera model, the determination of the values of the parameters of the lens, the selection of the lens model. The setting of the lighting range and the angle of light projection is executed with the use of fuzzy inference based on a Mamdani model. The determination of all the other output values is based on a classic two-valued logic in which a regression algorithm is used. In the process executed by the regression algorithm, individual hypotheses that are the goal of the inference, are either confirmed or abolished, based on the authenticity of the facts and rules. Such type of inference cannot be executed without thy hypothesis being determined and defined as goal driven. At each of the stages of the configuration of the vision system, the inference module is fed with knowledge necessary for the determination of the value of the required input parameters. In the case when the satisfactory configuration of the vision system that complies with all the design requirements cannot be set based on the knowledge accumulated in the knowledgebase, the combination of several configuration options into one functional structure is

allowed. In such case, the vision system can be composed of numerous illuminators or cameras. The defect detection process is then performed through the sequential analysis of images from individual configurations included in a complex structure of the vision system (Fig. 5).

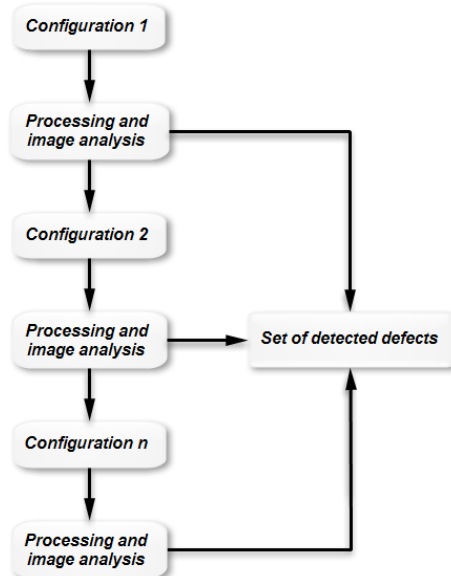


Figure 5. Defect detection process in a complex structure of the vision system

The next stage in the development of the AOI system consists in the determination of the structure of the detection algorithm intended for the processing and analysis of digital images.

4. METHODOLOGY FOR THE SELECTION OF THE STRUCTURE OF THE DETECTION ALGORITHM

Detection algorithms are built of numerous methods connected with image analysis and processing, therefore their selection has to be a complex process. The classification parameters in detection algorithms depend on the type of the inspected object and the types of defects that occur within the analysed surface. The main part of the algorithm is a set of methods for image processing and analysis (Fig. 6).

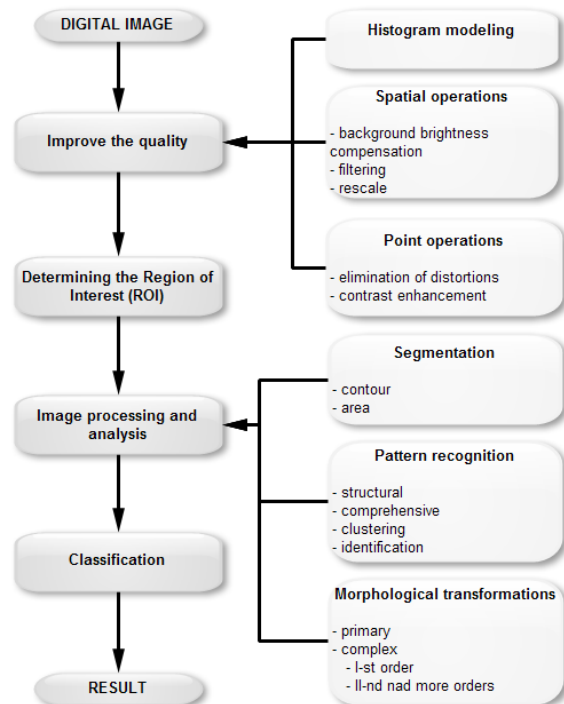


Figure 6. Structure of detection algorithms used in AOI systems for the detection of surface defects

The methods most commonly used in the structures of detection algorithms include the following: segmentation, morphological transformations, and image recognition. During the process of segmentation, the pixels are assigned to classes according to specific criteria such as location, or statistical distribution of brightness, or colour. Morphological methods enable the processing of the shapes of objects by image analysis using the so-called structuring elements [15], which are sections of the image with a highlighted focal point. Image recognition is an automatic identification of classes of objects and phenomena recorded in images [16]. The pattern recognition and pattern matching are related to image recognition. The inference concerning the structures of detection algorithms is performed based on the two-valued logic with the use of the progression model, where based on the facts and rules accumulated in the knowledgebase, new facts are generated up to the moment when a fact consistent with a proposed hypothesis, being an inference goal, can be found among the generated facts. A big advantage of such type of inference is the set of new facts, which can constitute valuable knowledge for the designers of detection algorithms. The methods included in the structure of detection algorithms are sequential, conditional or iterative, depending on the complexity of the defect detection problem. The developed methodology for the selection of the structure of the detection algorithm for use in the detection of surface defects involves the following stages: the determination of the area of image analysis, the verification of the need for the execution of the process for the improvement the

quality of images, the determination of the method for the improvement of image quality, the verification of the need for the image segmentation process, the determination of the method for image segmentation, and the determination of the image recognition method.

5. SUMMARY

The developed model for the support of the design of AOI systems significantly enhances the processes of vision system and detection algorithm creation, as it applies systematised knowledge and computing intelligence enabling the automatic inference. The adaptation of AOI systems to new types of products and surface defects occurring in technological lines is much easier, quicker and cheaper when the developed solution is applied. Through the application of the feedback loop between the set of faulty goods and the knowledgebase, a problem of information supply has been solved, which results in the increased effectiveness of the inference process. The formalisation of the structure of data representing selected thematic areas enables a quick exchange of information between the designers using the developed solution, whereas the separation of the expert knowledge from detection algorithms influences the reduction of numerical calculations. The opportunity to explore more efficient structures of detection algorithms for the analysis of digital images is an innovative approach that has not yet been taken into account in the literature. Knowledge presented in form of rules and facts has a lot of advantages, e.g. inference explanation facility. The mechanism of explanation presents how individual conclusions are drawn. Retrospective, hypothetical explanations and explanations against the facts are possible. The first enable the investigate the entire inference process from the stage of conclusion and comments to the rules, the second allows to check how the conclusion would change in the case when different values were assigned to the facts, whereas the third enable the explanation why it was impossible for a given conclusion to be drawn. The future extension and optimisation of the methodology is possible. It seems crucial to include the impact of external factors on the structure of the vision system. In such a case, the influence of the external factors could be included through the analysis of the probability of their occurrence with the use of Bayes networks or physical analysis employing numerous simulation methods based on the method of finite elements. Noteworthy are also data mining methods enabling the determination of associations (the creation of knowledge based on data) concerning the existing AOI systems, e.g. AIS, SETM, APriori, Elat, Levelwise, FreeSpan, etc. The methods of this kind are usually equipped with specific measures describing, inter alia, confidence,

which would also constitute a crucial element supporting the designers of AOI systems.

REFERENCES

- [1] Przybylski W., *Technologia maszyn i automatyzacja produkcji*. Wydawnictwo Politechniki Gdańskiej, Gdańsk, 2001.
- [2] Gawęcka J., Jędryka T., *Analiza sensoryczna. Wybrane metody i przykłady zastosowań*. Wydawnictwo Akademii Ekonomicznej w Poznaniu, Poznań, 2001.
- [3] Hamrol A., *Zapewnienie jakości w procesach wytwarzania*. Wydawnictwo Politechniki Poznańskiej, Poznań, 1995.
- [4] Batchelor B., Waltz F., *Intelligent machine vision*. Springer-Verlag Limited 2001, pp. 18-20.
- [5] Malamas E., Petrakis E., Zervakis M., *A survey on industrial vision systems applications and tools*. Image and Vision Computing 21(2), 2003.
- [6] Mery D., Berti M., *Automatic detection of welding defects using texture features*. Insight 45(10), 2003.
- [7] Yan T.S., Cui D.W., *The method of intelligent inspection of product quality based on computer vision*. 7th Int. Conf. on Computer-Aided Industrial Design and Conceptual Design (CAIDCD '06), Hangzhou, 2006.
- [8] Meola C., Carlomagno G., Squillace A., Vitiello A., *Non-destructive evaluation of aerospace materials with lock-in thermography*. Engineering Failure Analysis, vol. 13, issue 3, 2006.
- [9] Shih-Chieh L., Chih-Hsien C., Chia-Hsin S., *A development of visual inspection system for surface mounted devices on printed circuit board*. Proceedings of the 33rd Annual Conference of the IEEE Industrial Electronics Society (IECON) Taipei, Taiwan, 2007.
- [10] Gąsiorek E., *Podstawy projektowania inżynierskiego*. Wydawnictwo Akademii Ekonomicznej we Wrocławiu, Wrocław, 2006.
- [11] Gawrysiak M., *Mechatronika i projektowanie mechatroniczne*. Politechnika Białostocka, Białystok, 1997.
- [12] Kwaśnicka H., *Sztuczna inteligencja i systemy ekspertowe: rozwój, perspektywy*. Wydawnictwo Wyższej Szkoły Zarządzania i Finansów we Wrocławiu, Wrocław, 2005.
- [13] Kelton D., Law M., *Simulation Modeling and Analysis*. Third Edition, McGraw-Hill, 2000.
- [14] Russell S., Norvig P., *Artificial Intelligence. A Modern Approach* Third Edition, Prentice-Hall, 2010.
- [15] Tadeusiewicz R., Korohoda P., *Komputerowa analiza i przetwarzanie obrazów*. Wydawnictwo Fundacji Postępu Telekomunikacji, Kraków, 1997.
- [16] Hundt Ch., Liśkiewicz M., *Two-Dimensional Pattern Matching with Combined Scaling and Rotation*. Springer, Berlin, 2008.



Tomasz WÓJCICKI,
Employee of the
Information Technology
Department at the
Institute For Sustainable
Technologies in Radom,
author of IT solutions in
the field of image
analysis, artificial
intelligence, 3D
modeling, vision
systems in technical
diagnostics.

SCANNING TELEVISION OPTICAL MICROSCOPE FOR DIAGNOSTICS OF MICROOBJECTS IN MEDICINE

Ivan PRUDYUS, Volodymyr SHKLIARSKYI, Yuriy MATIIESHYN,
Anatoliy PEDAN, Yuriy BALANYUK, Volodymyr VASYLYUK

National University, Institute of Telecommunications, Radioelectronics and Electronic Devices
Bandera Street 12, 79013 Lviv, Ukraine, e-mail: shkliarskyi@polynet.lviv.ua

Summary

Scanning television optical microscope (STOM) developed by authors will enable to diagnose microobjects which size exceeds 0,1 microns. Diagnostics can be carried out by supervision over researched microobjects during influence on them of various reagents and catalysts, and also definition of parameters of microobjects: the sizes, speed of movement, acceleration, growth rate, change of density, etc.

Ways of the scanning television microscope construction which can be used for the biological microobjects research are analyzed. The Microscope capabilities are expanded due to a raster formation in television and little-frame modes. Ways of the raster size change are offered at preservation of the microobject image resolution.

Key words: scanning microscope, electron beam tube, microobject, diagnostics

SKANUJĄCY TELEWIZYJNY OPTYCZNY MIKROSKOP DLA DIAGNOSTYKI MIKROOBIEKTÓW W MEDYCYNIE

Streszczenie

Skanujący telewizyjny optyczny mikroskop (STOM) skonstruowany przez autorów pozwoli na diagnozowanie mikroobiektów których rozmiar nie przekracza 0,1 mikrona. Diagnoza może być przeprowadzona poprzez obserwowanie badanych mikroobiektów podczas oddziaływania różnych reagentów i katalizatorów, oraz w celu określenia parametrów fizycznych mikroobiektów: wielkości, prędkości, przyspieszenia ruchu, tempa wzrostu, zmian gęstości itp.

Sposób skonstruowania skanującego telewizyjnego optycznego mikroskopu powala na badania i analizy mikroobiektów biologicznych. Możliwości mikroskopu zostały rozszerzone w stosunku do skanowania rastrowego i trybów mało-kadrowych. Zaproponowane zostały sposoby rastrowej zmiany rozmiaru ekranu przy zachowaniu rozdzielczości zdjęcia mikroobiektu.

Słowa kluczowe: skanujący mikroskop, lampa kineskopowa, mikroobiekt, diagnoza

INTRODUCTION

Scanning television optical microscope (STOM) developed by authors will enable to diagnose microobjects which size exceeds 0,1 microns [1-3]. Diagnostics can be carried out by supervision over researched microobjects during influence on them of various reagents and catalysts, and also definition of parameters of microobjects: the sizes, speed of movement, acceleration, growth rate, change of density, etc [4-7]. As a light source in such microscope electron beam tube (EBT) of the high resolution is used. Very short time of afterglow such EBT allows to use a mode of a running beam. Advantage of such microscope in comparison with a video television microscope consists in an opportunity of formation of the image of microobject (MO) which will consist of 5000 elements of decomposition on each coordinate. In comparison with electronic microscope STOM

provides an opportunity to carry out researches in real time on alive MO. Advantage of the STOM in comparison with a laser microscope consists in much smaller energy of illumination that liquidates influence of a source of illumination on alive MO. Use of change of the sizes of a scanning raster will provide formation of image of MO with change of its scale without loss of the resolution of the image.

1. SCANNING MICROSCOPE STRUCTURAL SCHEME

The structural scheme of the STOM is submitted on fig. 1. Into its structure enter: the block of forming of scanning raster BFSR, block EBT of the high resolution BEBT, the block of management of operating modes scanning EBT BMOM, two block of the optical channel BOC1 and BOC2, researched microobject MO, the block of photoelectronic multiplier BPEM, the block of formation of video

signal BFVS, the television monitor TM, the block of processing of video signal BPVS, personal computer PC with its monitor M.

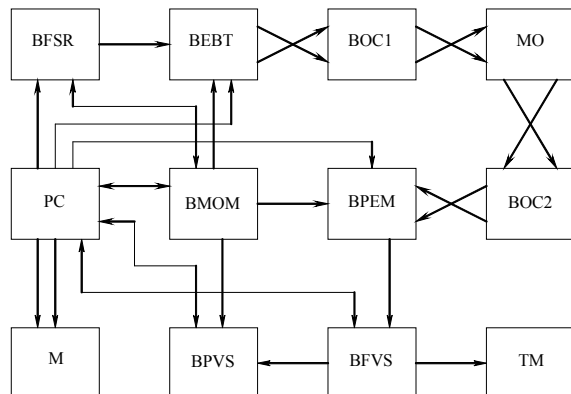


Figure 1. STOM provides formation of MO image on the screen of the television monitor which is used for the snap analysis of MO condition by the operator in real time. On results of the analysis by the operator it is made a decision on methods of the further research: increase in the image of all MO or its separate fragment, overlapping of a researched fragment with the center of EBT screen, discrete scanning with the increased resolution, increase of contrast of MO image, measurement of static and dynamic MO parameters, archiving of the image, etc. Results of processing of MO image are displayed on the monitor of a personal computer M

2. PRINCIPLE OF WORK

The principle of work of STOM will consist in the following. On screen of EBT the light scanning raster which with the help of optical channel block BOC1 is projected on researched microobject MO is formed. Light which has passed through MO, or was beat off from it moves on a photosensitive target of photoelectronic multiplier PEM. On an output of the block of the photoelectronic multiplier BPEM the signal which instant value is proportional to quantity of light which has arrived on a photosensitive target is formed. On an output of the block of formation of video signal BFVS the signal in the television standard which moves on television monitor TM and the block of processing of video signal BPVS is formed. BPVS makes an analog strip filtration of video signal and regulation of contrast. The block of management of operating modes BMOM chooses the following operating modes according to a command of the operator [1,7]:

- a television mode of formation of a scanning raster;
- a discrete mode of formation of a scanning raster with various resolution;
- a discrete mode of formation of a scanning raster with various frequency;
- a discrete mode of formation of a miniraster;
- a discrete and analog mode of formation of a scanning raster of the changeable sizes;

- a discrete and analog mode of moving of a scanning raster.

The personal computer is used for a choice of operating modes of STOM, processing of MO image by standard programs, archiving of the images, the automated definition of parameters MO - the sizes, the area, speed of movement, growth rate and others.

The internal structure of separate units of the STOM will be determined by a place of its possible use: a) research laboratories of the small medical organizations (the cheapest and simple STOM); b) research laboratories of the medical organizations (rather cheap with more wide opportunities); c) branch research laboratories for which the STOM should have the widest functionalities.

For the first case the most suitable is use of STOM with the minimal functionalities which works in a standard television mode. At use of PC cheap and standard systems of input and processing of images are applied to input of images researched MO in PC. Use in such microscope cheap EBT because in this case not necessarily to provide scaling the image researched MO due to change of the sizes of a scanning raster in wide borders is possible. Change of the sizes of a scanning raster and its displacement is expedient for making simple analog circuits.

In the second case use of an electron beam tube of the high resolution will be necessary. Formation of sweep which is equivalent to decomposition of the image 1000x1000 elements, it is possible to carry out as analog (with very small factor of nonlinearity of sweep), and digital way. Input of the image in a personal computer is necessary for carrying out with preliminary digitization of the image, therefore standard videoblasters for input of the image in a personal computer do not approach. Besides for processing images with the big digital files use of the difficult expensive specialized programs is necessary.

In the third case the STOM should have the greatest possible functionalities with the purpose of carrying out of the difficult specialized researches. Formation of sweep should provide decomposition of the image on 5000x5000 elements. For the snap analysis it is necessary to provide a television mode of formation of a scanning raster for input of the image in a personal computer, and for the detailed analysis digital sweeps which will provide high accuracy of formation of a scanning miniraster in any point of EBT screen with the purpose of detailed research of separate fragments of image MO can be used. In such microscope it is necessary to provide wide opportunities on change of factor of increase, sensitivity, regulation of contrast in wide borders, etc.

On fig. 2. the preparation of blood of the person on the monitor of a scanning electronic microscope (the top line) and blood unguent of the person on monitor of STOM (the bottom line) is represented.

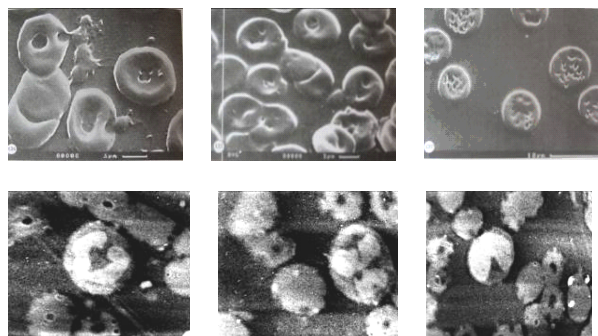


Figure 2. EBT together with electromagnetic electron-optical units of formation and management of electronic beam (focus-deflection complex) it is submitted on fig. 3. The basic condition of reception on EBT screen of a light spot of the minimal sizes is mutual adjustment axes of an electronic beam and an optical axis of a lens. Into the focus-deflection complex enter (from left to right): two electromagnetic systems of adjustment, the coil of focusing astigmatism correction and the coil of a coordinate deflection



Figure 3. The device will consist of liquid crystal display (LCD), control panel (CP), microcontroller (MC), the block of measurements (BM) and the switchboard (S) and has the following characteristics

Use of STOM in comparison with other devices which use for research of biological and medical microobjects (MO), has such advantages:

- very small exposition of illumination that allows to investigate alive MO in real time;
- ultrahigh resolution of used EBT for scanning MO in comparison with used devices of display (the monitor of the personal computer, the television video-control device) allows to change scale of formed image of MO without loss of resolution;
- flexibility of formation of a scanning raster allows to choose operatively fragment of MO and to display its image in the increased scale on the television monitor;
- considerably the big depth of sharpness of the formed image in comparison with optical and video microscopes;

- an opportunity of MO illumination in a ultra-violet range with use specialized EBT and formation of MO image in a seen spectrum;
- absence of necessity of a putting researched MO in vacuum;
- simplicity of MO preparation to research;
- an opportunity of research of MO internal structure;
- an opportunity of research dynamic MO, etc.

Essential advantages of CTOM in comparison with video, optical and electronic microscopes enable to speak about their wide use in those branches where it is necessary to diagnose and define parameters of alive MO in real time without preliminary processing and harmful influence on MO, first of all, in medicine and biology.

The basic technical parameters of a laboratory breadboard model of a microscope [7]:

- the maximal factor of increase – 20000^x;
- factor of smooth change of scale – 1...10;
- the minimal size of a scanning element on researched object – 0,1 microns;
- a maximum of a spectrum of a luminescence of the screen of a tube – 0,54 microns;
- the minimal size of a light spot on the screen of a tube – 10 microns;
- a mode of scanning – TV the standard.
- power consumption – 150 W;
- overall dimensions - 240×350×700 (mm);
- weight – 22 kg.

3. SUMMARY

The developed scanning television optical microscope provides diagnostics of medical and biological microobjects which sizes exceed 0,1 microns in a wide spectral range of illumination in real time.

REFERENCES

- [1] Prudyus I.: *Nanoluminescence a Scanning Optical Microscope for Research of Functioning of Microorganisms Under Influence of Low Temperatures* /I. Prudyus, A. Zaichenko, L. Palianyca, A. Pedan, V. Shkliarskyi// Modern Problem of Radio Engineering, Telecommunications and Computer Science TCSET'2012: XI intern. conf., February 21 – 24 2012 : Proceed. of the Conf. - Lviv-Slavske, Ukraine, 2012. – P. 38 – 39.
- [2] Balanjuk Y.: *Scanning Television Optical Microscope for Research of Biological Microobjects* /Y. Balanjuk, B. Lubinecka, Y. Matiieshyn, A. Pedan, I. Prudyus, Gennadiy Turkinov, Volodymyr Shkliarskyi// Modern Problem of Radio Engineering,

Telecommunications and Computer Science TCSET'2010: X intern. conf., 23 – 27 February 2010: Proceed. of the Conf. - Lviv-Slavske, Ukraine, 2010. - p.18.

- [3] Vasylyuk V.: *Raster Forming Block in Scanning Television Microscope* / V. Vasylyuk, V. Goy, V. Shkliarskyi // Modern Problem of Radio Engineering, Telecommunications and Computer Science TCSET'2010: X intern. conf., February 23 – 27 2010: Proceed. of the Conf. - Lviv-Slavske-Ukraine, 2010. - p. 67.
- [4] Balanjuk Y.: *Scanning Television Optical Microscope With Illumination of Microobject in a Ultra-Violet Range* / Y Balanjuk, Y. Matiieshyn, A. Pedan, V. Shkliarskyi. // Modern Problem of Radio Engineering, Telecommunications and Computer Science TCSET'2012: XI intern. conf., February 21 – 24 2012 : proceed. of the conf. - Lviv-Slavske, Ukraine, 2012. - P 113.
- [5] Matiieshyn Y.: *Research of Dynamic Microobjects of the Various Sizes and Forms With the Help of a Scanning Television Optical Microscope* // Y Matiieshyn, V Shkliarskyi, V Storozh // Modern Problem of Radio Engineering, Telecommunications and Computer Science TCSET'2012: XI intern. conf., February 21 – 24 2012 : proceed. of the conf. - Lviv-Slavske, Ukraine, 2012. - P 114.
- [6] Hudz B.: *Video Signal Forming Block in Scanning Television Microscope* / B. Hudz, Y. Matiieshyn, V. Shkliarskyi. // Modern Problem of Radio Engineering, Telecommunications and Computer Science TCST'2010: X intern. conf. February 23 – 27 2010: Proceed. of the Conf. - Lviv-Slavske, Ukraine, 2010. - p. 111.
- [7] Shkliarskyi V.I.: *Scanning Television Optical Microscopy: theory and practice: monography* / V.I. Shkliarskyi. – Lviv Polytechnic Press.– 2010.– 456 p.



PRUDYUS Ivan, Doctor of technical sciences, professor, director of the Institute of Telecommunications, Radio-electronics and Electronic Technics.

Basic directions of scientific researches are antennas, antenna systems, multispectral monitoring systems and complexes.

E-mail:

iprudus@polynet.lviv.ua



SHKLIARSKYI

Volodymyr., Doctor of technical sciences, professor of the Department of Radio-Electronic Devices and Systems.

Basic directions of scientific researches are television scanning systems.

E-mail:

shkliarskiy@polynet.lviv.ua



MATIIESHYN Yuriy

Candidate of technical sciences, The assistant of the Radioelectronic Devices and Systems department.

Basic directions of scientific researches: development of the precision television measuring equipment.

E-mail:

jumati@polynet.lviv.ua



PEDAN Anatoliy, The senior scientific employee of a research department of radio engineering systems. Institute of Telecommunications, Radio-Electronics and Electronic Technics.

Basic directions of scientific researches are television scanning systems.

E-mail: adpedan@gmail.com



BALANJUK Yuriy, The postgraduate of the Department of Radio-Electronic Devices and Systems, Institute of Telecom-munications.

Basic directions of scientific researches are television scanning systems.

E-mail:

Balanyuk.ya@gmail.com



VASILIUK Volodymyr

The postgraduate of the Department of Radio-Electronic Devices and Systems, Institute of Telecom-munications.

Basic directions of scientific researches are television scanning systems.

E-mail: evoreiner@gmail.com

FAULT DIAGNOSIS OF ROTATING MACHINES USING VIBRATION AND BEARING TEMPERATURE MEASUREMENTS

Adrian D. NEMBHARD^A, Jyoti K. SINHA^A, A. J. PINKERTON^B, K. ELBHBAH^A

^A School of Mechanical, Aerospace and Civil Engineering (MACE), The University of Manchester, Manchester M13 9PL

^B Department of Engineering, Lancaster University, Bailrigg, Lancaster LA1 4YR

Summary

Acquisition and subsequent processing of vibration data for fault diagnosis of rotating machinery with multiple bearings, such as Turbo-generator (TG) sets, can be quite involved, as data are usually required in three mutually perpendicular directions for reliable diagnosis. Consequently, the task of diagnosing faults on such systems may be daunting for even an experienced analyst. Hence, the current study aims to develop a simplified fault diagnosis (FD) method that uses just a single vibration and a single temperature sensor on each bearing. Initial trials on an experimental rotating rig indicate that supplementing vibration data with temperature measurements gave improved FD when compared with FD using vibration data alone. Observations made from the initial trials are presented in this paper.

Keywords: Vibration Monitoring, Condition Monitoring, Rotating Machinery, Fault Diagnosis, Principal Component Analysis

1. Introduction

Acquisition and subsequent processing of vibration data for rotating machinery fault diagnosis can be quite intricate; as data are usually required in three mutually perpendicular directions for accurate fault diagnosis (British Standards Institution, 2009). To say the least, the processing of data acquired from complex systems such as turbo generating sets that consist of several stages of operations with multiple bearings is tedious, data intensive and consequently costly. Though traditional practice in vibration-based condition monitoring (VCM) is a mature technique for fault diagnosis of rotating machines, it is a relatively involved process that mandates judgment and expertise from a trained analyst. Additionally, the task of diagnosing faults on these systems may be daunting, if not impossible, for even an experienced analyst. Thus a more simple but robust technique is usually required and would be well appreciated by the relevant industries.

Recent studies (Elnady, et al, 2012; Elbhah and Sinha, 2013; Sinha and Elbhah, 2013) have suggested VCM methods that require significantly reduced number of vibration sensors. Elnady, et al (2012) proposed the use of the on-shaft vibration (OSV) measurement technique that requires special arrangement of the measurement instrumentation. Elbhah and Sinha (2013) and Sinha and Elbhah (2013) used just a single vibration sensor on each bearing by fusion of data in; the composite spectrum and higher order spectra respectively. However both methods were slightly computationally involved. The present study aims to keep both data acquisition and processing simple

and develop a diagnosis technique that uses fewer sensors while preserving moderate computational load. With the wide availability of temperature monitoring systems on rotating machines in industries and studies confirming the sensitivity of temperature to rotating machinery faults (Gaberson, 1996; Sabnavis, et al., 2004; Craig, et al, 2006; Nembhard, 2011; Yong-Wei and Jian-Gang, 2011), an opportunity exists to integrate temperature and vibration data for effective fault diagnosis. Hence, a simplified fault diagnosis (FD) method is proposed that uses just a single vibration and a single temperature sensor on each bearing. The temperature measurement is expected to compensate for the reduction in vibration sensors while replacing the need for advanced and complex signal processing of the vibration data in the fault diagnosis process.

The proposed vibration and the temperature measurements are made on an experimental rotating rig with two coupled rotors supported through 4 ball bearings (Nembhard, et al, 2013a). Different faults are simulated in the rig and both vibration and temperature measurements are collected and analysed in Section 2. Earlier studies used Principal Component Analysis (PCA) as a tool for the diagnosis in rotating machines (Li, et al, 2003; Liying, et al, 2012; Elnady, et al, 2012), so this method is applied in the present study. Results from analyses done are presented and discussed in this paper.

2. Experimental set up

Figure 1 shows a photograph of the experimental rig used for the experiment

(Nembhard, et al, 2013a). The set up consists of two 20 mm nominal diameter dissimilar length (100 mm and 50 mm) rigidly coupled rotors that are supported by four grease lubricated ball bearings. These are secured atop flexible steel pedestals that are bolted to a large lathe bed secured to the

concrete flooring. Machined sections accommodating balancing disks are mounted on each rotor. System drive is provided by a 0.75kW, 3 phase, 3000 rpm motor that is mated to the rotor-bearing system via a semi-flexible coupling. The main dimensions of the rig are provided in Figure 2.

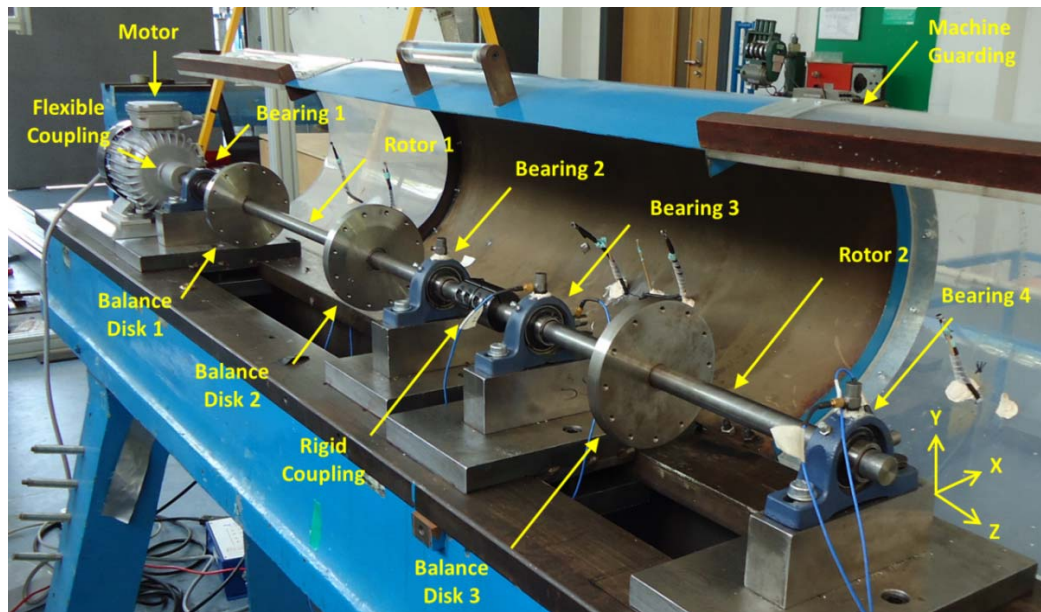
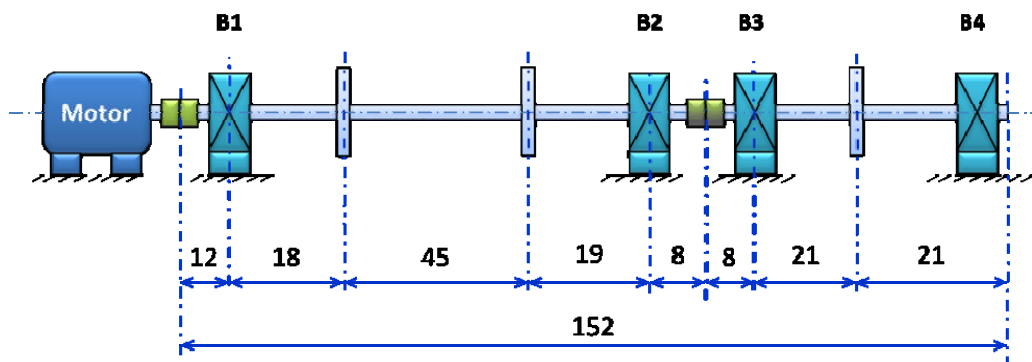


Figure 1. Experimental rig mechanical layout



Note: All dimensions shown in cm

Figure 2. Schematic of experimental rig with dimensions

The instrumentation and software schematic for the set-up is depicted schematically in Figure 3 (Nembhard, et al, 2013a). Rig speed is varied with a speed controller that is operated from a personal computer. The dynamic response of the system is then measured with 100 mV/g accelerometers. Each bearing location has two accelerometers that are mounted with adhesive in mutually perpendicular directions. The vibration data are transmitted through two four channel signal conditioners to a 16 Bit Analogue to Digital (A/D)

Data Acquisition System. Data logging software then stores the digitized vibration data on the personal computer. To measure the thermal response of the system, K-type thermocouples are attached between the bearing casing and outside of the outer race of each bearing. This mounting position was used to get the most immediate and accurate temperature measurements possible. All four temperature readings were captured with an eight channel data logger and saved to the personal computer for later analysis.

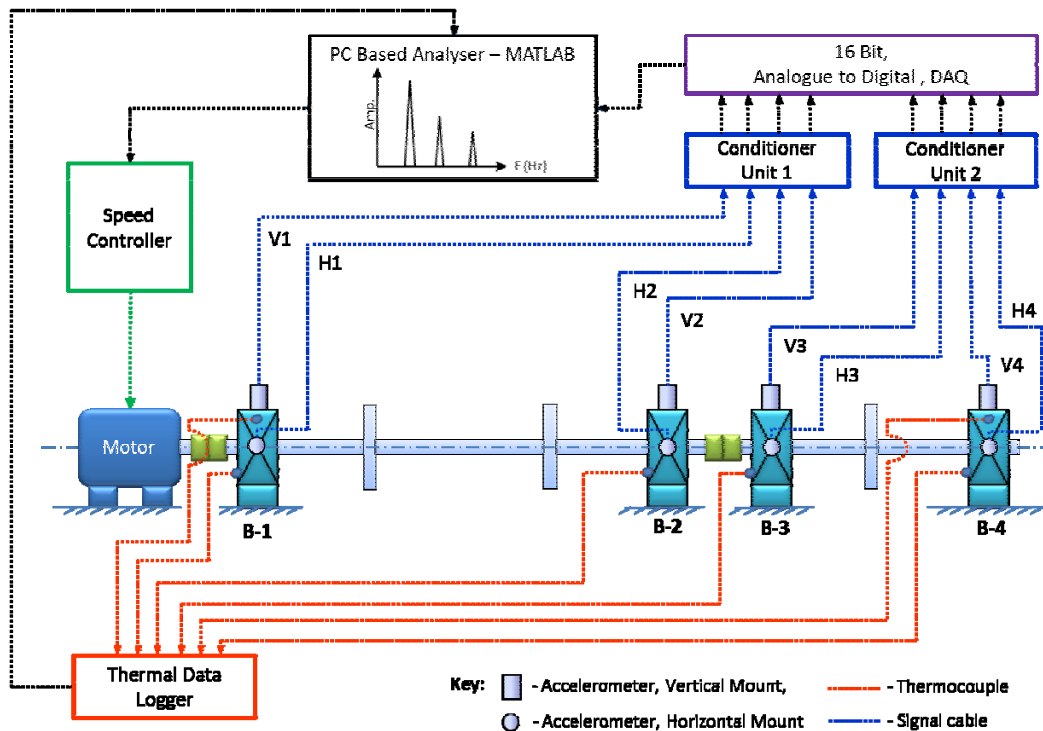


Figure 3. Schematic of software and instrumentation

3. Experiments

On starting system from rest, bearing temperatures were recorded for a period of ten minutes at 5 second intervals. Vibration data, at a sampling frequency of 10 kHz, was collected at the ten minute point for a total sample time of one minute. After each experiment the system was allowed to cool to ambient temperature before configuring the rig for a different scenario. Experiments were performed at 2400 rpm (40 Hz). Data for the healthy machine condition was first collected in order to establish baseline conditions for the rig. Data were then collected for three fault conditions; cracked rotor, rotor rub and coupling misalignment. The cracked rotor condition was simulated with the crack in three different positions. In each case a “breathing crack” (Sabnavis et al, 2004),

with a depth of 20% shaft diameter was created (see Figures 4(a),(b)).

Rub was simulated by a Perspex apparatus consisting of a base bolted to the lathe bed (at 115 mm from bearing 4) and a stand with a 22 mm diameter hole drilled parallel to the axial centre line of the shaft. The shaft passes through the hole and rub its inner bore (see Figure 5). Misalignment was the final scenario tested in order to minimise the effect of any residual misalignment that could be retained in the system after testing. A steel shim was installed under Bearing 3 housing to induce angular misalignment in the y-z plane across the rigid coupling located between Bearing 2 and Bearing 3 (see Figure 6). Further details of experiments done are given by Nembhard, et al (2013b). Table 1 summarizes the experiments and data collection procedure employed.

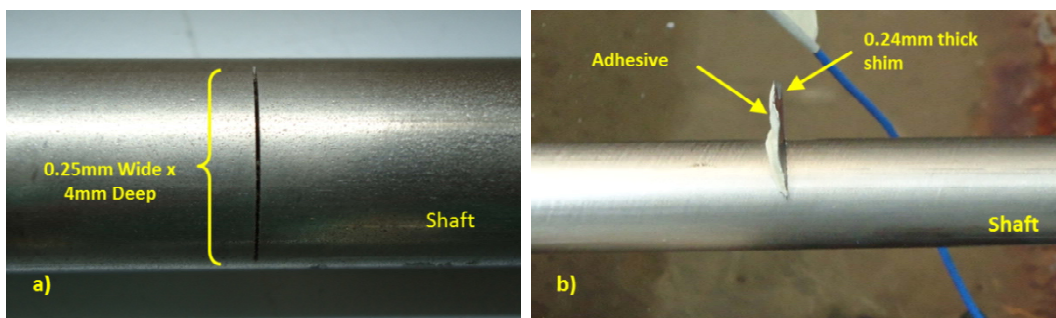


Figure 4. Details of apparatus used for rub simulation

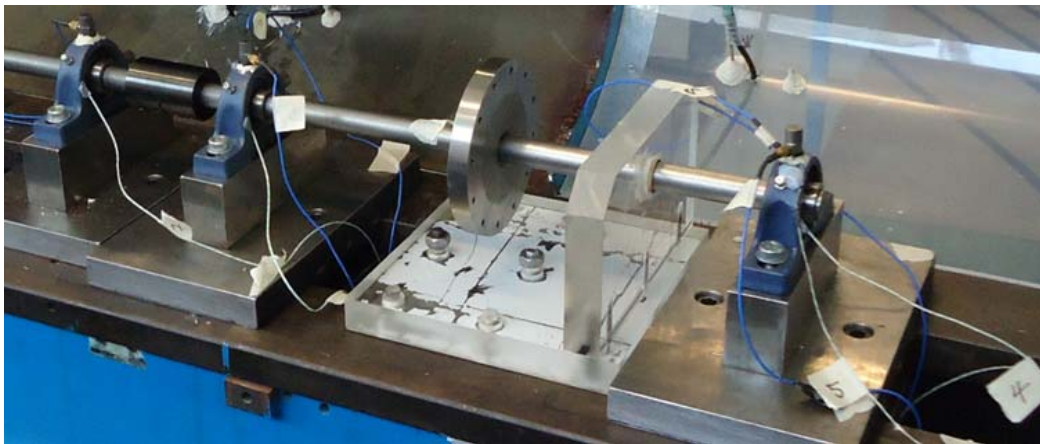


Figure 5. Close up of apparatus used for rub simulation between bearing 3 and bearing 4

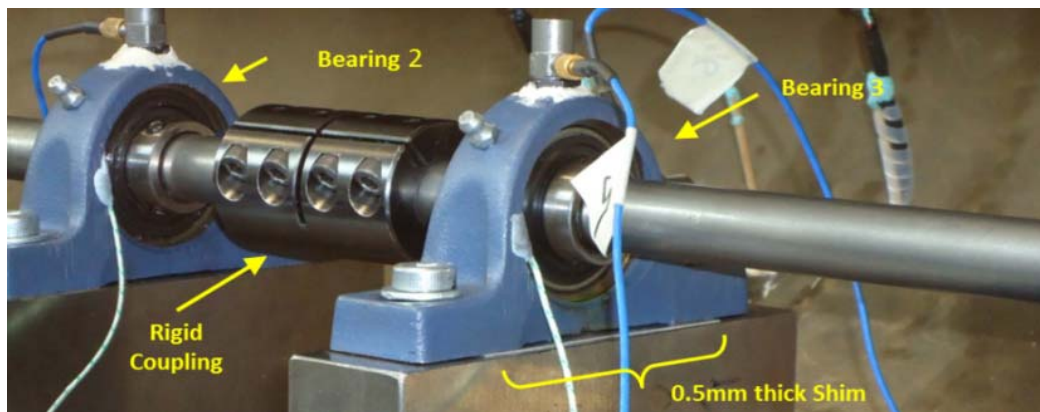


Figure 6. Details of Misalignment simulation at Bearing 3.

Table 1. Summary of experimental procedure used. One fault scenario was simulated at a time

No	Code*	Scenario Name
1	Healthy	Healthy
2	Cr Nr1	Crack near Bearing 1
3	Cr Nr2	Crack near Bearing 2
4	Cr Nr3	Crack near Bearing 3
5	Mlign	Misalignment
6	Rb Nr4	Rub near Bearing 4

*Same nomenclature is used in figures throughout rest of paper

4. Data Analysis

For each machine condition, the acceleration spectrum was generated from data measured in the horizontal radial direction between 5 Hz and 1 kHz. Each spectrum was analysed to gain insight into to the condition.

Principal Component Analysis (Jolliffe, 2002) was then performed; first with vibration data only and then with vibration and temperature data. Firstly, for each machine condition, the measured vibration data was segmented into 20 observations. Each observation was used to compute one time domain feature (root mean square [rms]) and three

frequency domain features (amplitudes of 1x, 2x and 3x harmonic components). Each bearing location was treated as a separate set of features. Hence a total of 16 features (4 bearings x 4 features) were computed. These were used to populate a feature matrix, X_v , for loading to the PCA algorithm. Each scenario simulated was treated as a different set of observations; hence matrix X_v would have 16 rows (features) and 120 columns (6 scenario x 20 observations). Before computing of Principal Components (PCs), each element in X_v was converted to zero mean and unit variance (Jolliffe, 2002; Elnady, et al, 2012).

Temperature measurements were processed to add to this vibration data. Since temperatures were recorded during machine run up it was necessary to extrapolate it to obtain steady state bearing temperatures and for this a simple thermodynamic model of the bearing plus curve fitting process were used. Assuming the majority of heat loss from a bearing was via conduction to the steel pedestals, which could have acted as a large heat sink, the bearing temperature change values would be as shown in Equation (1).

$$\Delta T = (T_{max} - T_o)e^{-At} \quad (1)$$

(where ΔT is temperature increase, T_{max} is steady state temperature, T_o is ambient temperature, A is an arbitrary variable and t is time).

Unknown variables in the equation for each condition were adjusted until the model (dashed lines) matched the warm up curves (solid lines) as shown in Figure 7(a). These variables were then used to generate full steady state curves (as shown in Figure 7(b)) for each fault condition. Full interrogation of the acceleration spectra was also done to ascertain if any bearing fault was present; as this would have affected the temperature measurements. The steady state temperatures calculated for each bearing were included as an additional feature, which resulted in a 20 x 120 feature matrix, X_{t+v} . The process of normalizing elements in X_{t+v} was repeated and PCs were calculated.

5. Results and Discussion

5.1 Spectral Analysis of vibration data only

Figure 8 shows the typical amplitude spectra at Bearing 2 for all conditions tested. It can be seen that the method did give an indication of the presence of fault conditions, as there were noticeable increases in the 1x component for all fault conditions relative to the healthy spectrum. However, fault diagnosis was not possible as different faults generated similar spectral features. In an attempt to improve the diagnosis, the amplitudes of the 4x, 3x and 2x harmonic components for each bearing location at all conditions tested was normalized with their respective 1x component. These were used to generate plots of the normalized 3x harmonic component against the normalized 2x harmonic component and the normalized 4x harmonic component against the normalized 2x harmonic component, as shown in Figures 9(a) and 9(b) respectively. The main objective of normalizing with the 1x component is to remove the effects of unbalance which would be present across the spectrum. Consequently this would leave the spectral features present fully representative of the condition present on the rig. It was expected that different faults would form clusters in each plots, however, the results obtained did not show any useful discriminative feature. As expected, it seems the simple spectrum is not adequate for the diagnosis of these simulated faults without phase information (Sinha, 2002; Sinou, 2009).

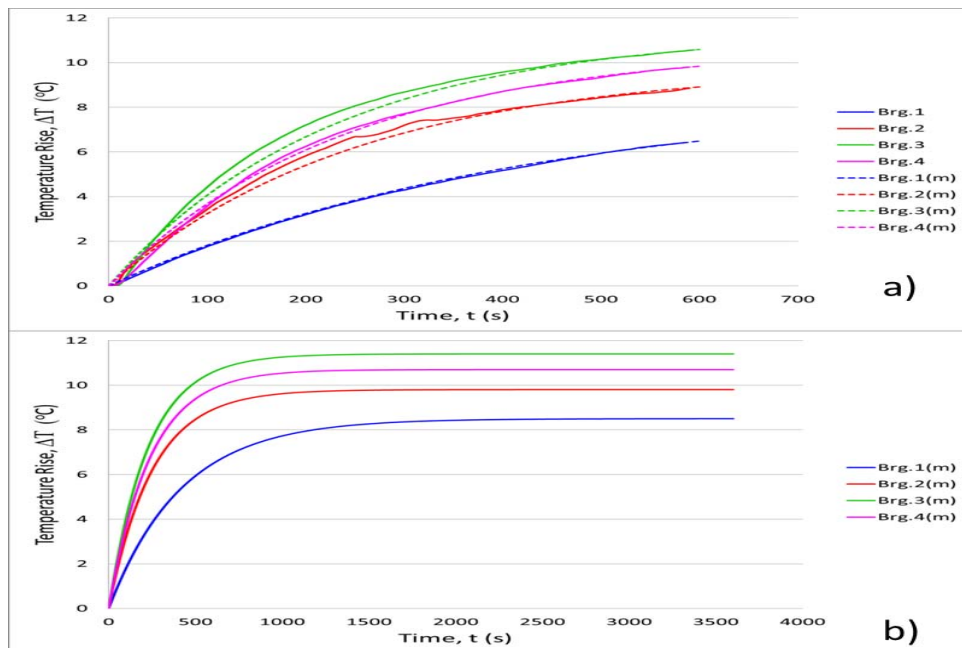


Figure 7. Sample showing progression of temperature trends in curve fitting process: a) transient curve fitting and b) generation of steady state curves

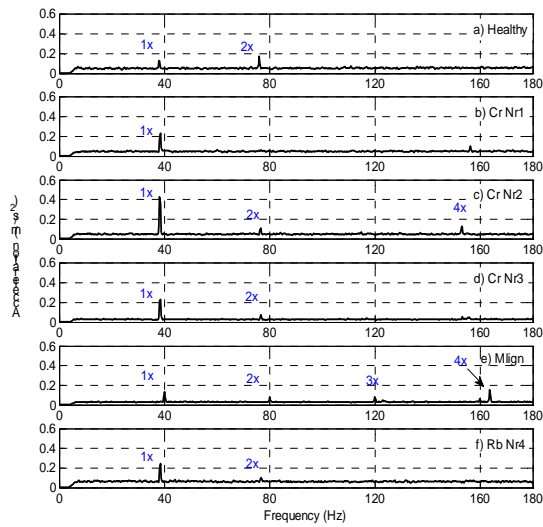


Figure 8. Typical amplitude spectra at Bearing 2 for all conditions tested.

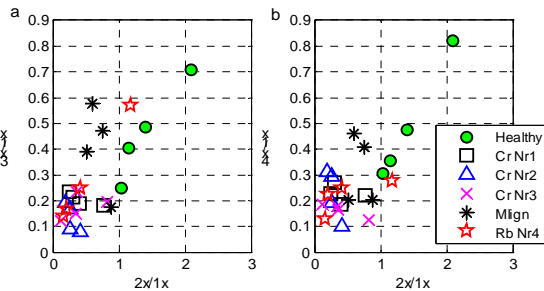


Figure 9. Comparison of spectral features for all conditions tested at 40 Hz: Healthy, Crack near Bearing 1, Crack near Bearing 2, Crack near Bearing 3, Misalignment and Rub near Bearing 4.

5.2 Fault Classification with vibration data only

Figure 10 shows a two dimensional (2D) PC plot which correlates the 2nd PC (PC2) against the 1st PC (PC1). Healthy condition did not occupy a defined space as there was some overlap with it and the Rub near bearing 4 data points. It was also observed that there was overlap between Misalignment and Crack near bearing 1 and 3 data. This is analogous to results obtained in the spectrum analysis (see Figure 8) where it was not possible to distinguish cracked rotor from misalignment. It therefore appears that PCA with vibration data alone is no more useful than spectrum analysis in this case.

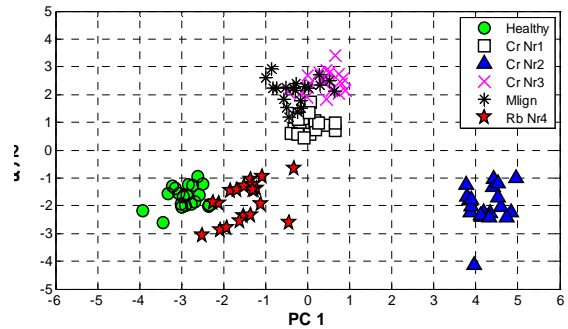


Figure 10. Fault Classification by PCA without Temperature - 40 Hz

5.3 Fault Classification with vibration and temperature data

Figure 11 shows the 2D PC plot that was produced. It can be seen that the addition of temperature fully separates healthy from all faulty data. The overlap between Misalignment and Crack near bearing 1 and 3 that was noticed in PCA with vibration data only (in Figure 10) does not exist in this plot. It was interesting to note that the Crack near bearing 2 condition was mostly unperturbed by the addition of temperature. Notwithstanding, the addition of temperature puts each fault condition in a clearly defined region, which may be useful for fault diagnosis. Additionally, when compared to the simple spectrum in Figure 8(c); where Crack near bearing 2 was observed to be the most severe fault (possessing the largest 1x component and with noticeable increase in 2x harmonic component with respect to the healthy spectrum), a similar observation is made here, as the said condition has the greatest separation from the healthy case. Therefore, in addition to fault classification, it seems this method may be able to provide useful information on fault severity. Further experimentation would be required to verify this.

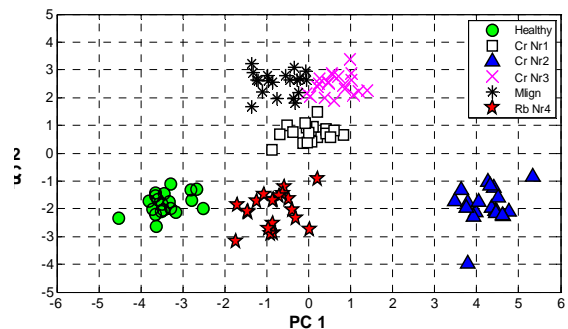


Figure 11. Feature classification by PCA, with Temperature - 40 Hz.

Conclusion

A fault diagnosis technique for rotating machinery, rotor-related faults is proposed using a single vibration sensor together with a simple temperature sensor on each bearing. Initial trials show that supplementing vibration data with

temperature measurements gives better separation of healthy and faulty data, allowing clearer diagnosis of faults when compared with vibration data alone. The proposed method also seems to be simple and non-intrusive and thus have the potential for future application. However further experimentation on different rigs with different faults is required to fully explore the potential and validate the usefulness of the method.

Acknowledgments. A. D. Nembhard wishes to sincerely thank the Commonwealth Scholarship Commission for affording him the PhD Commonwealth Scholarship to the UK from Jamaica to pursue the current research. The author also wishes to acknowledge that the contents of this paper is a slight modification of works presented at the 2013 Conference on Condition Monitoring of Machinery in Non-Stationary Operations (CMMNO 2013).

References

1. British Standards Institution, 2009. *ISO 10816-1:1995+A1:2009 Mechanical vibration – Evaluation of machine vibration by measurement of on non-rotating parts – Part 1: General guidelines*. London: BSI.
2. Craig, M., Harvey, T. J., Wood, R. J. K., Masuda, K., Kawabata, M. and Powrie, H. E. G., 2009. *Advanced condition monitoring of tapered roller bearings, Part 1*. Tribology International, 42(11-12), pp. 1846-1856.
3. Elbhbah, K and Sinha, J. K. *Vibration-based condition monitoring of rotating machines using a machine composite spectrum*. Journal of Sound and Vibration, 332 (2013), pp. 2831-2845.
4. Elnady, M. E., Sinha, J. K. and Oyadiji, S. O., 2012. *Condition monitoring of rotating machines using on-shaft vibration measurement*. In: IMechE, 9th International Conference on Vibrations in Rotating Machinery. London, UK 11-13 Sep 2012. Springer.
5. Gaberson, H. A., 1996. *Rotating machinery energy loss due to misalignment*. Energy Conversion Engineering Conference 1996, IECEC 96, Proceedings of the 31st Intersociety, 3, pp.1809-1812.
6. Jolliffe, I. T., 2002. *Principal Component Analysis*. 2nd ed. New York: Springer.
7. Li, W., Shi, T., Liao, G. and Yang, S., 2003. *Feature extraction and classification of gear faults using principal component analysis*. Journal of Quality in Maintenance Engineering, 9(2), pp. 132-132.
8. Liying, J., Xinxin, F., Jianguo, C. and Zhonghai, L., 2012. *Fault detection of rolling element bearing based on principal component analysis*. In: Proceedings of the 2012 24th Chinese Control and Decision Conference (CCDC). New Jersey, USA 23-25 May 2012. IEEE.
9. Nembhard, A. D., 2011. *Comparison of Thermal and Vibration Analyses for the Condition Monitoring of Rotating Machines*. MSc. The University of Manchester.
10. Nembhard, A. D., Sinha, J. K., Pinkerton, A. and Elbhbah, K., 2013a. *Condition Monitoring of Rotating Machines using Vibration and Bearing Temperature Measurements*. In: International Conference on Condition Monitoring of Machinery in Non-Stationary Operations (CMMNO). Ferrara, Italy 8-10 May 2013. Springer.
11. Nembhard, A. D., Sinha, J. K., Pinkerton, A. J., and Elbhbah, K., 2013b. *Combined Vibration and Thermal Analysis for the Condition Monitoring of Rotating Machinery*. Manuscript under preparation.
12. Sabnavis, G., Kirk R. G., Kasarda, M. and Quinn, D., 2004. *Cracked shaft detection and diagnostics: A literature review*. The Shock and Vibration Digest, 36(4), pp. 287-296.
13. Sinha, J. K., 2002. *Health Monitoring Techniques for Rotating Machinery*. Ph.D. University of Wales Swansea (Swansea University).
14. Sinha, J. K. and Elbhbah, K., 2013. *A future possibility of vibration based condition monitoring of rotating machines*. Mechanical Systems and Signal Processing, 34(1-2), pp. 231-240.
15. Sinou, J. J., 2009. *Experimental response and vibrational characteristics of a slotted rotor*. Communications in Nonlinear Science and Numerical Simulation, 14(7), pp. 3179-3194.
16. Yong-Wei, T. and Jian-Gang, Y., 2011. *Research on vibration induced by the coupled heat and force due to rotor-to-stator rub*. Journal of Vibration and Control, 17(4), pp. 549-566.

NOVEL INTUITIVE HIERARCHICAL STRUCTURE FOR CONDITION MONITORING SYSTEM OF WIND TURBINES

Tomasz BARSZCZ, Marcin STRĄCZKIEWICZ

AGH University of Science and Technology, Department of Robotics and Mechatronics,
al. Mickiewicza 30, 30-059 Kraków, Poland, e-mail: tbarszcz@agh.edu.pl

Summary

The field of condition monitoring (CM) systems has developed significantly in recent decade. Due to constant improvement of embedded computing, complex vibration data processing can be now implemented for a much larger group of machines, e.g. wind turbines.

One of the key outcomes of this process is increase in the number of signal features calculated online. Instead of a dozen of broadband values, we now have more than a hundred for a typical wind turbine. Such a situation creates information overload for the operators. On one hand, it is now possible to detect machine failure at an early stage, but on the other – a person monitoring a few dozens of turbines, each generating over a hundred features is not able to properly organize all the information from CM systems.

Therefore, we have proposed the hierarchical informational structure for condition monitoring system of wind turbines, based on the data fusion methods. The information about feature values and statuses is combined into higher levels, e.g. main bearing, gearbox and generator together with the information about its severity and novelty.

Keywords: data fusion, condition monitoring, fault detection and identification, vibration, wind turbines

NOWATORSKA INTUICYJNA STRUKTURA HIERARCHICZNA SYSTEMU MONITOROWANIA STANU TURBIN WIATROWYCH

Streszczenie

Na przestrzeni ostatniego dziesięciolecia zaobserwować można było szczególny rozwój na polu monitorowania stanu maszyn i urządzeń. Stało się tak dzięki wykorzystaniu bardziej zaawansowanych systemów wbudowanych oraz skomplikowanych algorytmów przetwarzania sygnałów drgań, które obecnie mogą być zastosowane do oceny stanu znacznie większej grupy maszyn, takich jak np. turbiny wiatrowe.

Jednym z najważniejszych efektów tego procesu jest zwiększenie ilości wskaźników diagnostycznych, które mogą zostać obliczone w czasie rzeczywistym – zamiast kilkunastu wartości szerokopasmowych, obecnie otrzymuje się ich ponad sto dla typowej turbiny wiatrowej. W rezultacie prowadzi to do przeciążenia ilością informacji, jakie jest stanie przetworzyć wykwalifikowany pracownik utrzymania ruchu. Z jednej strony, istnieje obecnie możliwość wykrycia uszkodzenia maszyny w najwcześniejszym jego stadium, z drugiej natomiast – inżynier utrzymania ruchu monitorujący kilkadziesiąt turbin, z których każda generuje ponad sto wskaźników informujących o stanie maszyny, nie jest zdolny do właściwej oceny wszystkich informacji z systemu diagnostycznego.

W związku z tym, zaproponowana została hierarchiczna struktura informacyjna dla systemów monitorowania stany turbin wiatrowych oparta na metodach integracji danych. Informacja o wartościach oraz stanach wskaźników diagnostycznych łączy się na wyższych poziomach, tj. łożyska głównego, przekładni oraz generatora razem z informacją o ich o ważności oraz aktualności.

Słowa kluczowe: integracja danych, monitorowanie stanu, wykrywanie i identyfikacja uszkodzenia, analiza drgań, turbiny wiatrowe

1. INTRODUCTION

Nowadays condition monitoring (CM) systems are much more robust than, for instance, 10 years ago [1]. This is due to the accelerated development of complex signal processing techniques and computing effectiveness caused by demanding applications. Important field is wind power generation especially offshore [2, 3]. That in turn makes the diagnostic process of machinery more precise and quicker, since it

enables the maintenance engineer to detect fault development at the earliest stage it occurs. Many researchers develop new fault detection methods using numerous approaches, ranging from knowledge-based methods [4, 5] to numerous natural/soft computing techniques [6, 7]. There are also practical approaches, using data available from SCADA systems [8]. Important review papers in this field is [9].

On the other hand, the rapid development of diagnostic capabilities causes the information overload.

For example, in wind turbine industry, the maintenance engineer typically is obligated to analyze more than a hundred different diagnostic features that describe the technical state of each turbine. Examples of such might be root mean square, peak to peak and kurtosis as broadband indicators, and ball passing frequency of outer ring and higher harmonics presence as the narrowband ones. Gears are probably the most important component of wind turbines, therefore several new methods have been recently proposed [10, 11, 12, 13]. Taking into account all the features calculated from 6-8 vibration signals, for a wind park consisting of few dozens of wind turbines the amount of information is overwhelming. Responding to individual threshold violations may as a consequence lead to the situation when alarms that are crucial for the operation of machine and thus should be analyzed in the first place are pushed to the side by the minor ones.

Therefore there is a need to organize the diagnostic analyses (i.e. features) into the reasonable order (also referred as structure) to improve embracing diagnosis of machinery with growing number of diagnostic features by maintenance engineer. The proposed structure shall be both intuitive and accessible in order to increase proper justification of a problem and simplify the further maintenance steps.

The paper is organized as follows. After the introductory part the wind turbine design is briefly discussed along with typically used wind turbine diagnostic hierarchical structures that are used to describe technical state of the machine. Next, the proposal of more intuitive approach is presented. The block diagram is described together with new way of categorizing alarm level violations. Ideas of data fusion, alarm novelty and severity are discussed in the

separate subsections. The results are described and followed by the conclusions.

2. STATE OF THE ART

Since organization of diagnostic features is supposed to be easily interpretable for the maintenance engineer it shall be based on the scheme of turbines operation. Such arrangement is aimed at proper justification of machine operation, easier fault recognition and proper planning of further actions. Thus it is important to describe the kinematic chain of a typical wind turbine.

Such a kinematic scheme is presented in Fig. 1. The main rotor is driven by three blades and supported by the main bearing. It passes the torque to the planetary gearbox. Second bearing supporting the rotor is incorporated into the gearbox. The planetary gear has three planets, which are driven by the planet carrier. The planets transmit the torque to the sun gear, in the same time increasing the rotational speed. The sun shaft passes the torque from the planetary gear to the two-stage parallel gear. The parallel gear contains three shafts: the slow shaft clutched to the sun shaft, the intermediate (sometimes called middle) shaft and the high speed shaft, which drives the generator.

Typical requirement for wind turbine drive-train condition monitoring systems is to measure vibrations with six measurement channels that each covers separate area of drive-train [1, 3]. Namely: main bearing, planetary gearbox, 1st stage of parallel gearbox, 2nd stage of parallel gearbox, front of the generator (driven end – DE) and back of the generator (non-driven end – NDE).

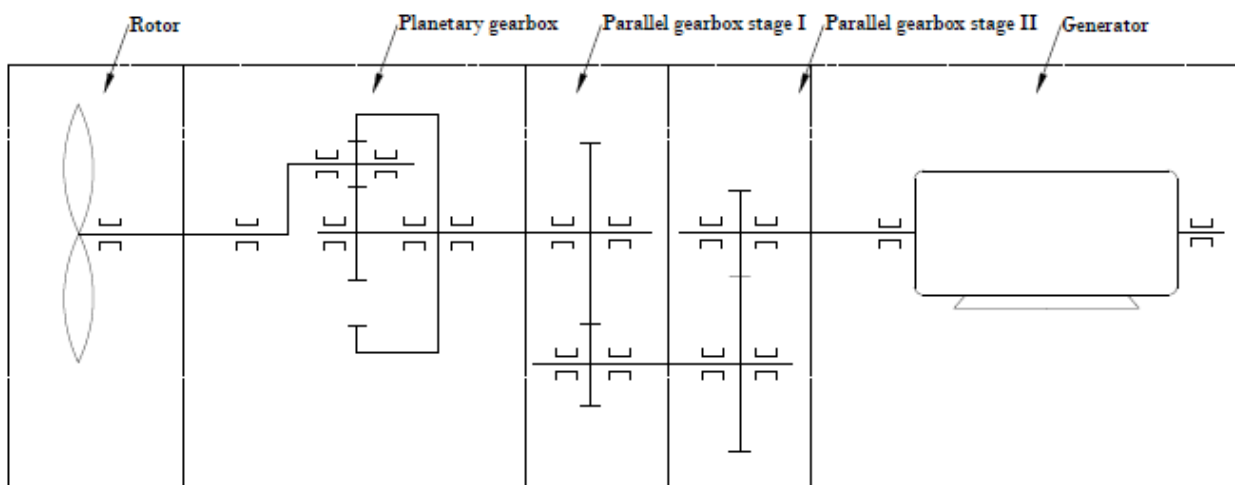


Figure 1. Kinematic scheme of a typical geared wind turbine

Additional required measurement covers rotational speed in order to assess acquired vibration data to proper operational state. In majority of condition monitoring systems dedicated for wind turbines value of generated power and wind speed are measured along with calculation of the diagnostic features.

There are two standard types of condition monitoring structural trees used in industrial condition monitoring systems that cover typical vibration analysis used in diagnostic process. The main idea in each of them is to reveal the information about the state of machine from the analysis level in the most convenient way.

2.1. Sensor based hierarchy

The first type of a structure is based on the measurement channels. It is presented in Fig. 2. As each of the hierarchical structures, it consists of information levels (or layers), which narrow down from the vibration signal analyses via the channel layer to the machine which is monitored, i.e. wind turbine. It is easy to notice that the channel layer corresponds with the (typically) six vibration sensors used for CM of wind turbine. First, the vibration data should be validated, as it was shown that wind turbines vibration depend highly on the operational state and are prone to multiple noise sources [14, 15]. Data acquired from the sensor is a subject of numerous analyses concerning energy levels, the character of its fluctuation and presence of particular frequency components in signals. The number of such signal features, and therefore elements on the analysis level, is typically in range of 150 as presented in Tab.1. The analyses most commonly used in wind turbine diagnostics are listed in the table attached at the end of the article (Tab. 2).

Tab. 1 Summary of basic commonly used wind turbine diagnostic features

Kinematic elements	Number of features per kinematic element	Total number of kinematic elements
Broadband	8	48
Narrowband bearings	4	72
Narrowband shafts	3	15
Narrowband gears	3	9
Total	-	144

In practice, the information about violated threshold limit on particular analysis is propagated directly to the higher level, i.e. to the channel layer and then to the examined machine. Such an approach impedes quick defect diagnosis and is time consuming.

It is due to the fact that the condition monitoring engineer receives information about raised level of one or more analyses located in the ‘analyses layer’. The features are not divided into segments regarded to the kinematic elements (whether it concerns gears, shafts or bearings) they indicate about. Therefore in such situation, one has to refer the particular (raised) analysis to the appropriate fault-susceptible element and estimate the severity of the problem by himself. Moreover, in the presented approach there is no separation between crucial alarms and simple informative warning. Similarly, such structure suffers lack of indication of novelty of the alarm. For example, if the engineer decides to deal with some major alarm at first, the remaining alarms verified as less important after time will still be unmarked, just as new ones, what might be misleading afterwards. As a result, the hierarchy presented in the Fig. 2 looks transparently, however it does require additional substantial time and effort to identify the severity of information

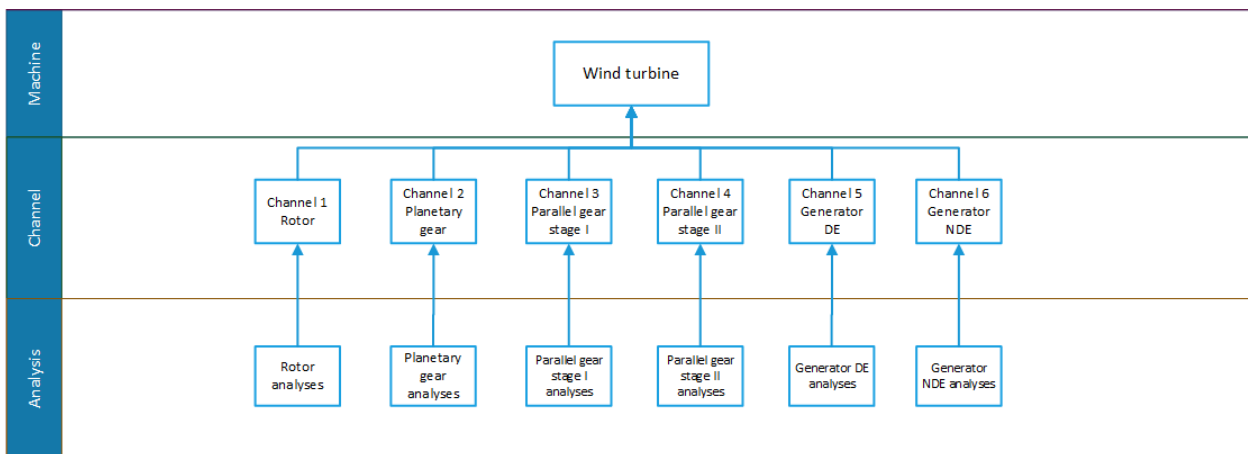


Figure 2. Hierarchical structure based on measurement channels

2.2. Component based hierarchy

The second standard type of condition monitoring hierarchy is based on the real mechanical elements in wind turbine, i.e. gears, shafts, bearings and rotor. It is intuitive from the practical point of view. It is presented in Fig. 3. For a single wind turbine the structure is divided into 5 main layers, namely:

- the machine that is being monitored,
- types of kinematic elements, i.e. gears, shafts, bearings and rotor,
- particular kinematic elements, e.g. planetary gear, generator shaft or main bearing,
- location of a sensor, one of six typically used sensor locations used for wind turbines, as mentioned above,
- signal features (i.e. analyses), used for fault detection of particular kinematic element at particular sensor location.

The main advantage of this approach is the ability to localize fault development according to the kinematic element, however it is hindered as well. Practically, the maintenance engineer has to deal with mix of the sensor locations within the structure. In fact it does not concern the engineer from which sensor the faulty signal used for the particular feature comes from. It is important whether the analysis level is high, its dynamic changes rapidly over time and whether the machinery may run for the time necessary for preparation of the repair or it has to be stopped immediately to prevent more serious breakdown.

It is always worth mentioning that early detection and preventing crash of machinery is one of the basic objective of CM systems. For instance, if the alarm

threshold violates for the middle shaft harmonic analysis, the system informs of the exceeding within the group of shafts, then on the middle shaft. Next the structure of the system reveals that the violation is obtained from signal measured on either stage I or II of parallel gearbox. Finally, the analysis related to particular harmonics of the shaft rotation are obtained. Such diffuse can be confusing. Separating shafts or bearings without placing them within the kinematic scheme makes finding the reason of potential fault more complex. Furthermore, the described structure does not carry information about the severity nor about the novelty of the alarm, similarly to the first type of hierarchy.

3. NEW HIERARCHICAL STRUCTURE

The proposed hierarchical structure aims to overcome problems and difficulties related to previously described structures. As presented in Fig. 4 the information about feature values and statuses is combined into higher levels, i.e. rotor, gearboxes and generator that correspond with the kinematics of a wind turbine. If diagnosis concerns bigger kinematic element it is categorised under such label, e.g. a malfunction of one of middle shaft's bearings falls into the following sections: middle shaft bearing, middle shaft, parallel gearbox, gears generally. It is because, at the first place, defect of the bearing affects operation of this particular shaft, subsequently parallel gearbox (it is not important which stage of the gearbox), and gears altogether.

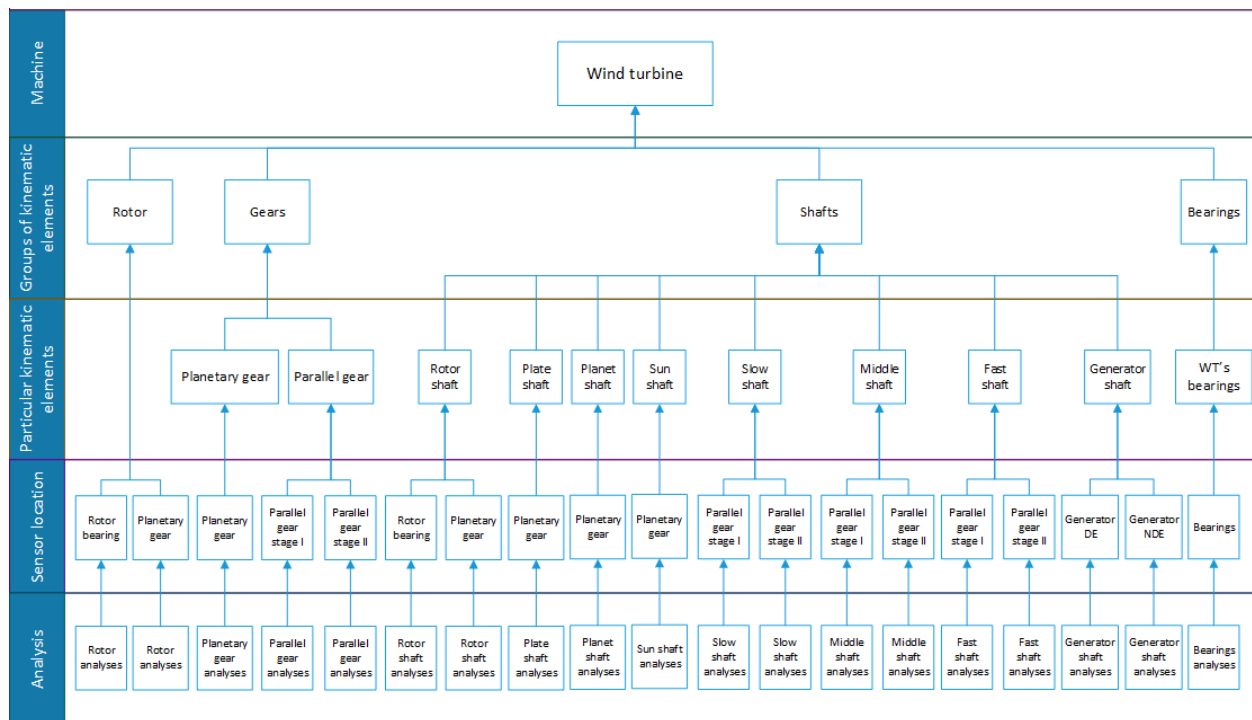


Figure 3. Hierarchical structure based on groups of kinematic elements

The significant amount of techniques performed within the analysis layer may be reduced using data fusion methods with no harm or even with a benefit to the correctness of evaluation. It is discussed in the subsections below along with procedures used to define the severity and novelty of alarms. The propagation of the alarm in the proposed structure assumes its flexibility and is described afterwards.

3.1 Severity

The main reason for introducing the severity feature is to help to distinguish the important information from not-so-important. The main approach to avoid the information overload is extension of signal parameters by adding the field of priority, which we will later call severity. The severity parameter should inform the operator how important is the message about a violation of an alert threshold. There should be 4-6 levels of severity, e.g.:

- critical,
- important,
- early warning,
- information

For example, the increase in the overall signal energy with dominant first harmonic component on the generator should be treated with the upmost priority. This can be a sign of an unbalance, leading to a catastrophic failure. On the other hand, a relatively small increase on the BPFO frequency is typically not

critical. It should be monitored, but there is no need to stop the machine and perform a maintenance action.

Severity should also depend on the rate of change of the feature. For a majority of mechanical faults in wind turbines, the process of the development is relatively slow and takes weeks or even months. If a situation is detected when the rate of change suggests a problem within a shorter time, e.g. hours, the user must be notified with much higher priority.

3.2 Novelty

The next extension of signal parameters, which we propose to take into account is the novelty of the information. Such an approach shall create a dynamic system, which uses the rules of human perception. In a live situation, when a small team must supervise several hundred machines, generating all together many thousands of features it is a normal situation that many threshold violations are active in the same time. There must be a method to attract the attention of operators to newly detected events. This should be achieved by increasing the weight of the information right after it is detected and decreasing it as it gets older.

One way to implement at least a part of this mechanism is to adopt the acknowledgement of events. The operator must manually acknowledge the information from the system about the threshold violation. The system shall store the time of detection and the time of acknowledgment. This is, however, only the basic level of such an approach.

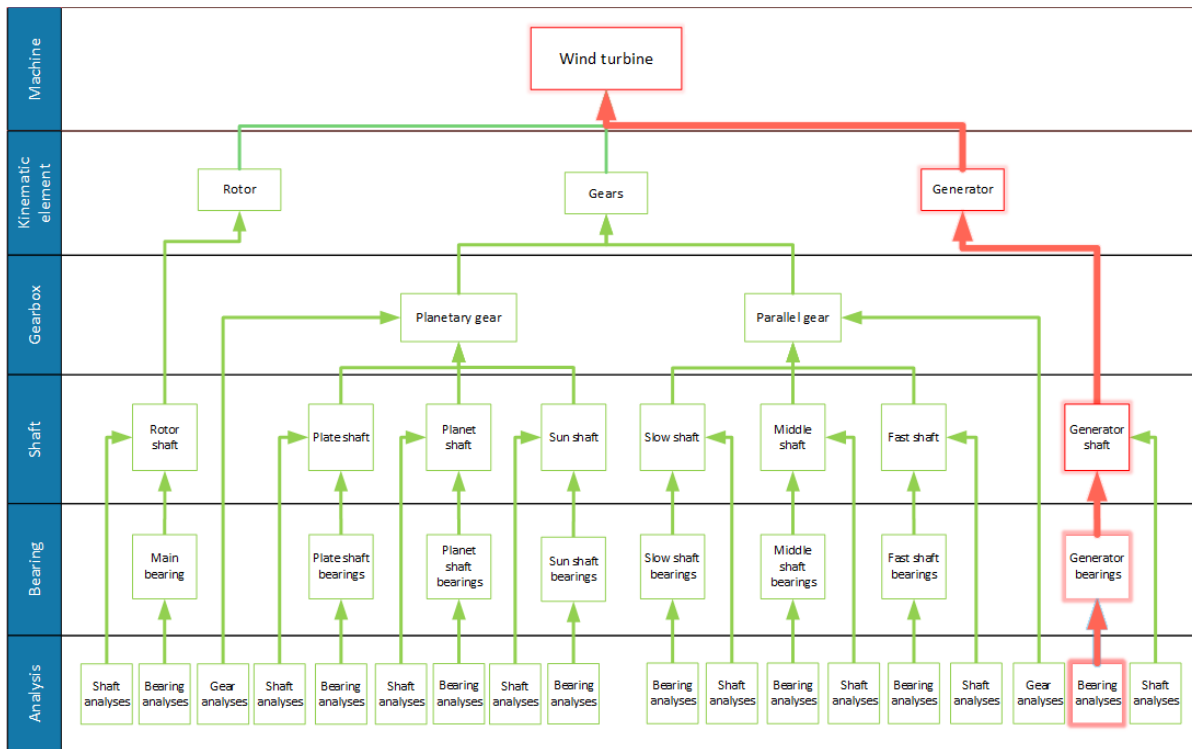


Figure 4. Hierarchical structure based on kinematic elements

3.3 Data fusion

The main reason to use the data fusion method is to decrease the amount of information [16, 17, 18]. The idea of employing data fusion methods for diagnostics of wind turbine comes from two facts. Firstly, for a single wind turbine one may distinguish more than a hundred diagnostic features, which creates information overload for the operators. Secondly, one does not need to know, for instance, which particular component of a rolling bearing generates an alarm, because the maintenance staff will replace the whole bearing anyway. Thus, information should be integrated to a form comprehensible for people without detailed diagnostic knowledge.

The integration of data is carried out at the analysis level. Its block design, presented in Fig. 5, enables synthesis of the features regarding to particular kinematic element of the machine.

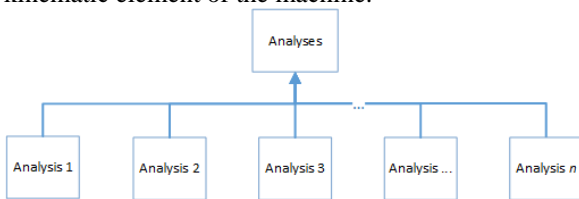


Figure 5. Hierarchical structure based on kinematic elements

The most efficient method available for data fusion is the weighted average of lower level signal features. It can be used for a single estimator of a gearbox state and it can be obtained from integration of harmonics using weighted average [19]:

$$\bar{x} = \frac{\sum_{i=1}^n w_i n_i}{\sum_{i=1}^n w_i} \quad (1)$$

where n_i represents i^{th} analysis and w_i stands for weight assigned to the i^{th} analysis. Such an approach does not need to follow exact model, where all the analyses are only at the lowest level. It is possible that more complex features, e.g. referring to modulations coming from the gearbox or from faulty bearings [20] or even to the whole machine [21, 22] can be integrated at a higher level.

Such a simple approach may also be used for combining information related to shaft's rotational speed harmonics or gear mesh harmonics.

3.4 Flexibility

If an informational hierarchy should be efficient, it also needs to be flexible. The hierarchy should take into account all the three proposed features. In such a system, if a threshold violation is detected on a lowest level, the information is propagated up to the top level of the wind turbine (see Figure 4). The different groups of users will move from the top to the level, which gives sufficient information for the observer. On the Fig. 4, such levels are:

- wind farm: the turbine number X has a problem
- single WT level: there is a problem with generator

- component: the generator bearing has a problem
- analysis: one of bearing parts (e.g. outer race) is damaged

In order to achieve the flexibility, users should be able to view the data from different angles. For example, one may need to see the most critical events, the most recent events, all the events referring to the generator etc.

4. CONCLUSIONS

In the paper we have proposed transparent, expanded and unequivocal hierarchical structure that simplifies diagnostic process for the maintenance engineer and enhances the correct fault recognition. The structure is built based on the approaches of severity and novelty were presented. Data fusion algorithms are proposed in order to limit diffuse of diagnostic information. Only relatively simple elements of the proposed hierarchy were shown in this paper, this issue is our main area of research.

Further research are necessary in this field. Main directions should be:

- determine the detailed structure for certain wind turbine types
- selection of more efficient data fusion techniques
- definition of normal states and a method to calculate the distance between one of "good" states and the current one

The real data (laboratory data, real wind turbines) should be applied to the proposed structure in order to fine tune the proposed information system.

The ultimate goal is implementation of the proposed method in a real world condition monitoring system.

REFERENCES

- [1] T. Gellermann, „Requirements for Condition Monitoring Systems for Wind Turbines,” Allianz, 2003
- [2] Wiggelinkhuizen, E., Verbruggen, T., Braam, H., Rademakers, L., Xiang, J., Watson, S., *Assessment of condition monitoring techniques for offshore wind farms*, (2008) Journal of Solar Energy Engineering, Transactions of the ASME, 130 (3), pp. 0310041-0310049
- [3] T. Barszcz, „Concept of monitoring and diagnostics of small and medium power rotating machinery”, *Diagnostyka*, nr 35, pp. 49-56, 2005
- [4] Lethe G., Kinne D., Terna I., *Dynamic simulation of a windturbine system calculating vibrations, loads, durability and acoustic response in a single cae environment*, European Wind Energy Conference and Exhibition 2009, EWEC 2009; Marseille; France; 16-19 March 2009
- [5] Barszcz T., Bielecka M., Bielecki A., Wójcik M., „Wind speed modelling using Weierstrass function fitted by a genetic algorithm”, *Journal of Wind Engineering and Industrial Aerodynamics*, Volume 109, October 2012, pp. 68-78
- [6] Barszcz T., Bielecki A., Wójcik M., „ART-type artificial neural networks applications for classification of operational states in wind

- turbines”, Lecture Notes in Computer Science, Volume 6114 LNAI, Issue PART 2, 2010, pp. 11-18
- [7] Barszcz T., Bielecka M., Bielecki A., Wójcik M., „Wind turbines states classification by a fuzzy-ART neural network with a stereographic projection as a signal normalization”, Lecture Notes in Computer Science, Volume 6594 LNCS, Issue PART 2, 2011, pp. 225-234
- [8] Yang, W., Tavner, P.J., Crabtree, C.J., Wilkinson, M., “Cost-effective condition monitoring for wind turbines”, (2010) IEEE Transactions on Industrial Electronics, 57 (1), pp. 263-271
- [9] Jardine A.K.S., Lin D., Banjevic D., "A review on machinery diagnostics and prognostics implementing condition-based maintenance", Mechanical Systems and Signal Processing Volume 20, Issue 7, October 2006, pp. 1483–1510
- [10] Zappala D., Tavner P.J., Crabtree C.J., “Gear fault detection automation using WindCon frequency tracking”, European Wind Energy Conference 2012, EWEC 2012; Copenhagen; Denmark; 2012.
- [11] Sawalhi N., Randall R. B., “Gear parameter identification in a wind turbine gearbox using vibration signals”, Mechanical Systems and Signal Processing, in press, DOI: 10.1016/j.ymssp.2013.08.017
- [12] Soua S., Van Lieshout P., Perera A., Gan T.H., Bridge B., “Determination of the combined vibrational and acoustic emission signature of a wind turbine gearbox and generator shaft in service as a pre-requisite for effective condition monitoring”, Renewable Energy Volume 51, March 2013, pp. 175-181
- [13] Jabłoński A., Barszcz T., “Instantaneous circular pitch cyclic power (ICPCP) - A tool for diagnosis of planetary gearboxes”, Key Engineering Materials Volume 518, 2012, pp. 168-173
- [14] Jabłoński A., Barszcz T., Bielecka M., „Automatic validation of vibration signals in wind farm distributed monitoring systems”, Measurement: Journal of the International Measurement Confederation Volume 44, Issue 10, December 2011, pp. 1954-1967
- [15] Jabłoński A., Barszcz T., “Validation of vibration measurements for heavy duty machinery diagnostics”, Mechanical Systems and Signal Processing Volume 38, Issue 1, 5 July 2013, pp. 248-263
- [16] Worden K, Staszewski WJ & Hensman JJ, *Natural computing for mechanical systems research: A tutorial overview*. Mechanical Systems and Signal Processing, Volume 25, Issue 1, 2011, pp. 4-111
- [17] Khazaei, M., Ahmadi, H., Omid, M., Moosavian, A., “Vibration condition monitoring of planetary gears based on decision level data fusion using Dempster-Shafer theory of evidence”, Journal of Vibroengineering 14 (2), pp. 838-851
- [18] Brodowski S., Bielecki A., “New specifics for a hierarchical estimator meta-algorithm”, Lecture Notes in Computer Science, Volume 7268 LNAI, Issue PART 2, 2012, pp. 22-29
- [19] T. Barszcz, A. Jabłoński, “Selected methods of finding optimal center frequency for amplitude demodulation of vibration signals”, Diagnostyka, nr 35, pp. 25-28, 2010/2
- [20] J. Urbanek, J. Antoni i T. Barszcz, „Detection of signal component modulations using modulation intensity distribution”, Mechanical Systems and Signal Processing, nr 28, pp. 399-413, April 2012
- [21] Urbanek J., Barszcz T., Zimroz R., Antoni J., „Application of averaged instantaneous power spectrum for diagnostics of machinery operating under non-stationary operational conditions”, Measurement: Journal of the International Measurement Confederation Volume 45, Issue 7, August 2012, pp. 1782-1791
- [22] Urbanek J., Barszcz T., Sawalhi N., Randall R.B., „Comparison of amplitude-based and phase-based methods for speed tracking in application to wind turbines”, Metrology and Measurement Systems Volume 18, Issue 2, 2011, Page 11



dr hab. inż. Tomasz BARSZCZ

Graduate of Electronic Eng at Politechnika Gdańska (1993r.). Received PhD in mechatronics in 1997r. (AGH). Has long experience of working with companies like ABB Zamech and ALSTOM Power. Author of many papers and books on machinery diagnostics.

Monitoring systems developed under his supervision were installed on several hundred machines worldwide.



mgr inż. Marcin STRĄCZKIEWICZ

PhD student in the Department of Robotics and Mechatronics, AGH University of Science and Technology. The main areas of his interests are digital signal processing and monitoring of machinery working in non-stationary conditions.

Appendix

Tab. 2 Diagnostic features assigned to kinematic elements of a typical wind turbine

Kinematic element	Bandwidth	Feature	Formula
General	Broadband	RMS – root mean square	$u_{rms} = \sqrt{\frac{1}{T} \int_0^T u^2(t) dt}$ (2)
	Broadband	PP – peak to peak	$u_{pp} = \max_{0 < t < T} (u(t)) - \min_{0 < t < T} (u(t))$ (3)
	Broadband	ZP – zero to peak	$u_{zp} = \max_{0 < t < T} (u(t))$ (4)
	Broadband	Crest factor	$C = \frac{u_{zp}}{u_{pp}}$ (5)
	Broadband	Kurtosis	$K = \frac{\mu^4}{\sigma^4} = \frac{\sqrt{\frac{1}{N} \sum_{i=1}^N (x_i)^2}}{\sqrt{\frac{1}{N} \sum_{i=1}^N (x_i - \bar{x})^2}}$ (6)
Bearing	Narrowband	BPFO – ballpass frequency of outer race	$f = \frac{n}{2} f_r \left(1 - \frac{d}{D} \cos \alpha\right)$ (7)
	Narrowband	BPFI – ballpass frequency of inner race	$f = \frac{n}{2} f_r \left(1 + \frac{d}{D} \cos \alpha\right)$ (8)
	Narrowband	FTF – fundamental train frequency	$f = \frac{1}{2} f_r \left(1 - \frac{d}{D} \cos \alpha\right)$ (9)
	Narrowband	BSF (RSF) – ball (roller) spin frequency	$f = \frac{D}{2d} \left(1 - \left(\frac{d}{D} \cos \alpha\right)^2\right)$ (10)
	Narrowband	Cepstrum	$C_A(\tau) = F^{-1}\{\log A(f)\}$ (11)
	Narrowband	Bispectrum	$bisp(f_1, f_2) = \frac{1}{M} \sum_{m=1}^M X_m(f_1) \cdot X_m(f_2) \cdot X_m^*(f_1 + f_2)$ (12)
Shaft	Narrowband	Higher harmonics of rotational speed	$\begin{aligned} f &= f_r, \\ f &= 2f_r, \\ f &= 3f_r. \end{aligned}$ (13)
Gear	Narrowband	TSA – time synchronous averaging	$y_a(t) = \frac{1}{N} \sum_{n=0}^{N-1} y(t + nT)$ (14)
	Narrowband	GMF – gear meshing frequency	$\begin{aligned} f_{GMF} &= GMF = f_1 \cdot v_1 = f_2 \cdot v_2 \\ f_{GMF} &= 2GMF \\ f_{GMF} &= 3GMF \end{aligned}$ (15)
	Narrowband	Cepstrum	As above
	Narrowband	Bispectrum	As above

Notation in the table:

u – time domain signal, f_r - shaft speed, n - number of rolling elements, α - the angle of the load from the radial plane, d - ball diameter, D - pitch diameter (distance between opposing balls in a bearing); F - Fourier transform, A - Amplitude, f - narrowband frequency; f_1 - fundamental frequency, f_2 - first harmonic frequency, X_m - short-time Fourier transform, t - time, T - time interval for avering.

COINTEGRATION METHOD FOR TEMPERATURE EFFECT REMOVAL IN DAMAGE DETECTION BASED ON LAMB WAVES

Phong Ba DAO

AGH University of Science and Technology, Faculty of Mechanical Engineering and Robotics,
Department of Robotics and Mechatronics, Aleja Mickiewicza 30, 30-059 Krakow, Poland
E-mail: phongdao@agh.edu.pl

Summary

The paper presents an application of the cointegration technique for temperature effect removal in Lamb wave data. The method is based on the analysis of cointegration residuals and stationary statistical characteristics. The experimental results on Lamb wave responses from undamaged and damaged aluminium plates show that the cointegration process can remove undesired temperature effects and accurately detect damage.

Keywords: structural health monitoring, Lamb waves, cointegration, temperature effect removal

WYKRYWANIE USZKODZEŃ PRZY POMOCY FAL LAMBA - KOMPENSACJA WPŁYWU TEMPERATURY OPARTA O METODĘ KOINTEGRACJI

Streszczenie

Fale Lamba stosowane są do wykrywania uszkodzeń w konstrukcjach płytowych. Wpływ temperatury na amplitudę oraz fazę fal Lamba jest jedną z głównych przeszkód w powszechnym zastosowaniu tej metody w praktyce inżynierskiej. W pracy zastosowano metodę kointegracji do kompensacji wpływu temperatury na propagację fal Lamba. Metoda oparta jest na badaniu stacjonarności sygnałów. Zastosowane podejście pokazane jest na przykładzie wykrywania szczelin zmęczeniowych w płytach aluminiowych. Wyniki pokazują, że metoda kointegracji skutecznie usuwa z fal Lamba wszystkie efekty związane z wpływem temperatury, przyczyniając się do wykrycia badanych uszkodzeń.

Słowa kluczowe: wykrywanie uszkodzeń w konstrukcjach, fale Lamba, kointegracja, kompensacja wpływu temperatury

1. INTRODUCTION

Lamb waves are the most widely used guided ultrasonic waves for structural health monitoring (SHM) applications. Various damage detection methods – based on Lamb waves – have been developed for the last few decades, as reported and reviewed in [1–5]. However, despite many research developments, practical engineering applications are still limited. This is not only due to complex physical wave propagation mechanisms (e.g. multiple modes or dispersive nature) but also due to damage sensitivity that is often affected by operational and environmental conditions [6]. It appears that temperature variability (instantaneous, daily or seasonal) is one of the major problems [7,8]. Therefore it is important for practical applications of Lamb waves to develop methods that are sensitive only to damage but insensitive to operational-environmental conditions, to avoid false-positive and false-negative damage detection scenarios.

Various approaches were developed to deal with undesired effects of operational and environmental variability in SHM data, as presented in [6]. The

cointegration method – developed originally from the field of econometrics [9] – has been proposed recently in process engineering for abnormality detection [10] and in structural damage detection for the removal of temperature effect from bridge vibration data and Lamb wave responses [11, 12]. The major idea used in these investigations is based on the concept of stationarity of time series. Monitored variables are cointegrated to create a stationary residual whose stationarity represents normal condition. Then any departure from stationarity can indicate that monitored structures are no longer operating under normal condition.

This paper builds upon previous investigations on the cointegration technique for trend removal in Lamb wave data. The major objective is to present a new approach based on cointegration for the removal of temperature variability and damage detection based on Lamb waves. The augmented Dickey-Fuller (ADF) test [13] is used not only to test the degree of non-stationarity of variables, but also to create a damage detection indicator.

2. PREVIOUS STUDY ON TEMPERATURE EFFECT REMOVAL IN LAMB-WAVE-BASED SHM

Lamb-wave-based SHM in principle is based on guided ultrasonic waves introduced into a structure at one point and sensed at a different location. Damage in a structure can be then identified by monitoring changes in the output signal. Signal attenuation and/or mode conversion is sufficient to detect various types of damage such as cracks in metallics or delamination in composites [2]. Lamb-wave-based damage detection techniques have shown great potential for SHM applications since they feature [3]: (1) the ability to inspect large structures as well as insulated structures (e.g. pipeline under water); (2) the ability to examine the entire cross-sectional area of a structure including both internal damage and surface defects; (3) the capability of classifying various types of damage using different wave modes; (4) excellent sensitivity to damage with high precision of identification; and (5) low energy consumption and great cost-effectiveness.

However, as discussed above temperature variability has a dominant effect on Lamb waves therefore various approaches have been proposed to overcome this effect in which some representative works are summarised hereinafter.

The early proposed approaches are based on soft computing [14, 15]. The first publication reported a unique combination of time series analysis, neural networks, and statistical inference techniques. Several methods – such as feature extraction based on signal decomposition and principle component analysis – were investigated in the second publication. Various machine learning tools that could be used in these approaches were reviewed and extensively discussed in [16].

Two different methods were presented in [17]. The first one proposed to record reference signals over a range of temperatures and then to use these signals in the ensemble that best matches a subsequent signal for subtraction. The second method relies on the improvement of sensitivity via an exact compensation scheme for the temperature change. Both methods would require large reference databases in practical applications. This could be often expensive and not always possible. Efficient modeling could ease this task, as demonstrated in [18].

A reference-free approach – based on properties of fundamental Lamb wave mode propagation – has been proposed in [19]. Baseline subtraction methods – based on multiple baselines – have been proposed in [8]. Instead of using a single baseline for subtraction purposes, a series of baselines are used, covering the range of operating conditions of the structure. This approach is known as Optimal Baseline Selection (OBS). More recently, a new Baseline Signal Stretch (BSS) method have been

proposed in [20]. A combined strategy that uses both OBS and BSS was also considered in this work.

A model that accounts for relevant temperature-dependent Lamb wave propagation parameters was investigated in [7]. This work underlines the effect of temperature on transducer properties. The role of piezoceramic adhesive layers in structures exposed to elevated temperatures was investigated.

3. COMMON TREND REMOVAL BY USING THE COINTEGRATION METHOD

For the sake of completeness this section briefly introduces the concept of cointegration. Firstly, stationarity and non-stationarity are explained.

For a given time series y_t presented in the form of the first-order Auto-Regressive process $AR(1)$, which is defined as

$$y_t = \phi y_{t-1} + \varepsilon_t \quad (1)$$

where ε_t is an independent Gaussian white noise process with zero mean, three different time series can be distinguished. These are [21]:

- stationary time series ($|\phi| < 1$) – the process looks irregular, but always oscillates around the mean;
- non-stationary time series ($\phi > 1$) – the process is initially smooth but eventually becomes rough;
- random walk ($\phi = 1$) – the process moves up and down; it behaves as a non-stationary time series, but slowly.

In practice time-invariant behaviour can be indicated by statistical moments of the process. A stationary process would have time invariant moments while a non-stationary process would exhibit some time dependence in moments. It is well known that the most simple stationary time series is the independent Gaussian white noise process [21]. The time series y_t in Eq. (1) is an integrated series of order 1, denoted $I(1)$, if it has the form of random walk (i.e. $\phi = 1$) without a trend [22]. When $\phi = 1$, Eq. (1) yields

$$\Delta y_t = y_t - y_{t-1} = \varepsilon_t \quad (2)$$

This clearly shows that, the first difference of y_t is just a white noise process ε_t , i.e. a stationary time series. The consequence is that a non-stationary $I(1)$ time series becomes a stationary $I(0)$ time series after the first difference. In a similar way, a non-stationary $I(2)$ time series would require differencing twice to induce a stationary $I(0)$ time series. The number of differences required to achieve stationarity is called the order of integration. Thus time series of order d are denoted as $I(d)$.

Following this short introduction, the concept of cointegration can be introduced. Let

$Y_t = (y_{1t}, y_{2t}, \dots, y_{nt})^T$ denote an $(n \times 1)$ vector of $I(1)$ time series. Then Y_t is cointegrated if there exists an $(n \times 1)$ vector $\beta = (1, -\beta_2, \dots, -\beta_n)^T$ such that

$$\underbrace{\beta^T Y_t}_{\text{Cointegration residual}} = \underbrace{[1 \quad -\beta_2 \quad \dots \quad -\beta_n]}_{\text{normalized cointegrating vector}} \underbrace{\begin{bmatrix} y_{1t} \\ y_{2t} \\ \vdots \\ y_{nt} \end{bmatrix}}_{\text{cointegrated variables}} \sim I(0)$$

In other words, the non-stationary $I(1)$ time series in Y_t are cointegrated if there exists (at least) a linear combination of them that is stationary or has the $I(0)$ status. The linear combination, denoted $\beta^T Y_t \sim I(0)$, is referred to as a *cointegration residual* or a long-run equilibrium relationship between time series [22]. The β vector is called a *normalized cointegrating vector*. It can be noticed that the action of creating the cointegration residual ($u_t = \beta^T Y_t$) is the action of projecting the $(n \times 1)$ Y_t vector on the cointegrating vector β , or in other words applying the cointegrating vector β to the $(n \times 1)$ Y_t vector.

Testing for cointegration is in essence testing for the existence of long-run equilibriums (or stationary linear combinations) among the elements of Y_t [22]. However, before any attempt is made to test for that existence, two constraints (or pre-requirements) related the time series in Y_t need to be fulfilled. Firstly, the analysed time series must *have at least a common trend*. Secondly, the analysed time series must *have the same degree of non-stationarity*, i.e. they must be integrated of the same order.

If the $(n \times 1)$ vector of $I(1)$ time series in Y_t is cointegrated with $0 < r < n$ cointegrating vectors then there are $n - r$ common stochastic trends [22]. For n variables, the cointegration process may create as many as $n - 1$ linearly independent cointegrating vectors. To illustrate the duality between cointegration and common trends, let

$$Y_t = (y_{1t}, y_{2t})^T \sim I(1) \quad \text{and} \quad \varepsilon_t = (\varepsilon_{1t}, \varepsilon_{2t}, \varepsilon_{3t})^T \sim I(0) \quad (3)$$

and suppose that Y_t is cointegrated with the normalized cointegrating vector $\beta = (1, -\beta_2)^T$. This cointegration relationship may be represented as

$$y_{1t} = \beta_2 \sum_{s=1}^t \varepsilon_{1s} + \varepsilon_{3t} \quad \text{and} \quad y_{2t} = \sum_{s=1}^t \varepsilon_{1s} + \varepsilon_{2t} \quad (4)$$

where the common trend is $\sum_{s=1}^t \varepsilon_{1s}$. As illustrated below, the cointegration process removes the common stochastic trend and the cointegration residual $\beta^T Y_t$ obtained is a stationary $I(0)$ time series, i.e.

$$\begin{aligned} \beta^T Y_t &= y_{1t} - \beta_2 y_{2t} \\ &= \beta_2 \sum_{s=1}^t \varepsilon_{1s} + \varepsilon_{3t} - \beta_2 \left(\sum_{s=1}^t \varepsilon_{1s} + \varepsilon_{2t} \right) \\ &= \varepsilon_{3t} - \beta_2 \varepsilon_{2t} \sim I(0) \end{aligned} \quad (5)$$

One of the most common approaches used to determine the existence of cointegration and the number of linearly independent cointegrating vectors (or relationships) among multivariate non-stationary time series in Y_t were developed in [23]. This so-called *Johansen's cointegration procedure* basically is a combination of cointegration and error correction models in a Vector Error Correction Model (VECM) form. This is a sophisticated sequential procedure and thus is not presented in this paper. For a complete description of the Johansen procedure, readers are referred to [23]. In this study, the Johansen's cointegration procedure was realized by using the Econometrics Toolbox [24].

Next, an example that uses the Johansen's cointegration procedure to remove common trends in the simulated data is presented. The Weierstrass-Mandelbrot (W-M) cosine fractal function is used in the analysis because of its non-linear and non-stationary nature. The W-M cosine fractal function is given by [25]

$$W_i = \sum_{j=-N}^N \frac{\left(1 - \cos B^j \frac{i}{N_p} \right)}{B^{(2-D)j}} \quad (6)$$

where $i = 1 \dots N_p$, with N_p is the total number of data samples; and the parameter D and B must be in the range $1 < D < 2$ and $B > 1$, respectively.

In this example, three W-M cosine fractal functions (e.g. variables x, y, z) are used (see Fig. 1). Clearly, they share one common stochastic trend, i.e. the positive drift (or upward trending). When these three variables – sharing a common trend – are cointegrated, the cointegration process results in two cointegrating vectors (i.e. $r = 2$), in which The first cointegrating vector is:

$$\beta_1 = [1 \quad -1.62 \quad 1.99 \quad 0.16]^T \quad (7)$$

The second cointegrating vector is:

$$\beta_2 = [1 \quad 0.12 \quad -1.21 \quad 2.03]^T \quad (8)$$

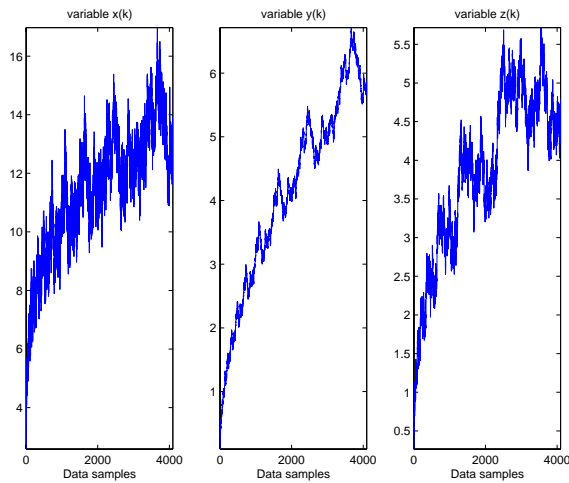


Fig. 1. Three W-M cosine fractal functions (x, y, z).

Next, projecting three variables (x, y, z) on the two obtained cointegrating vectors that results in two cointegration residuals in Fig. 2 and Fig. 3. It is easy to observe that the cointegration residual in Fig. 2 – which uses the first cointegrating vector is more stationary than the one in Fig. 3 – which uses the second cointegrating vector. The results obtained in Fig. 2 and Fig. 3 also showed that the positive drift trending was removed from the W-M variables.

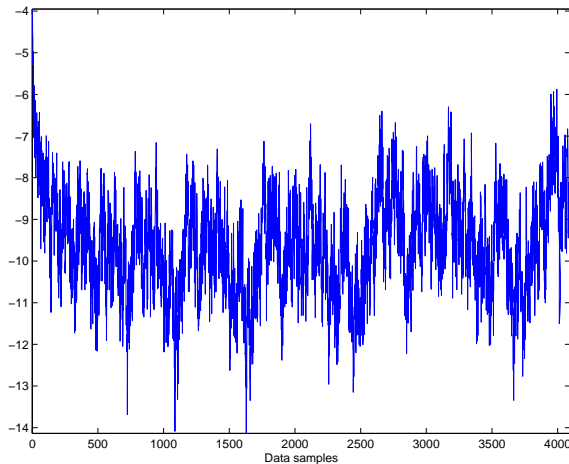


Fig. 2. The first cointegration residual obtained when three W-M variables are projected on the first cointegrating vector.

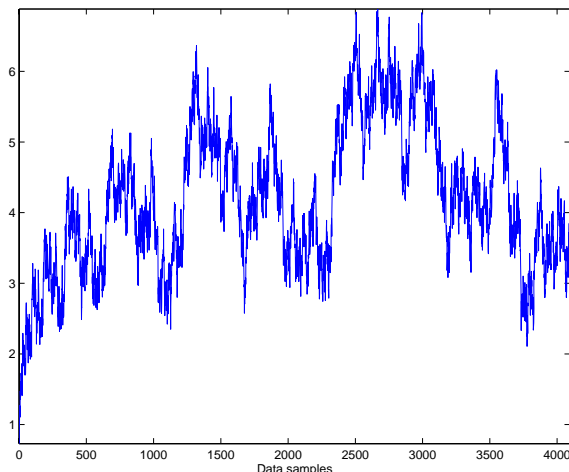


Fig. 3. The second cointegration residual obtained when three W-M variables are projected on the second cointegrating vector.

4. LAMB WAVE EXPERIMENTAL DATA WITH TEMPERATURE TRENDS

Experimental data used in this paper originate from a series of tests described in [15]. Lamb waves were propagated in an aluminium plate (200 x 150 x 2 mm) aluminium plate of 2 mm thickness was used in these experiments. Two low-profile, surface-bonded piezoceramic *Sonox P155* transducers (diameter 10 mm and thickness 1 mm) were used for Lamb wave generation and sensing.

A five-cycle 75 kHz cosine burst signal was used for Lamb wave generation. The excitation signal was enveloped using a half-cosine envelope. The maximum peak-to-peak amplitude of the excitation signal was equal to 10 V. This excitation led to the so-called single Lamb wave mode propagation, i.e. the A0 fundamental Lamb wave mode was generated whereas the amplitude of the S0 mode was negligible. The excitation signal was generated using the *TTi TGA 1230* arbitrary waveform generator. Lamb wave responses were acquired using a digital 4-channel *LeCroy LT264 Waverunner* oscilloscope. Both instruments, i.e. the signal generator and the oscilloscope, were controlled in MATLAB through the General Purpose Control Bus (GPIB) protocol standard, running on a standard PC. Fig. 4. shows a schematic diagram of the experimental arrangement.

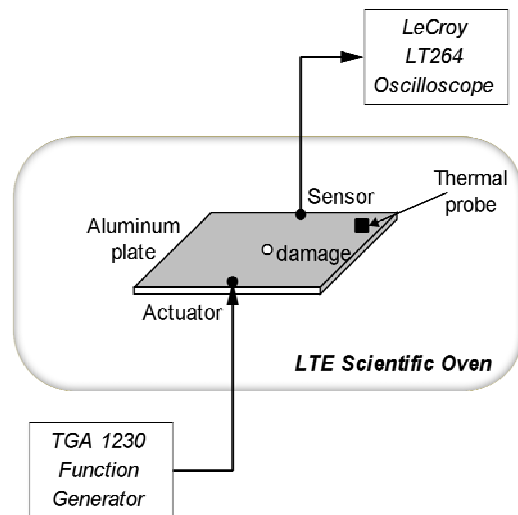


Fig. 4. Experimental arrangement.

The plate was placed in a 100 liter *LTE Scientific* oven to obtain data for various temperature levels. The temperature on the surface of the plate was measured using a thermal probe. Firstly, the experimental tests were performed using the intact plate. The plate was firstly heated up (from 35°C to 70°C) and then cooled down (from 70°C to 35°C) with a step change of 5°C. The heating and cooling cycles were performed twice to address the problem of repeatability and check for possible hysteresis

between cycles. Then, a hole was drilled the middle of the plate and the entire experimental work was repeated.

The analysis presented in this paper utilised lamb wave data for the *undamaged plate* and the *damaged plate with 5 mm hole* – measured at four different temperatures (i.e. 35, 45, 60 and 70°C). Altogether twenty Lamb wave responses were used for each single combined damage-temperature condition and each response measurement consists of 5000 data samples acquired using the sampling rate of 10 MHz. Strong influence of temperature on lamb wave responses was observed, as reported previously in [15, 18].

5. EXPERIMENTAL RESULTS

This section presents the temperature effect removal and damage detection results based on the proposed cointegration-based method. Lamb wave experimental data described in the previous section were used in this analysis.

The cointegration analysis and the ADF test were performed using the Lamb wave experimental data. The entire procedure consists of three schemes:

- (1) ADF test on the “pre-cointegrated data”;
- (2) Cointegration of Lamb wave responses;
- (3) ADF test on the “post-cointegrated data”.

It is well known that whenever the cointegration method is used, the ADF test is firstly performed to measure the degree of stationarity or non-stationarity of the analysed variables. In principle, *the more negative the ADF t-statistic value is obtained, the more stationary the signal is*, as shown in [11,12]. The assumption is that damage introduced to the plate can change stationarity of Lamb wave data. In addition, different severities of damage can produce Lamb wave responses with different stationary characteristics. If this is the case, then not only the existence of damage can be detected, but also its severity can be assessed. Hence, the ADF test can be used not only to test for stationarity but also to detect damage and judge its severity. Following [12], the average ADF t-statistics are used in this study to assess the degree of stationarity of the analysed data and to detect possible damage.

In the first scheme, twenty Lamb wave responses from each single combined damage-temperature condition were directly used in the ADF test. This analysis resulted in ADF t-statistic features, in which each feature consists of twenty ADF t-statistic values that correspond to twenty Lamb wave responses used in the ADF test. The results in Fig. 5 are presented for the undamaged plate and the damaged plate with 5 mm hole at four different temperatures investigated. All statistics vary abruptly and do not exhibit any immediate patterns. Lamb wave responses are corrupted by temperature and the relevant average ADF t-statistics are also influenced by this effect. The

average ADF t-statistics for the undamaged plate and the damaged plate are relatively separated when the temperature is equal to 35°C. However, once the temperature increases these statistics are overlapped.

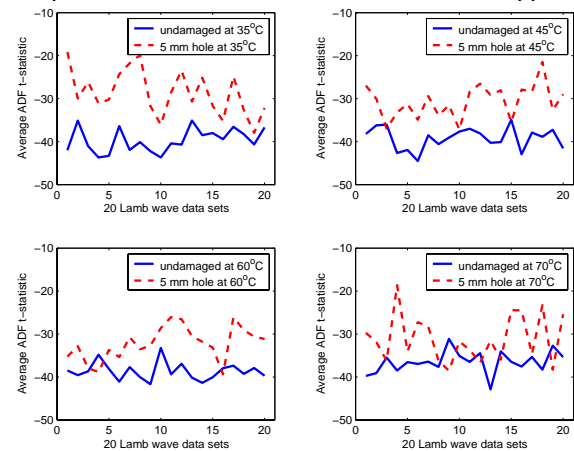


Fig. 5. ADF test results for the pre-cointegrated Lamb wave data.

In the second scheme, twenty Lamb wave responses from each single combined damage-temperature condition were cointegrated by using the Johansen’s cointegration procedure. For the data used the cointegration process creates as many as nineteen linearly independent cointegrating vectors, which subsequently can be used to produce *nineteen cointegrating residuals* (i.e. post-cointegrated Lamb wave responses) after the data projection process.

In the third scheme, nineteen cointegrating residuals obtained from the second scheme were used in the ADF test (or in other words, the ADF test was performed on the post-cointegrated Lamb wave responses). This analysis resulted in *ADF t-statistic features*, in which each feature consists of nineteen ADF t-statistic values that correspond to nineteen cointegrating residuals obtained from the cointegration process.

The results in Fig. 6 for different temperatures investigated show that the average ADF t-statistics for the undamaged plate and the damaged plate are very well separated. Interestingly, these statistics display large negative values (i.e. smaller than -25) for the first cointegrating residual; whereas, the relevant statistics for the remaining residuals are relatively stable and remain between -10 and -5. In this case, the 1st cointegrating vector created the most stationary cointegrating residual. The statistics for the damaged plate with the 5 mm hole increase monotonically from the 2nd to the 19th residual. It is important to emphasize that these statistics are quite similar for all temperatures investigated. This is due to the fact that the temperature effect was purged from the Lamb wave data by the cointegration process. Therefore, the ADF test was applied effectively to the cointegrating residuals that were free from temperature variations. This is why these statistics are relatively stable if compared with the relevant statistics in Fig. 5.

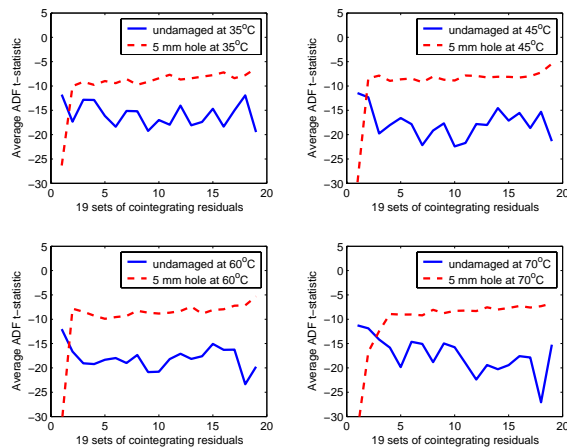


Fig. 6. ADF test results for the post-cointegrated Lamb wave data.

6. CONCLUSIONS

By applying the cointegration analysis, the varying temperature effect is successfully removed from Lamb wave responses and therefore the cointegrating residuals obtained are free from temperature variations.

When the ADF test is applied to the temperature-effect-purged cointegrating residuals, the damaged plate with 5 mm hole can be easily detected.

Although, the results obtained are interesting, further research work is required to confirm these findings. This work should focus on: more complex structures, real damages (e.g. fatigue cracks in metals or delaminations in composites) and different damage detection strategies (wave propagation paths, transducer schemes, etc.).

ACKNOWLEDGEMENT

The work presented in this paper was supported by funding from WELCOME research project no. 2010-3/2, sponsored by the Foundation for Polish Science (Innovative Economy, National Cohesion Programme, EU).

The experimental tests have been performed in the Department of Mechanical Engineering at Sheffield University, UK. The technical assistance of Dr Boon Lee in these tests is greatly acknowledged.

BIBLIOGRAPHY

[1] Kessler S. S., Spearing S. M., Soutis C., *Damage detection in composite materials using Lamb wave methods*, Smart Mater. Struct. 11 (2002) 269–278.
 [2] Staszewski, W. J., *Structural health monitoring using guided ultrasonic waves*, in: J. Holnicki-Szulc and C.A. Mota Soares (ed.), *Advances in Smart Technologies in Structural Engineering*, Springer, Berlin, 2004, pp. 117–162.

[3] Su Z., Ye L., Lu Y., *Guided Lamb waves for identification of damage in composite structures: A review*, J. Sound Vib. 295 (2006) 753–780.
 [4] Croxford A. J., Wilcox P. D., Drinkwater B. W., Konstantinidis G., *Strategies for guided-wave structural health monitoring*, Proc. R. Soc. A 463 (2007) 2961–2981.
 [5] Raghavan A., Carlos C. E. S., *Review of guided-wave structural health monitoring*, The Shock and Vibration Digest 39 (2007) 91–114.
 [6] Sohn H., *Effects of environmental and operational variability on structural health monitoring*, Phil. Trans. R. Soc. A 365 (2007) 539–560.
 [7] Lanza di Scalea F., Salamone S., *Temperature effects in ultrasonic Lamb wave structural health monitoring systems*, J. Acoust. Soc. Am. 124 (2008) 161–174.
 [8] Konstantinidis G., Drinkwater B. W., Wilcox P. D., *The temperature stability of guided wave structural health monitoring systems*, Smart Mater. Struct. 15 (2006) 967–976.
 [9] Engle R. F., Granger C. W. J., *Co-integration and error-correction: representation, estimation, and testing*, Econometrica 55 (1987) 251–276.
 [10] Chen Q., Kruger U., Leung A. Y. T., *Cointegration testing method for monitoring non-stationary processes*, Ind. Eng. Chem. Res. 48 (2009) 3533–3543.
 [11] Cross E. J., Worden K., Chen Q., *Cointegration: A novel approach for the removal of environmental trends in structural health monitoring data*, Proc. R. Soc. A 467 (2011) 2712–2732.
 [12] Dao P. B., Staszewski W. J., *Cointegration approach for temperature effect compensation in Lamb wave based damage detection*, Smart Mater. Struct. 22 (2013) 095002.
 [13] Dickey D., Fuller W., *Likelihood ratio statistics for autoregressive time series with a unit root*, Econometrica 49 (1981) 1057–1072.
 [14] Sohn H., Worden K., Farrar C., *Statistical damage classification under changing environmental and operational conditions*, J. Intell. Mater. Syst. Struct. 13 (2002) 561–574.
 [15] Lee B. C., Manson G., Staszewski W. J., *Environmental effects on Lamb wave responses from piezoceramic sensors*, Materials Science Forum: Modern Practice in Stress and Vibration Analysis, Trans Tech Publications, Switzerland, 440–441 (2003) 195–202.
 [16] Worden K., Staszewski W. J., Hensman J. J., *Natural computing for mechanical systems research: a tutorial overview*, Mech. Syst. Signal Process. 25 (2011) 4–111.
 [17] Croxford A. J., Wilcox P. D., Konstantinidis G., Drinkwater B. W., *Strategies for overcoming the effect of temperature on guided wave structural health monitoring*, Proc. SPIE

Health Monitoring of Structural and Biological Systems (SPIE 6532 65321T1), Bellingham, WA, USA, 2007.

- [18] Kijanka P., Radecki R., Packo P., Staszewski W. J., Uhl T., *GPU-based local interaction simulation approach for simplified temperature effect modelling in Lamb wave propagation used for damage detection*, Smart Mater. Struct. 22 (2013) 035014.
- [19] Sohn H. *Reference-free crack detection under varying temperature*, KSCE J. Civ. Eng. 15 (2011) 1395–1404.
- [20] Croxford A. J., Moll J., Wilcox P. D., Michaels J. E., *Efficient temperature compensation strategies for guided wave structural health monitoring*, Ultrasonics 50 (2010) 517–528.
- [21] Golder M., *Time series models*, Lecture Note on Methods IV: Advanced Quantitative Analysis, September 2012 (available from: <https://files.nyu.edu/mrg217/public/timeseries.pdf>).
- [22] Zivot E., Wang J., *Modeling Financial Time Series with S-PLUS*, 2nd ed., Springer, New York, 2006.
- [23] Johansen S., *Statistical analysis of cointegration vectors*, Journal of Economic Dynamics and Control 12 (1988) 231–254.
- [24] LeSage J. P., *Applied econometrics using Matlab*, Department of Economics, University of Toledo (www.spatial-econometrics.com).
- [25] Staszewski W. J., *Wavelets for Mechanical and Structural Damage Detection* ((in Series Studia i Materialy) Monograph no. 510/1469/2000) (Gdansk: Polish Academy of Sciences Press, IMP-PAN), 2000.



Phong Ba DAO received an M. Sc. degree in electrical engineering from Hanoi University of Science and Technology, Hanoi, Vietnam, and a Ph.D. degree in control engineering from the University of Twente, Enschede, The Netherlands in 2003, and 2011, respectively. Since July 2011 he has been an Assistant Professor at the Department of Robotics and Mechatronics, AGH University of Science and Technology in Krakow, Poland. His current research interests are structural health monitoring and damage detection, multi-agent control systems, intelligent control, and mechatronics.

EVALUATION OF THE WEAR OF FRICTION PADS RAILWAY DISC BRAKE USING SELECTED FREQUENCY CHARACTERISTIC OF VIBRATIONS SIGNAL GENERATED BY THE DISC BRAKE

Wojciech SAWCZUK, Franciszek TOMASZEWSKI

Poznan University of Technology, Faculty of Working Machines and Transportation, Institute of Combustion Engines and Transport, Division of Rail Vehicles, Piotrowo 3 street, 60-965 Poznan, fax (61) 665-2204, e-mail wojciech.sawczuk@put.poznan.pl

Summary

The article presents a new method for diagnosis of the wear of friction pads railway disc brake through analysis of the braking vibration during braking with the constant braking power and during braking to stop by making the analysis of signals in the frequency domain. At the time of research there are vibration acceleration generated by the caliper with brake pads during two types of braking.

Keywords: railway disc brake, diagnostics of brake, frequency analysis

OCENA ZUŻYCIA OKŁADZIN CIERNYCH KOLEJOWEGO HAMULCA TARCZOWEGO NA PRZYKŁADZIE WYBRANYCH CHARAKTERYSTYK WIDMOWYCH SYGNAŁU DRGANIOWEGO GENEROWANEGO PRZEZ HAMULEC

Streszczenie

Artykuł przedstawia autorską metodę diagnozowania zużycia okładzin ciernych poprzez analizę drgań układu hamulcowego na przykładzie hamowania na spadku jak i hamowania zatrzymującego, dokonując analizy sygnałów w dziedzinie amplitud. W czasie badań rejestrowano przyspieszenia drgań generowane przez obsady hamulcowe z okładzinami w czasie hamowania.

Słowa kluczowe: kolejowy hamulec tarczowy, diagnostyka hamulca, analiza widmowa

1. INTRODUCTION

Because of complex braking system in rail cars and locomotive, most often consisting of 8 individual brake cylinders, application of one diagnostic system to assess the wear of all friction sets is impeded [8]. Few disadvantages of disc brake include a lack of possibility of controlling the condition of the friction set: brake and pad in the whole operation time. It is particularly observable in rail cars, where disc brakes are mounted on the axle of the axle set between the wheels (Fig. 1) [9]. To check the wear of friction pads and brake discs it is necessary to apply specialistic station e.g. inspection channel to carry out inspections, and to carry out replacement of friction parts in case they reach their terminal wear. A system for video inspection and diagnostics worked out in Rail Vehicle Institut TABOR in Poznan is the most advanced system to diagnose disc brake. Diagnosing system [3] provides complete information about the wear of friction pads and brake disc in each operation moment. Worked out solutions, because of complex and expensive measuring set consisting of a digital film camera and a software to convert the picture, after successful

tests at reasearch station, have not been applied by railway industry yet.



Fig. 1. View of two friction set mounted on axle passenger car

In rail technique, also rail track stations are used to diagnose the wear of friction pad. At these stations friction set consisting of disc brake and friction pad is photographed during train ride. However, it is not a very precise method because, on the basis of registered pictures the thickness of friction pads of disc brake is only assessed. When pads' thickness amounts to approx. 10mm tram

driver receives information that limitary acceptable wear of pads on a certain axle of axle set has been reached. Rail track stations to diagnose the wear of friction pads are used by German, British and French railways.



Fig. 2. System of signaling braking mounted on passenger car 136: a) excluded brake, b) other state of the brake: 1 – green colour it is excluded brake, 2 – rectangle crossed out that is other the state of the brake e.g. is missing airs in the brake installation, 3 – manometer pressures

In railway vehicles, systems signaling braking process and easing process, visible for the service from the inside and outside of the vehicle, are the most often applied. Those systems enable to check during train ride in which car braking system is blocked (Fig. 2). Nevertheless, rail technique lacks an objective method of quantitative assessment of the wear of friction pads.

The purpose of this research is to apply frequency analysis to evaluation of the wear of friction pads on the base vibration signal generated by caliper with pads disc brake lever set.

2. METHODOLOGY AND RESEARCH OBJECT

The research was carried out at internal station for tests of railway brakes. A brake disc type 590×110 with ventilation vanes and three sets of pads type 175 FR20H.2 made by Frenoplast constitute the research object. One set was new - 35mm thick and two sets were worn to thickness of 25mm and 15mm. A research program 2B1 (II) according to instructions of UIC 541-3 was applied.

The braking was carried out from speed of 80km/h and it was the braking with the constant braking power $P=45\text{kW}$. During the research pad's pressures to disc N of 25kN was realized as well as braking masses per one disc of $M=5.7T$ and during braking to stop [6].

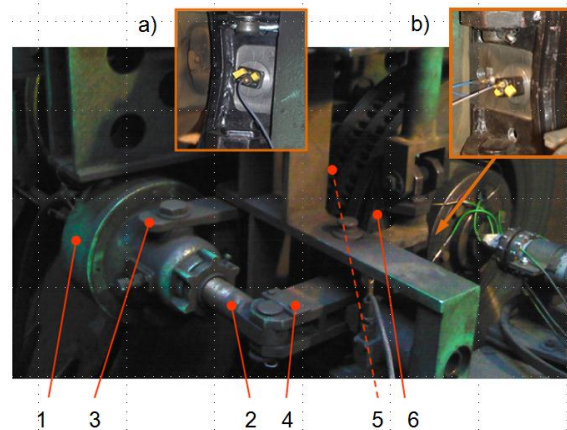


Fig. 3. View of disc brake lever set: a) caliper with vibration converter mounted in side of cylinder casing (is not visible in the picture), b) caliper with vibration converter mounted in side of piston rod, 1- brake cylinder casing, 2- brake cylinder piston rod, 3- left main level, 4- right main level, 5- caliper with vibration converter (is not visible in the picture)

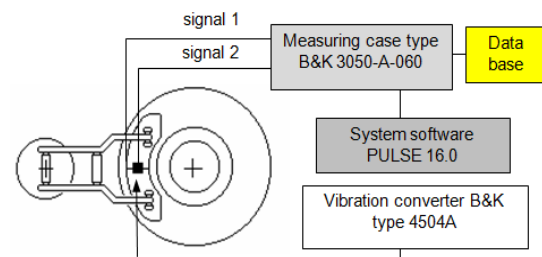


Fig. 4. Measurement set of vibrations generated by caliper with pads

This research was carried out in accordance with principles of active experiment [4]. After carrying out a series of brakings the friction pads were changed and values of instantaneous vibration accelerations were registered.

Vibration converters were mounted on pad calipers with a mounting metal tile, which is presented in Fig. 3a and 3b. During the research signals of vibration accelerations were registered in three reciprocally orthogonal directions [10]. To acquire vibration signal a measuring system consisting of piezoelectric vibration accelerations converter and measuring case type B&K 3050-A-060 with system software PULSE 16.0 was used. Fig. 4 presents the view of the measurement set [1, 2].

3. RESEARCH RESULTS

The purpose of spectrum analysis of signals of vibration accelerations was to determine frequency bands connected with change of pad's thickness during operation of braking system. Figure 5, 6, 7 and 8 presents exemplary amplitude spectra of vibration accelerations for various pad's thicknesses received during braking with constant braking power from speed of 80km/h and braking to stop with the

same speed braking. Spectrum received on measurement of vibrations in direction perpendicular to friction surface of the disc (direction Y).

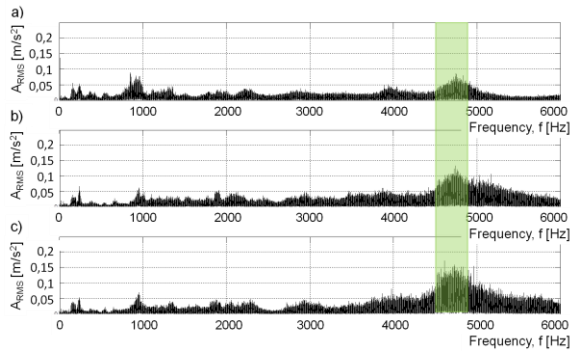


Fig. 5. Dependence of amplitude of vibration accelerations on frequencies for different pad's thicknesses during braking with constant braking power from speed of 80km/h in direction Y1: a) pad's thickness G1=35mm, b) pad's thickness G2=25mm, c) pad's thickness G3=15mm

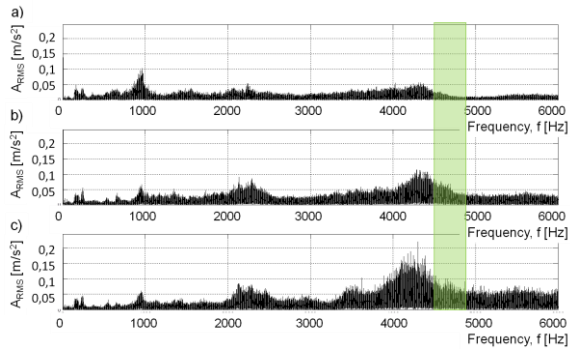


Fig. 6. Dependence of amplitude of vibration accelerations on frequencies for different pad's thicknesses during braking with constant braking power from speed of 80km/h in direction Y2: a) pad's thickness G1=35mm, b) pad's thickness G2=25mm, c) pad's thickness G3=15mm

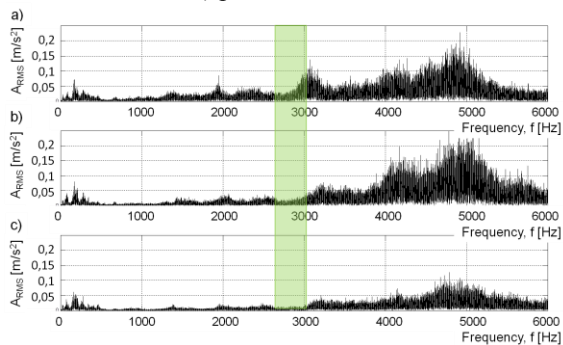


Fig. 7. Dependence of amplitude of vibration accelerations on frequencies for different pad's thicknesses during braking to stop (speed at the beginning of braking v=80km/h) in direction Y1: a) pad's thickness G1=35mm, b) pad's thickness G2=25mm, c) pad's thickness G3=15mm

Frequency analysis were part of the first 20 seconds with a constant braking power and the last 5 seconds to stop braking. In the case of braking to

stop only last 5 seconds allows braking to observe changes in the spectrum of vibration accelerations.

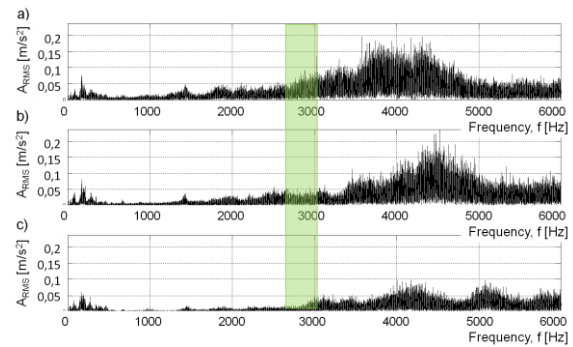


Fig. 8. Dependence of amplitude of vibration accelerations on frequencies for different pad's thicknesses during braking to stop (speed at the beginning of braking v=80km/h) in direction Y2: a) pad's thickness G1=35mm, b) pad's thickness G2=25mm, c) pad's thickness G3=15mm

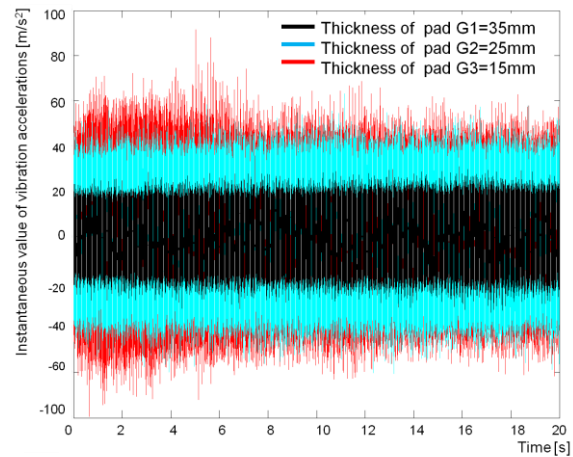


Fig. 9. Signal of vibration accelerations registered on pad caliper in direction Y, for different thickness of pads during braking with the constant braking power

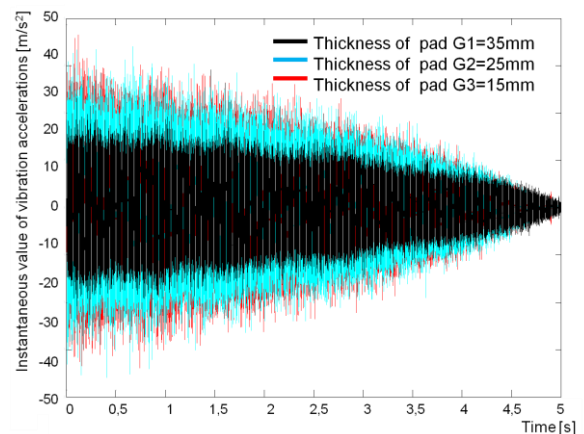


Fig. 10. Signal of vibration accelerations registered on pad caliper in direction Y, for different thickness of pads during braking to stop (Speed at beginning of braking v=80km/h)

Figure 9 and 10 shows an exemplary signal of instantaneous values of vibration accelerations of

caliper and pad registered in direction Y_1 (orthogonal to the disc) during station research.

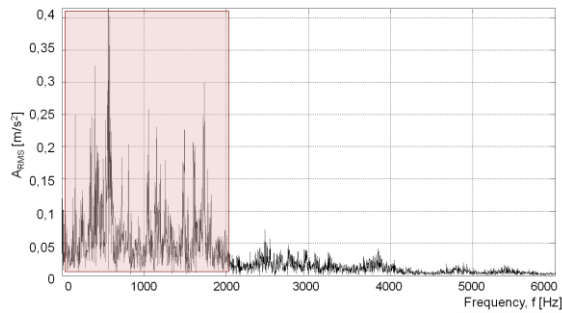


Fig. 11. Dependence of amplitude of vibration accelerations on frequencies for internal station for tests of railway brakes after brake (speed at the beginning of braking $v=80\text{km/h}$)

Frequency analysis has been also the vibrations generated by the internal station for tests of railway brakes during speed $v = 80 \text{ km/h}$, it was found that 2kHz do not analyze the spectrum changes depending on the thickness of the friction pads

Research on measurement of vibration accelerations of brake calipers in frequency domain showed that it is possible to find frequency bands, in which dependence of RMS value of vibration accelerations A_{RMS} (equation (1)) [4] on various pad's thicknesses in considered range of speeds at the beginning of braking is observed.

$$A_{RMS} = \sqrt{\frac{1}{T} \int_0^T [s(t)]^2 dt} \quad (1)$$

where:

T – average time [s],
 $s(t)$ – instantaneous value of vibration accelerations, in $[\text{m/s}^2]$.

Table 1 and 2 presents frequency range, in which dependence of amplitude value of vibration accelerations on the wear of pads is observed. Additionally, dynamics of changes according to dependence (2) [6] of an examined diagnostic parameter for a certain frequency band and at a certain speed at the beginning of braking and values of correlation coefficients for linear dependence of amplitude value of vibration accelerations on examined friction pad's thicknesses is presented. On this basis it was concluded that diagnosing the wear of frictions pads can be carried out independently from the type of braking for certain frequency bands.

$$D = 20 \lg \left(\frac{A_2}{A_1} \right) \quad (2)$$

where:

A_1 – the value of point parameter determined for pad G_3 or G_2 , in $[\text{m/s}^2]$,
 A_2 – the value of point parameter determined for pad G_1 , in $[\text{m/s}^2]$.

Table 1 measurement results for braking with the constant braking power

Measurement of vibrations in direction Y_1					
Frequency Hz	Value of RMS value m/s^2			Dynamics of changes dB	
	Pad 35mm	Pad 25mm	Pad 15mm	G2/G1	G3/G1
4600-4800	1,68	2,75	3,76	4,27	6,96
Measurement of vibrations in direction Y_2					
4600-4800	0,45	1,44	2,11	10,1	13,4

Table 2 measurement results for braking to stop

Measurement of vibrations in direction Y_1					
Frequency Hz	Value of RMS value m/s^2			Dynamics of changes dB	
	Pad 35mm	Pad 25mm	Pad 15mm	G2/G1	G3/G1
2800-3000	0,345	0,148	0,078	-7,36	-12,88
Measurement of vibrations in direction Y_2					
2800-3000	0,443	0,231	0,142	-5,65	-9,26

Figure 12 and 13 presents dependence of friction pad's thickness of disc brake G on RMS value of selected two bands frequency. selected point parameters of vibration accelerations. For RMS value of band frequency, also obtained from measurement in direction Y_1 by using linear approximating functions described with dependences (3-6) for speeds at the beginning of braking $v=80\text{km/h}$ during braking with the constant braking power and during braking to stop, the following equations defining friction pads' thickness were introduced:

$$G = 69,682 \cdot A_{RMS(Y1, BS)} + 11,733 \quad (3)$$

$$G = -9,6426 \cdot A_{RMS(Y1, BP)} + 51,372 \quad (4)$$

$$G = 64,396 \cdot A_{AVERAGE(Y1, BS)} + 7,2718 \quad (5)$$

$$G = -11,862 \cdot A_{AVERAGE(Y1, BP)} + 40,871 \quad (6)$$

where:

G – thickness of pad [mm],
 $A_{(.,)}$ – RMS value from band frequency $[\text{m/s}^2]$,
 BS – braking to stop (band frequency 2800-3000Hz),
 BP – braking with constant braking power (band frequency 4600-4800Hz).

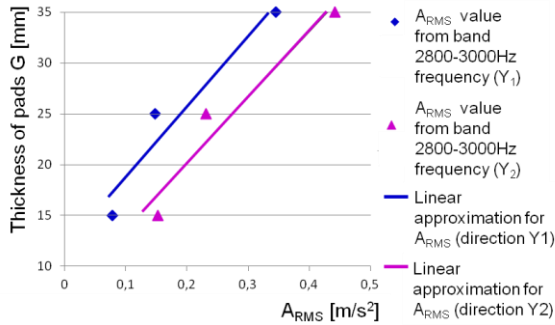


Fig. 12. Dependence of pad's thickness in function of RMS value of vibrations accelerations for frequency band 2800-3000Hz

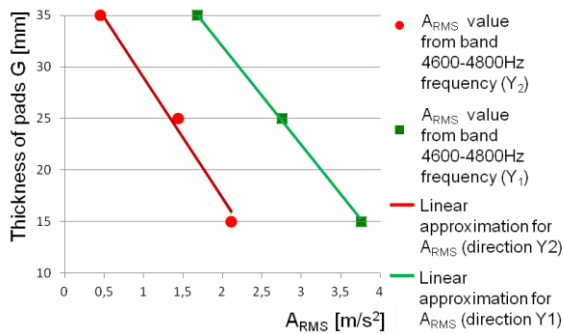


Fig. 13. Dependence of pad's thickness in function of RMS value of vibrations accelerations for frequency band 4600-4800Hz

The inaccuracy of the linear regression models described dependencies (3-10) present table 3 and 4.

Table 3 Error in % in the application models in estimating linear regression actual thickness of brake pad for braking with the constant braking power

Measurement of vibrations in direction Y ₁			
Frequency Hz	For brake pad G ₁ =35mm	For brake pad G ₂ =25 mm	For brake pad G ₃ =15 mm
4600-4800	0,29	0,87	0,74
Measurement of vibrations in direction Y ₂			
4600-4800	1,44	5,08	4,82

Table 4 Error in % in the application models in estimating linear regression actual thickness of brake pad for braking to stop

Measurement of vibrations in direction Y ₁			
Frequency Hz	For brake pad G ₁ =35mm	For brake pad G ₂ =25 mm	For brake pad G ₃ =15 mm
2800-3000	2,16	11,84	12,73
Measurement of vibrations in direction Y ₂			
2800-3000	2,16	11,43	12,20

The analysis of results of research in frequency function showed that for frequency band 4600-4800Hz it is possible to diagnose the wear of friction pads independently during braking with constant braking power P=45kW. The dynamics of changes of RMS values of vibration accelerations for pads: G₁, G₂ and G₃ can be found in the range between 2,3 and 13,4dB.

4. CONCLUSION

The research at internal station for tests of railway brakes showed that it is possible to diagnose the wear of friction pads by using analysis of the values of the vibration acceleration caliper by defining in frequency domain.

Analysis of caliper vibrations in frequency domain enables to diagnose the wear of friction pads in band: 4600-4800Hz during braking with the constant braking power P=45kW. Another band 2800-3000Hz of frequency analysis of vibrations signals also checked during braking to stop at the beginning of speed braking v=80km, pressures to disc N of 25kN and braking masses per one disc of M=5,7T.

For analysis in frequency domain, coefficients of dynamics of changes equals 4-6dB (direction Y₁), 10-13dB (direction Y₂) for braking with the constant braking power. And coefficients of dynamics of changes equals 7-12dB (direction Y₁), 5-9dB (direction Y₂) for braking to stop. Using RMS value of vibration accelerations it is possible to use diagnostic models to define the wear of friction pads during braking with the constant braking power. Error diagnosis using regression diagnostic models equaled 0,3-5% for braking with the constant braking power (for both direction measurement) and 2-12% for braking to stop also for both direction measurement.

The project is funded by the National Center for Science, N N504 644840

BIBLIOGRAPHY

- [1] Brüel & Kjær: *Piezoelectric Accelerometer Miniature Triaxial Delta Tron Accelerometer – Type 4504A*, oferta firmy Brüel & Kjær.
- [2] Brüel & Kjær: *Measuring Vibration*, Revision September 1982.
- [3] Boguś P., Bocian S.: *Shape deformation analizys of rail car brakes with image processing techniques*, Book of Abstracts of European Mechanics Society EUROMECH 406 Colloquium – Image Processing Methods in Applied Mechanics, Warszawa, 6-8 maj 1999, s.47-49.
- [4] Cempel C.: *Podstawy wibroakustycznej diagnostyki maszyn*. WNT Warszawa 1982.
- [5] Gruszewski M.: *Wybrane zagadnienia eksploatacji hamulca tarczowego*. Technika Transportu Szynowego 1995, nr 6-7, s. 84-86.
- [6] Kodeks UIC 541-3: *Hamulec-Hamulec tarczowy i jego zastosowanie. Warunki dopuszczenia okładzin hamulcowych*. Wydanie 6, listopad 2006.
- [7] Piechowiak T., *Hamulce pojazdów szynowych*, Wydawnictwo Politechniki Poznańskiej 2012.

- [8] Rail Consult Gesellschaft für Verkehrsberatung mbH.: *Wagon osobowy Z1 02, układ jezdny-tom 2. Dokumentacja Techniczno-Ruchowa.*
- [9] Sawczuk W.: *Assessing the Wear of Friction Pads in Disc Braking System of Rail Vehicle by Using Selected Frequency Characteristics of Vibration Signal*, *Vibration In Physical Systems*, Volume XXV s. 355-360.
- [10] Serridge M., Licht T. R.: *Piezoelectric accelerometers and vibration preamplifiers*, Brüel & Kjær 1987.



Wojciech SAWCZUK

DEng. from 2010, an adjunct at the Institute of Combustion Engines and Transport of Poznan University of Technology, Faculty of Working Machines and Transportation. In his work

deals with the scientific discipline which is the construction and operation of machines, specialty diagnostic machines. In particular research interests concern the research vibration braking of vehicles which run on rails, engine diagnostics and thermal tests of means of transport.

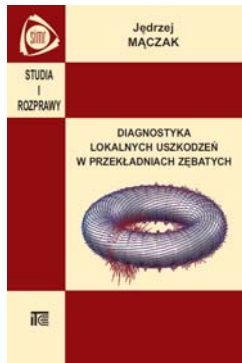


Franciszek TOMASZEWSKI

DSc., DEng. in the period 2002-2012, Head of the Division of Rail Vehicles, Dean of the Faculty of Working Machines and Transportation from 2012 at Poznan University of Technology. Research interests: study of

durability and reliability vehicles which run on rails, vibration diagnostics of internal combustion engines, testing and evaluation of the vibration and noise generated by land vehicles.

Participation in numerous research work, including as Director of grants and research, development and grants KBN and work for industry.



Jędrzej MAĆZAK

Diagnostyka lokalnych uszkodzeń w przekładniach zębatych

W monografii opisano metody diagnostyczne umożliwiające identyfikację lokalnych uszkodzeń przekładni zębatych. Takie ujęcie pozwala na dokładną lokalizację miejsc ich

wystąpienia. W odróżnieniu od metod globalnych przydatnych w detekcji uszkodzeń przekładni, metody prezentowane w monografii zdecydowanie przewyższają dotychczasowe podejście odnośnie identyfikacji i lokalizacji uszkodzeń związanych ze współpracą poszczególnych par zębów przekładni.

Zaproponowane metody, w części odwołujące się do transformat różniczkowych (np. operator energetyczny Teagera-Kaisera), pokazują, że możliwe jest dotarcie do źródła informacji diagnostycznej bez używania powszechnie stosowanych transformat całkowych. Pozwalają na identyfikację rodzajów uszkodzeń i ich lokalizację zarówno w kategoriach uszkodzeń poszczególnych wałów (np. pojawienie się bicia, czy uszkodzenie sprzęgła), jak i uszkodzeń poszczególnych zębów zębniaka lub koła. Odwołują się bezpośrednio do sygnałów czasowych pomijając w większości skomplikowane procedury całkowania. Ich zaletą jest prostota i szybkość działania mające ogromne znaczenie w autonomicznych systemach diagnostycznych przekładni oraz rozproszonych systemach diagnostycznych pracujących online.

W książce zaprezentowano szereg nowych metod diagnostycznych. Część z nich wykorzystuje sygnał przekładni synchronicznie uśredniony w ramach pojedynczego obrotu wału zębniaka. Tak wykonane uśrednianie sygnału eliminuje wpływ szumów oraz zakłóceń związanych z pracą pozostałych wałów przekładni. Umożliwia segmentację sygnału pozwalając na powiązanie wydzielonych jego fragmentów z kinematyką współpracy zębów koła na wale zębniaka. Pozwala tym samym na lokalizację uszkodzeń z rozdzielczością pojedynczych zębów i łatwiejsze diagnozowanie przyczyn występowania miejscowych zmian w sygnale związanych z rozwojem uszkodzeń wału i zębów. Opracowane metody analizy sygnałów umożliwiają wykrywanie chwilowych niestacjonarności sygnału spowodowanych lokalnymi uszkodzeniami przekładni. Metody te wykorzystują m.in. entropię Shannona i dywergencję Kullbacka oraz analizę chwilowych zmian mocy sygnału prowadzoną zarówno z wykorzystaniem obwiedni sygnału, jak i operatora energetycznego Teagera-Kaisera. Do wykrywania lokalnych zaburzeń wykorzystano obwiedniowy wskaźnik przyporu (ECF), porównujący segmenty sygnałów związane z kolejnymi przyporami zębów zębniaka.

Zaproponowana w monografii parametryczna reprezentacja sygnału przekładni na torusie T^2 stała się punktem wyjścia do budowy nowej przestrzeni obserwacji sygnału nazwanej lokalną płaszczyzną zążeń. Metoda bazuje na segmentacji sygnału przekładni lub sygnału z niego przetworzonego. Poszczególne segmenty są powiązane z kinematyką współpracy zążeń, zaś wynik jest prezentowany we współrzędnych *zęby zębniaka* \times *zęby koła*. Definicja płaszczyzny lokalnej umożliwia tabelaryzację segmentów sygnałów związanych ze współpracą poszczególnych par zębów. Poszczególne rodzaje uszkodzeń pozostawiają na tej płaszczyźnie swoją sygnaturę, po której można rozpoznać rodzaj i wielkość uszkodzenia. Metoda ta, wiążąc zmiany w sygnale ze współpracą określonych par zębów zębniaka i koła, pozwala na obserwację trendów tej współpracy podczas życia maszyny, umożliwiając ocenę jakości współpracy poszczególnych par zębów.

Opracowane metody diagnostyczne zostały przebadane na modelu symulacyjnym przekładni pozwalającym na uzyskiwanie przebiegów czasowych poprawnie odwzorowujących zachowanie rzeczywistej przekładni w obecności symulowanych uszkodzeń zmęczeniowych zębów oraz błędów wykonawczo-montażowych. Model przekładni został również wykorzystany do prezentacji zjawisk mających wpływ na sposób generacji sygnału wibroakustycznego przez współpracujące pary zębów. Jego zastosowanie pozwoliło na zbadanie korelacji między miejscem wystąpienia lokalnych zakłóceń w sygnale, a kinematyką i dynamiką pracy przekładni, szczególnie wchodzeniem w przypór i wychodzeniem z przyporu par zębów. Jak wykazały symulacje obserwacja tych miejsc w sygnale jest szczególnie informacyjna w kontekście pojawiania się wczesnych faz rozwoju uszkodzeń par zębatych.

Metody diagnostyczne przetestowano na stanowisku mocy krążącej podczas badań trwałościowych przekładni zębatych dotyczących zjawisk pittingu oraz wyłamania zębów a także na przekładni przemysłowej. Eksperymenty te, w części przytoczone w pracy, potwierdziły skuteczność opracowanych metod. Pozwoliły na zaproponowanie nowej procedury oceny stanu technicznego przekładni bazującej na obserwacji sygnałów na płaszczyźnie lokalnej zążeń. Takie podejście, z uwagi na prostotę metody i małe wymagania sprzętowe, może wypełnić lukę polegającą na braku metod diagnostycznych pozwalających na jednoznaczną ocenę poprawności współpracy zążeń poprzez pomiar wibroakustyczny.

W monografii przedstawiono nowe ujęcie metod numerycznych mających zastosowanie w diagnostyce przekładni. Analiza sygnału na płaszczyźnie lokalnej pozwala na ocenę jakości współpracy poszczególnych par zębów. Opracowane metody pozwalają prowadzić modelowo wspartą analizę lokalnych uszkodzeń przekładni zębatych i uzyskiwać informacje o pracy przekładni niemożliwe do otrzymania dotychczas stosowanymi metodami.

Diagnostyka

APPLIED STRUCTURAL HEALTH, USAGE AND CONDITION MONITORING

Obszar zainteresowania czasopisma to:

- ogólna teoria diagnostyki technicznej
- eksperymentalne badania diagnostyczne procesów i obiektów technicznych;
- modele analityczne, symptomowe, symulacyjne obiektów technicznych;
- algorytmy, metody i urządzenia diagnozowania, prognozowania i genezowania stanów obiektów technicznych;
- metody detekcji, lokalizacji i identyfikacji uszkodzeń obiektów technicznych;
- sztuczna inteligencja w diagnostyce: sieci neuronowe, systemy rozmyte, algorytmy genetyczne, systemy ekspertowe;
- diagnostyka energetyczna systemów technicznych;
- diagnostyka systemów mechatronicznych i antropotechnicznych;
- diagnostyka procesów przemysłowych;
- diagnostyczne systemy utrzymania ruchu maszyn;
- ekonomiczne aspekty zastosowania diagnostyki technicznej;
- analiza i przetwarzanie sygnałów.

Wszystkie opublikowane artykuły uzyskały pozytywne recenzje wykonane przez niezależnych recenzentów.

Topics discussed in the journal:

- General theory of the technical diagnostics,
- Experimental diagnostic research of processes, objects and systems,
- Analytical, symptom and simulation models of technical objects,
- Algorithms, methods and devices for diagnosing, prognosis and genesis of condition of technical objects,
- Methods for detection, localization and identification of damages of technical objects,
- Artificial intelligence in diagnostics, neural nets, fuzzy systems, genetic algorithms, expert systems,
- Power energy diagnostics of technical systems,
- Diagnostics of mechatronic and antropotechnic systems,
- Diagnostics of industrial processes,
- Diagnostic systems of machine maintenance,
- Economic aspects of technical diagnostics,
- Analysis and signal processing.

All the published papers were reviewed positively by the independent reviewers.

Redaktorzy działowi:

dr hab. inż. Tomasz BARSZCZ, prof. AGH
dr hab. Andrzej BIELECKI, prof. AGH
prof. dr hab. inż. Wojciech CHOLEWA
prof. dr hab. Wojciech MOCZULSKI
prof. dr hab. inż. Stanisław RADKOWSKI
prof. dr hab. inż. Wiesław TRAMPCZYŃSKI
prof. dr hab. inż. Tadeusz UHL

Kopia wszystkich artykułów opublikowanych w tym numerze dostępna jest na stronie www.diagnostyka.net.pl

Druk:

Centrum Graficzne „GRYF”, ul. Pieniężnego 13/2, 10-003 Olsztyn, tel. / fax: 89-527-24-30

Oprawa:

Zakład Poligraficzny, UWM Olsztyn, ul. Heweliusza 3, 10-724 Olsztyn
tel. 89-523-45-06, fax: 89-523-47-37

Wszystkie opublikowane w czasopiśmie artykuły uzyskały pozytywne recenzje, wykonane przez niezależnych recenzentów.

Redakcja zastrzega sobie prawo korekty nadesłanych artykułów.

Kolejność umieszczenia prac w czasopiśmie zależy od terminu ich nadesłania i otrzymania ostatecznej, pozytywnej recenzji.

Wytyczne do publikowania w DIAGNOSTYCE można znaleźć na stronie internetowej:

<http://www.diagnostryka.net.pl>

Redakcja informuje, że istnieje możliwość zamieszczania w DIAGNOSTYCE ogłoszeń i reklam.

Jednocześnie prosimy czytelników o nadsyłanie uwag i propozycji dotyczących formy i treści naszego czasopisma.

Zachęcamy również wszystkich do czynnego udziału w jego kształtowaniu poprzez nadsyłanie własnych opracowań związanych z problematyką diagnostyki technicznej. Zwracamy się z prośbą o nadsyłanie informacji o wydanych własnych pracach nt. diagnostyki technicznej oraz innych pracach wartych przeczytania, dostępnych zarówno w kraju jak i zagranicą.